Synthesis Of Halo Alkyl And Alkenyl Ortho-Carboxy Aryls And Bromo Nitro

Lactones As Inhibitors Of Protein Tyrosine Phosphatases And Cancer Cell

Growth

by

Casey Joseph Fadgen

A Dissertation in Partial Fulfillment
of the Requirements for the Degree
Doctor of Philosophy

Approved November 2012 by the
Graduate Supervisory Committee:

Seth D. Rose, Chair
Wilson Francisco
Ian Gould

ARIZONA STATE UNIVERSITY

December 2012

ABSTRACT

Changes to a cell's DNA can result in cancer, which is permanently sustained cellular proliferation. When malfunctioning genes, oncogenes, were verified to be of human origin in the 1970s, drugs were designed to target their encoded, abnormal enzymes. Tyrosine kinases have been established as an oft-modified oncogene enzyme family, but the protein tyrosine phosphatases (PTPs) were not investigated as thoroughly. PTPs have gradually been established as relevant enzymes that work in tandem with tyrosine kinases in cell signaling and are not just "house-keeping" enzymes. Some PTPs are thought to initiate tumorigenesis, and others may play a complementary role after the onset of cancer by extending the duration of cellular signals. Reversible inhibition of these enzymes by an oxalylamino group substituted on an *ortho*-carboxy aryl have been described in the literature. Modification of the oxalylamino group to favor irreversible inhibition of these cysteine-dependent enzymes may prevent inhibitor efflux by cells and subsequent mutation to gain resistance. Replacement of the oxalylamino group with halogenated propanoate and propenoate esters minimally inhibited cancer cell growth but did not inhibit activity of PTPs. Of the *ortho*-carboxy aryl structures, a methyl dichloropropanoate (compound 24) and a lactone alkene (compound 29) inhibited cell growth by 50% (GI-50) at micromolar concentrations. The GI-50s for compounds 24 and 29 were 19.9 (DU-145, prostate carcinoma) and 9.4 micromolar (A549, lung cancer), respectively. In contrast, brominated nitro lactones were able to inhibit both cancer cell growth and the activity of PTPs. In a sulforhodamine B assay, these compounds were

able to achieve GI-50s as low 5.3 micromolar (compound 33 against BXPC-3, pancreatic adenocarcinoma), and some killed 50% of cancer cells (LC-50) at micromolar concentrations. Compound 33 displayed LC-50 of 23.3 micromolar (BXPC-3), and compound 35 had LC-50s of 32.9 and 32.7 micromolar against BXPC-3 and colon adenocarcinoma (KM20L2), respectively. A single concentration (100 micromolar) inhibition assay of inhibitor PTPs resulted in no enzyme activity for 4 out of 5 PTPs tested with compound 33. Similar results were obtained for compounds 35 and 37. Future analysis will determine if these bromo nitro lactones are irreversibly inhibiting PTPs.

TABLE OF CONTENTS

Page

LIST OF TABLES

LIST OF FIGURES

vii

LIST OF SCHEMES

ABBREVIATIONS

$\times$	times
2-CCA	2-carboxycinnamic acid
2-FA	2-formylbenzoic acid
Å	angstrom(s)
AcOH	acetic acid
Anal.	combustion elemental analysis
app	apparent (spectral)
aq	aqueous
BNLA	bromo nitro lactone alkene
br	broad (spectral)
bteac	benzyltriethylammonium chloride
°C	degrees Celsius
Calcd	calculated
cm	centimeter
δ	chemical shift in parts per million downfield from tetramethylsilane
d	doublet (spectral)
DBU	1,8-diazabicyclo[5.4.0]undec-7-ene
DCM	dichloromethane
dd	doublet of doublets (spectral)
DFP	difluorophosphonate
DIFMU	6,8-difluoro-7-hydroxy-4-methylcoumarin
DIFMUP	6,8-difluoro-4-methylumbilliferyl phosphate
DMSO	dimethyl sulfoxide
DNA	deoxyribonucleic acid
DTT	DL-dithiothreitol
ε	molar absorptivity
E2	bimolecular elimination
EDTA	ethylenediaminetetraacetic acid
eq	equivalents
eqn	equation
EtOAc	ethyl acetate
EtOH	ethanol
g	gram(s)
GI_{50}	50% growth inhibition
GID	general inhibitor design
h	hour(s)
HSQC	heteronuclear single-quantum correlation spectroscopy
Hz	hertz
IR	infrared
J	coupling constant (in NMR spectroscopy)
kDa	kilodalton
λ	wavelength
L	liter(s)

LC$_{50}$	50% lethal concentration
μg	microgram(s)
μL	microliter(s)
μM	micromolar (micromoles per liter)
M	molar (moles per liter)
m	multiplet (spectral)
MALDI-TOF	matrix-assisted laser desorption/ionization time-of-flight
MeCN	acetonitrile
MeOH	methanol
MESNA	β-mercaptoethanesulfonate sodium salt
mg	milligram(s)
MHz	megahertz
min	minute(s)
mL	milliliter
mM	millimolar (millimoles per liter)
mm	millimeter(s)
mmol	millimole(s)
mol	mole(s)
mp	melting point
mRNA	messenger ribonucleic acid
MSDS	material safety data sheet
MTT	methylthiazolyldiphenyl-tetrazolium bromide
N	normal (equivalents per liter)
NAC	*N*-acetylcysteamine
NaOMe	sodium methoxide
NBS	*N*-bromosuccinimide
NCI	National Cancer Institute
NEt$_3$	triethylamine
nm	nanometer(s)
NMR	nuclear magnetic resonance
OBA	2-(oxalylamino)-benzoic acid
pBpB	pyridinium bromide perbromide
PBS	phosphate-buffered saline
pH	-log a$_H^+$
pNP	*para*-nitrophenolate
pNPP	*para*-nitrophenyl phosphate
ppm	part(s) per million
PTK	protein tyrosine kinase(s)
PTP	protein tyrosine phosphatase(s)
R*,R*	relative configurations; stereocenters have identical configurations (refers to R,R and S,S isomers)
R*,S*	relative configurations; stereocenters have opposite configurations (refers to *R,S* and *S,R* isomers)
RBF	round-bottom flask
R$_f$	retention factor (in chromatography)
RNA	ribonucleic acid

rt	room temperature
s	singlet (spectral)
SDS-PAGE	sodium dodecyl sulfate-polyacrylamide gel electrophoresis
SRB	sulforhodamine B
t	triplet (spectral)
TBNS	*trans*-β-nitrostyrene
TGI	total growth inhibition
THF	tetrahydrofuran
TLC	thin-layer chromotagraphy
TMS	tetramethylsilane
TMSCl	trimethylsilyl chloride
UV	ultraviolet

1 INTRODUCTION

1.1 Cancer and Proteins as Targets

Cancer is one of the leading causes of death in America. More than 1.6 million new cases of cancer are expected to be reported in 2012. As many as 577,000 people are expected to die from cancer in 2012.[1] Cancer is caused by changes in DNA that result in development of abnormal cells. The abnormal cells usually arise from the expression of oncogenes, inactivation of a tumor-suppressing gene or microRNA genes becoming abnormal.[2] In general, cancer cells are permanently sustained (do not undergo apoptosis), they are able to grow despite contacting other cells (ignore "contact inhibition") and they are capable of spreading to new, non-native tissues (metastasis).

The most aggressive cancers afflicted patients with a recognizable phenotype of excessive and abnormal tissue growth, which was treated by radiotherapy and surgery, and later, drugs. Treating cancer patients with drugs was generally not accepted among the medical community in the early to mid 1900s. However, lethal sulfur mustard gases used in World War I were studied as potential drug leads during WWII. Those studies led to nitrogen mustard drugs being used as some of the earliest candidates for clinical investigations. These compounds are effective DNA alkylators that become reactive after an intramolecular displacement of a halogen atom by the nitrogen (Scheme 1). The resulting product is very electrophilic at the ring carbons. After alkylation of DNA, another ring can form to react with DNA a second time.

1

Scheme 1. Nitrogen mustard, "mustine"
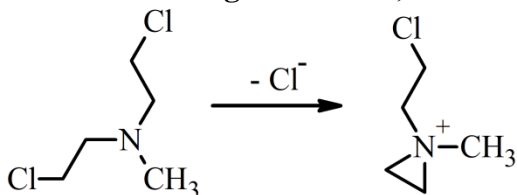
Initially, mustards were used on late-stage cancer patients who no longer showed a positive response to radiotherapy.[3] Unfortunately, providing a safe dosage to limit the cytotoxicity of these drugs was difficult, and most symptoms returned after promising remission. However, nitrogen mustards like chlorambucil and phosphoramide were developed despite these initial failures. These drugs have unsafe side-effects (e.g., mutations and cancerous development), but they are still used in the clinic.

By the 1960s and 1970s, tumor viruses were being thoroughly investigated as the potential origin of cancer cells. Studies of the Rous sarcoma virus (RSV), which is an avian RNA tumor virus, identified a viral gene, later termed *v-src*, that appeared to cause cancer.[4] A homologue of *v-src*, called *c-src*, was later found within non-cancerous cells, however. This proto-oncogene, *c-src*, was recognized as originating within the cellular genetic code,[5] and it can turn normal cells into cancerous ones when mutated or overexpressed. Tumor viruses themselves were determined to be responsible for eliciting this cancerous activity, but they were not the origin of cancerous genes.

Src was later discovered to be a tyrosine kinase,[6] and inhibitors targeted toward many tyrosine kinases have since been developed.[7] In contrast to RNA tumor viruses, certain defective cellular proteins like p53 were arising from DNA

tumor viruses.[8] The p53 protein is a transcription factor that controls apoptosis, DNA repair and other important cellular functions. DNA tumor viruses were discovered to be affecting *p53*, resulting in a mutant, malfunctioning p53 protein. Thus, tumor suppressing genes like *p53*, sometimes called anti-oncogenes, cause cancer or allow it to proliferate when they are defective. Thus, inhibitors that target proteins need to selectively inhibit those that are responsible for tumorigenesis or proliferation.

1.2 Enzyme Inhibition

Enzyme inhibition by synthetic drugs can occur in many fashions. When the active site of an enzyme is targeted, the inhibitors are considered competitive since they will compete with the enzyme's natural substrate. If the enzyme substrate is known, it is also investigated to determine any favorable interactions that can be utilized. If inhibition targets an allosteric site that causes a structural change in the enzyme, then it is considered a noncompetitive inhibitor. Inhibitors that block the catalytic pocket can greatly reduce the enzyme activity, but they must compete with the natural substrate, which may have very high affinity for the enzyme. Noncompetitive inhibitors can reduce enzyme activity at a constant rate regardless of the concentration of substrate present.

Inhibitors need to bind to their target enzyme regardless of their type of inhibition. Designs attempt to facilitate an appropriate interaction that will lead to a molecule that is able to displace a natural substrate or effectively/permanently bind the target. Reversible inhibitors or slow-binding reversible inhibitors interact

3

with enzyme residues without permanently disabling it. This type of inhibition is desirable for cases when continuous treatment is necessary or if highly selective drugs cannot be developed to inhibit deleterious enzymes. Extended treatment can be undertaken that leads to growth of cancer cells being inhibited enough to reduce the tumor to an operable size or eliminate the cancer altogether. Irreversible inhibitors permanently bind enzymes to disable them. In these cases, the selectivity of a drug needs to be specific for a cancerous target. Even extended treatment with irreversible inhibitors that are selective is not ideal since they are likely to affect the same enzyme of normal cells too.

Targeting a unique feature of enzymes can help lead to selective drugs. Factoring in the environment that a drug should bind to will help in developing inhibitors with advantageous interactions. For enzymes, targeting the catalytic residue or unique residues within the binding pocket is one method utilized. Cysteine is generally a neutral amino acid, but ionization of the sulfhydryl group can increase in proteins.[9] When inside an enzyme binding pocket, the thiol can be deprotonated more readily, especially when basic amino acids are nearby, to become a good nucleophile. Cysteine's reactivity was recently utilized in the development of an HER-2 inhibitor, neratinib or HKI-272.[10] HER-2 is a tyrosine kinase that has a cysteine in the active-site. Even though it is not the catalytic residue, the authors hypothesized that it could still be targeted as a nucleophilic group. Neratinib is a Michael-acceptor that binds irreversibly to HER-2 and has progressed to several phase III clinical trials. A family of enzymes that work with tyrosine kinases in cell signaling are the tyrosine phosphatases. Similarly to HER-

2, there is a cysteine in the enzyme-binding pocket, but it is the catalytic residue for almost all of the enzymes of this family.

1.3 Relationship of Protein Tyrosine Phosphatases to Cancer and Other Diseases

The first tyrosine phosphatase to be discovered, PTP1B, was not isolated until ~ 10 years after the first tyrosine kinase.[11, 12] Thus extensive investigation was slow to arise in comparison to PTKs. However, PTP1B was found to be valuable in regulating metabolism and as a potential target for treating type II diabetes.[13] After this discovery and subsequent investigations, PTPs were given more attention for their roles in other diseases and cancer.

There are at least 107 recognized protein tyrosine phosphatases (PTPs) in the human genome, and they are grouped into 4 Classes.[14] Almost all PTPs are defined by a specific catalytic domain of the form $(H/V)C(X)_5R(S/T)$.[15] Depending on the source, the description of the catalytic pocket varies from the simple HCX_5R[16] to the more encompassing $[I/V]HCxAGxxR[S/T]G$.[17] The latter description covers "classical" PTPs, which are described next. PTPs utilize a cysteine as the main catalytic residue (Figure 1). Only Class IV does not follow this trend, as it utilizes an aspartic acid for catalytic activity without cysteine being present.

Class I has 99 PTPs, which are divided into "classical" PTPs and VH1-like PTPs. "Classical" PTPs were identified and isolated first, as can be deduced from their namesake. There are 38 "classical" PTPs which selectively dephosphorylate tyrosine residues.[19] The first PTP to be expressed and isolated

was PTP1B, from the *PTPN1* gene, and it is a "classical" nonreceptor PTP (NRPTP).[11] This is opposed to the "classical" receptor-like PTPs (RPTPs), which are trans-membrane proteins. The Class I VH1-like PTPs contain several enzymes that can dephosphorylate residues other than tyrosine, including mRNA and phosphoinositides. Therefore they are also called dual-specificity PTPs (DSPs).
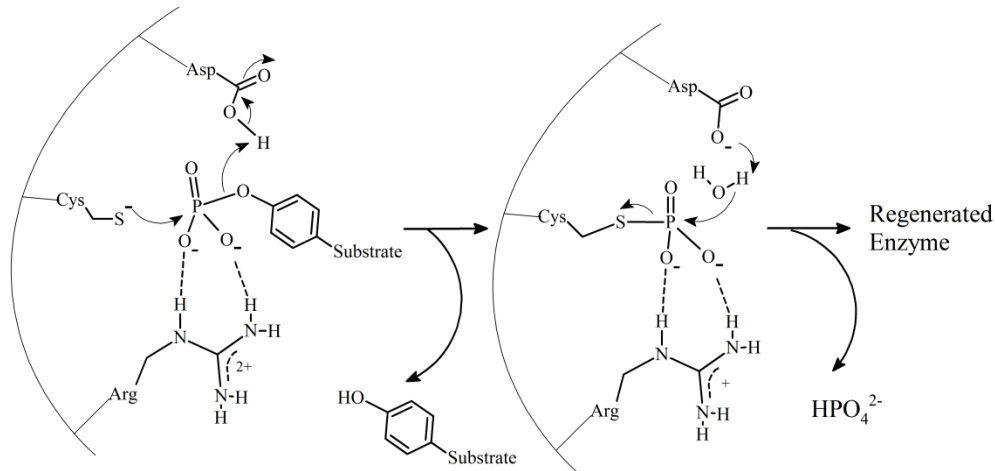
Figure 1. Important residues for catalysis in "classical" PTPs (see Dewang, et al.).[18]

Of the other three classes included in the PTP family, only Class III has been implicated as a target for disease initiation to a significant degree for this discussion. This class is made of three PTP homologs designated cell-division cycle 25, or CDC25A, CDC25B and CDC25C. In addition to tyrosine, they are also capable of dephosphorylating phosphothreonine and phosphotyrosine of Cdks (kinases) that are needed for cell cycle progression. The CDC25s may arise from oncogenes because of their increased expression in several cancers,[20] and they have been studied as therapeutic targets for several cancers.[21, 22] The CDC25s have not been established as arising from oncogenes, however.

Several genomic studies have been done to grasp a possible role for PTPs in disease initiation, progression, etc. Genetic deletions or overexpression of chromosomal locations in cancer cells have been used to implicate PTPs. While protein kinases, another signaling enzyme that phosphorylates proteins and other biomolecules, have been studied and established to arise from several oncogenes, as of 2012 only two PTP genes, *PTEN* and *PTPN11,* are recognized to have tumorigenic properties.[23, 24]

PTPN11 is the gene that encodes the SHP-2 enzyme. This is a classical NRPTP that can cause juvenile myelomonocytic leukemia after a somatic mutation. The mutation results in a more active enzyme. This particular enzyme, SHP-2, has an auto-inhibitory tail that inserts itself into the enzyme's catalytic pocket. The mutation results in a destabilized inhibitory interaction by changing the residues at or near the interface of the N-SH2 tail and the PTP catalytic domain. The mutation prevents the inhibitory tail from blocking the catalytic pocket causing increased RAS/MAPK signaling in certain cells. Furthermore, a germ-line mutation of SHP-2 causes Noonan syndrome, which is a developmental disorder. It too is a "gain-of-function" mutation with similar effects as the somatic mutations.[25, 26]

The *PTEN* gene encodes the PTEN enzyme (or MMAC1). It is also part of Class I, but it is not a "classical" enzyme. Instead, it belongs to the VH1-like PTP subclass. PTEN specifically dephosphorylates phosphatidylinositol 3,4,5-trisphosphate on internal cell membranes.[27] In contrast to *PTPN11*, mutation of

PTEN in cancer cells results in a loss of function for the encoded enzyme. Therefore, *PTEN* is a tumor-suppressing gene when it is not mutated.[28]

Discovering mutated, deleted or over-expressed genes provides a basis to further investigate their roles in tumorigenesis or tumor suppression with genetic experiments. Genetically modified mice are used to breed mice that express either one allele or no alleles, i.e. knockout mice, of a particular gene. These studies allow investigations of positive or negative effects that a gene may have on mice, which could translate to humans. In the case of *Ptpn1* knockout mice, insulin sensitivity and a resistance to weight gain was observed when they were fed a high fat diet.[13] This led to increased interest in PTP1B, the enzyme associated with *PTPN1*, as a pharmaceutical target and resulted in further investigations into its possible role in other diseases.

A couple of studies were released in 2007 that related PTP1B to a proto-oncogene in the epidermal growth factor receptor family (EGFR) known as HER-2 (or ERBB2). HER-2 is a receptor tyrosine kinase that becomes cancerous when a point mutation occurs in the region encoding its transmembrane domain or when there is a deletion or insertion in the extracellular domain, ECD.[29] HER-2 is overexpressed in about 25% of breast cancers,[30] and overexpression of PTP1B has been associated with HER-2.[31]

The study by Bentires-Alj and Neel[32] utilized the mouse mammary tumor virus (MMTV) to promote the oncogenic form of ERBB2 with the transmembrane domain point mutation (MMTV-NeuNT). After breeding with *Ptp1b* knockout mice, less than 40% of the MMTV-NeuNT knockout mice, or

8

Ptp1b null mice, had developed tumors after ~ 3 years. In comparison, MMTV-NeuNT mice with one or both *Ptp1b* alleles developed tumors with an average latency period of ~ 13 months. Furthermore, 80–90% showed tumor onset within ~ 500 days. Finally, a separate mouse model was studied that would generate mammary cancer under the same MMTV promoter except it would be independent of HER-2. These mice, expressing polyoma middle T antigen (MMTV-P*y*MT), were crossbred with *Ptp1b* null mice. They showed no change in tumor onset when comparing the MMTV-P*y*MT mice that had one or both ptp1b alleles to the MMTV-P*y*MT *Ptp1b* null mice. In other words, *Ptp1b* is directly and specifically related to Her-2 facilitated tumorigenesis.

In the Julien[29] study, MMTV was also used, but it utilized the in-frame deletion of the extracellular segment of *Erbb2* (this mutation is also called *Neu*) when breeding with *Ptp1b* null mice. Mice expressing this altered form of *Erbb2* develop mammary tumors that frequently lead to lung metastasis lesions and mimic similar events in human breast cancers. These changes are designated as NDL2 mice. After breeding, tumor onset was delayed for ~ 35 days for the mice that had one *Ptp1b* allele or by ~ 85 days for *Ptp1b* null mice.[33] Furthermore, a decrease in lung metastasis was also noted in mice with one or zero *Ptp1b* alleles. PTP1B is generally not recognized as an oncogene (or proto-oncogene) despite its chromosomal location being amplified in some cancers. It only appears to have a complementary role that assists in the onset of some cancers. However, as a downstream signaling enzyme, targeting PTP1B to treat cancer may still be beneficial in combination therapy under the right circumstances.

In contrast to the *Ptp1b* null mice that showed obesity resistance, mice that were genetically modified to remove *Ptpn2* did not experience a beneficial phenotype. *Ptpn2* is a gene that codes for Tcptp. This is another ubiquitously expressed NRPTP, and it is very similar to PTP1B, with about 74% sequence identity in the catalytic domain (Figure 2).[34] TCPTP is a protein that is vital for hematopoiesis, immune cell development and cytokine signaling. When mice are bred with knocked out *Tcptp*, they die in 3–5 weeks.[35] However, there are two known active isoforms of TCPTP. A 45 kDa protein of TCPTP, which localizes in the nucleus, and a ~ 48 kDa protein of TCPTP, which is found mostly in the cytosol of cells, are both active.[36] It is not currently known if inhibition of one form will be tolerated. In other words, inhibiting the nucleus isoform may be detrimental if its function is unique, but inhibition of the cytosol isoform may have overlapping phosphatases that can take over. The survival information from genetic deletion experiments may be misleading since both enzyme isoforms are missing.

These two enzymes, PTP1B and TCPTP, have distinct physiological roles despite their sequence similarities based on the genetic deletion experiments. The design of inhibitors for PTP1B will necessitate testing for selectivity over TCPTP. However, there is some evidence that inhibition of TCPTP may be beneficial in limited cases.[37] Additionally, two pseudogenes of TCPTP exist that can express inactive enzymes,[19] which may somewhat reduce the selectivity requirement of a drug. If these inactive enzymes are produced and have no vital function, then their presence may act as a buffer for the vital and active TCPTP isoforms. It is certain,

however, that deleting *PTPN2* entirely, and thus not generating the required enzymes, is not tolerated.

While a variety of other potential cancer targets exist in the protein tyrosine phosphatase family, the evidence and research are still accumulating.[15] Potential PTP cancer targets and tumor suppressing PTPs continue to be investigated. However, there is a large number of protein tyrosine kinases that have been designated as arising from oncogenes.[24] Targeting of specific PTPs may complement PTK targeting and inhibition.
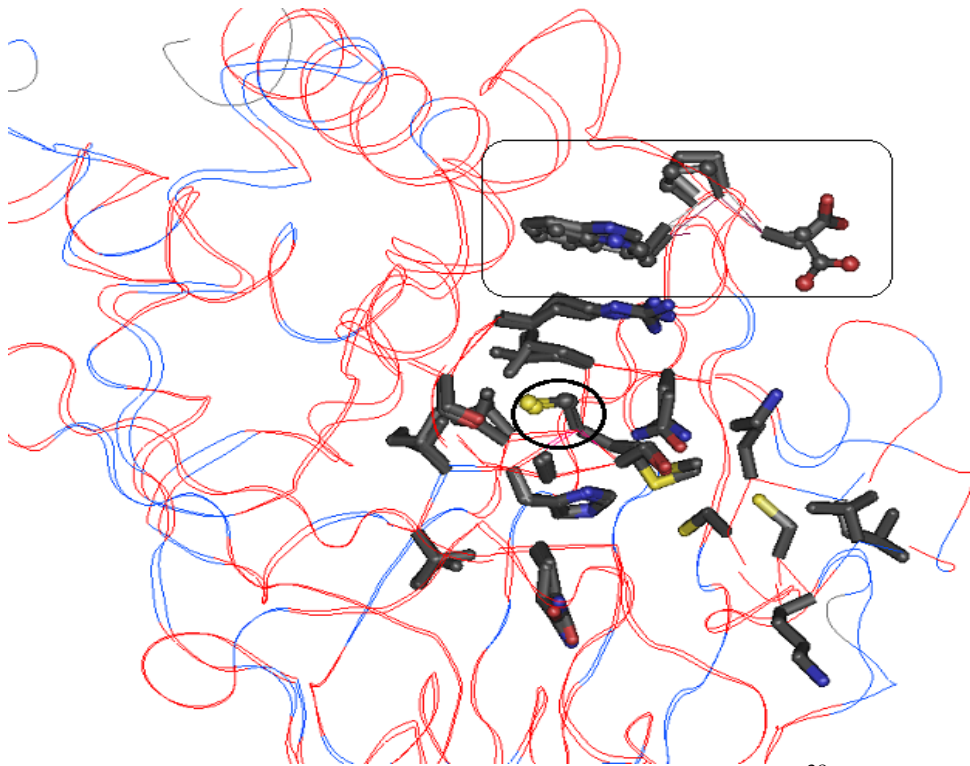
Figure 2. PTP1B and TCPTP enzymes. Acquired from VAST[38] and displayed using Cn3D.[39] PDB databank codes are in parenthesis. TCPTP (1L8K) and PTP1B (1ONZ) with WPD loops in a box (TCPTP: tubes, PTP1B: balls and sticks) and catalytic cysteines circled. Other amino acids within ~ 5 Å of the catalytic cysteines are also shown. The protein backbone is shown in red (matching amino acids) or blue (not matching) wire.

1.4 Reported Inhibitors of Protein Tyrosine Phosphatases

Because PTPs have an ionic binding pocket, developing drugs to interact within the pocket is difficult. Inhibitor interaction with the catalytic domain requires incorporation of ionic or polar functional groups, but compounds with these groups struggle to be cell permeable. Several early attempts at inhibition tried to incorporate a non-hydrolyzable phosphonate (Figure 3, DFP) to mimic tyrosine phosphates.[40, 41]
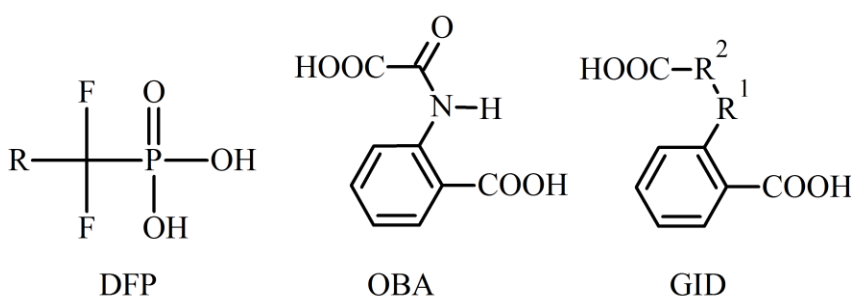
Figure 3. Reported inhibitors of PTPs and general design. Difluorophosphonate (DFP); 2-(oxalylamino)-benzoic acid; General Inhibitor Design (GID)

These inhibitor designs usually had various peptide attachments with the non-hydrolyzable difluorophosphonate (DFP) group. These were used to analyze X-ray structures for important interactions. Non-peptide structures were then synthesized after the X-ray studies and several assays. These non-peptide modifications were decent *in vitro* inhibitors, but the inhibition of the enzyme relied too heavily on the phosphonate group.

In 2000, a set of reversibly competitive inhibitors was described by researchers at Novo Nordisk.[42] These inhibitors utilized an oxalylamino group to mimic the phosphate and interact reversibly within the catalytic pocket. The initial structure used to probe the PTPs was just a benzene ring (Figure 3, OBA), but various other aromatic rings were also investigated. The *ortho*-substituted

12

carboxyl group was found to impart an important inhibitory effect, too. When these inhibitors were assayed with 7 PTPs (PTP1B, PTPβ, PTPε, PTPα, CD45, PTP-LAR and SHP1) using *para*-nitrophenyl phosphate (pNPP) as substrate, they could bind (K_i) PTPs at concentrations as low as 3.6 μM. A binding assay comparison was done between oxalylaminobenzene, i.e. *ortho*-carboxyl group absent, and 2-(oxalylamino)-benzoic acid (OBA). While OBA showed a K_i value of 23 μM against PTP1B, removal of the *o*-carboxyl group resulted in a K_i value >2000 μM under the same assay conditions. Additionally, X-ray analysis was done to compare these inhibitors to phosphotyrosine. PTPs undergo a conformational change of their WPD loop upon binding and hydrolyzing the phosphate group. The shift in the WPD loop from an "open" conformation to a "closed" conformation allows the aspartic acid (D^{181} for PTP1B) to act as a general catalyst.[43] Initially, aspartic acid donates a proton to the phosphate targeted by the catalytic cysteine. The catalytic sequence is complete upon aspartate deprotonating an occluded water molecule that is responsible for removing the phosphate from the cysteine to reconstitute the catalytic form of the enzyme (Figure 1).

Interestingly, the *o*-carboxy group of OBA was located very near (~ 2.9 Å) to the aspartic acid upon loop closure. Comparison of binding affinity at different pH values showed that OBA and its analogues bind 6–10 times better at pH 5.5 as opposed to neutral pH. This implies a potential salt bridge forming between the OBA analogues at low pH, and ionic repulsion at neutral pH. When several PTPs were assayed to find an optimum pH for catalytic activity,[44] only PTPβ had higher

turnover of pNPP at neutral pH as opposed to a pH below neutral. However, CD45 was the only PTP whose activity was found to be pH independent.

Inhibitors designed for this work attempted to utilize the *ortho*-carboxyl group in similar structures. However, the oxalylamino group that interacts reversibly and competitively is replaced in an attempt to incorporate an irreversible and competitive group (Figure 3, GID). The initial design would replace the reversibly binding oxalylamino with leaving groups. The R^1 and R^2 groups would replace the carbonyls with mono-halogenated sp^3 carbons. Additionally, R^2 would have the sp^2 halogenated product upon H-X elimination from R^2 and R^1, respectively. This would provide a halogenated Michael-acceptor for comparison to the halogenated alkyl analogue. Further design modifications from these initial tests were then going to be done by substitution on the aromatic ring and individual replacement of the two carboxyl groups shown in Figure 3 (GID) with nitro groups.
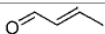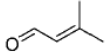
The selectivity of irreversible inhibitors is usually a greater concern compared to reversible inhibitors. Cellular nucleophiles and other macromolecules can be alkylated by irreversible inhibitors that are ambiguously active. If they are selective, however, then several issues can be overcome that reversible inhibitors face. Cellular expulsion is an issue that all inhibitors face, but a reversible inhibitor will face this issue each time it is released from its target. Furthermore, increased concentrations of a cellular substrate will influence the kinetics for binding of the reversible inhibitor. Additionally, cancerous cells that survive treatment with a reversible inhibitor could mutate to gain resistance.[45]

14

With regard to the general inhbitor design, several other inhibitors have been reported with these general structures. In fact, several precursor compounds of the planned inhibitors have been investigated in addition to similar analogues. In general, creating a reactive organic structure to bond with a PTP catalytic domain is focused on cysteine's reactivity, but investigations of these precursor compounds have found that it is not always the reactive residue.

Inhibition by acrolein was investigated against PTP1B long after it was found to react with just cysteine,[46] i.e. not in a protein. Cyclic products form upon a second reaction with another cysteine molecule. When PTP1B and acrolein are assayed together, PTP1B is inactivated. The enzyme activity is not recovered after gel filtration or dialysis to remove acrolein.[47] Kinetic data and MALDI-TOF of a trypsin digested enzyme implicate the catalytic cysteine for the site of reaction. Therefore, all evidence points to acrolein being an irreversible and competitive inhibitor. Furthermore, molecules with similar functional groups were investigated to determine the likelihood of attack at the β-carbon over the carbonyl carbon. Crotonaldehyde, acetaldehyde and several other compounds showed little to no inhibition when assayed under similar conditions (Table 1). Acrolein is a small molecule that can align with the more electrophilic beta carbon near the nucleophilic cysteine. Inhibition is noticeably reduced when bulky substituents on acrolein's beta carbon are substituted for a hydrogen. Additionally, small molecule aldehydes did not inhibit enzyme activity. This indicates a preference toward attack at the beta carbon of a conjugated carbonyl,

15

and it accounts for the reduced activity of alkyl-substituted acroleins, which will have reduced mobility inside the catalytic pocket to properly align.

Table 1. PTP1B Inhibition by Small-molecule Aldehydes

Compound	% Remaining Enzyme Activity[a]
Acrolein	4 ± 3%
Crotonaldehyde	85 ± 2%
Glyoxal	93 ± 2%
3-Methyl-2-butenal	95 ± 3%
Propanal	93 ± 4%
Acetaldehyde	> 95%

PTP1B (200 nM) with 500 µM of selected compound preincubated in assay buffer for 10 min with PTP1B enzyme. An aliquot was removed and used in an assay with pNPP as substrate (from Seiner, et al.).[47]

Compounds with unsaturated groups attached directly to an aromatic ring have been studied for their inhibition type and ability against PTPs, too. Cinnamyl aldehydes were shown to reversibly bind to the catalytic domain[48] (Figure 4). However, a guanidine group of an arginine residue, close to the catalytic cysteine, was said to be forming an enamine in preference to undergoing a thiolate reaction.
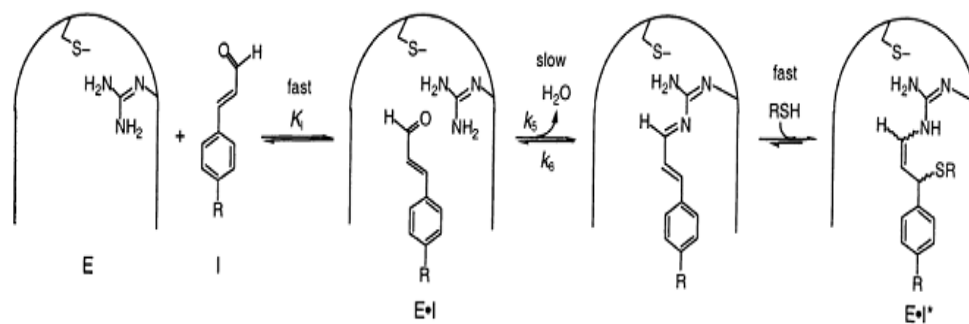
Figure 4. Proposed mechanism of inhibition of PTP1B by cinnamyl aldehyde analogue (from Fu, Park and Pei, 2002).[48]

Evidence of this formation was provided by heteronuclear single-quantum correlation spectroscopy (HSQC) with two ^{13}C labeled inhibitors on the aldehyde carbon (Figure 5, compound 14) and on the beta carbon, not shown. From Figure 5, the aldehyde proton peak and its carbon peak from compound 14 shift upfield upon addition of PTP1B. The appearance of three new peaks was believed to be from the newly generated enamine. Furthermore, a mutational study replaced the catalytic cysteine with alanine, and similar results were obtained from the HSQC experiment. Kinetic data showed these cinnamyl aldehydes to be binding slowly and reversibly as competitive inhibitors.

The cinnamic acid peptide matching the aldehyde compound was previously made by a separate group, and it was far more effective at inhibiting PTP1B, 0.079 μM[49] compared to ~ 5.42 μM[48] for the aldehyde. Detailed inhibition analysis was not described and no further published work could be found on the cinnamic acid analogue. While speculative, its inhibition may have been more favorable as a phosphate mimetic interacting with the cysteine, as opposed to reacting with guanidine.
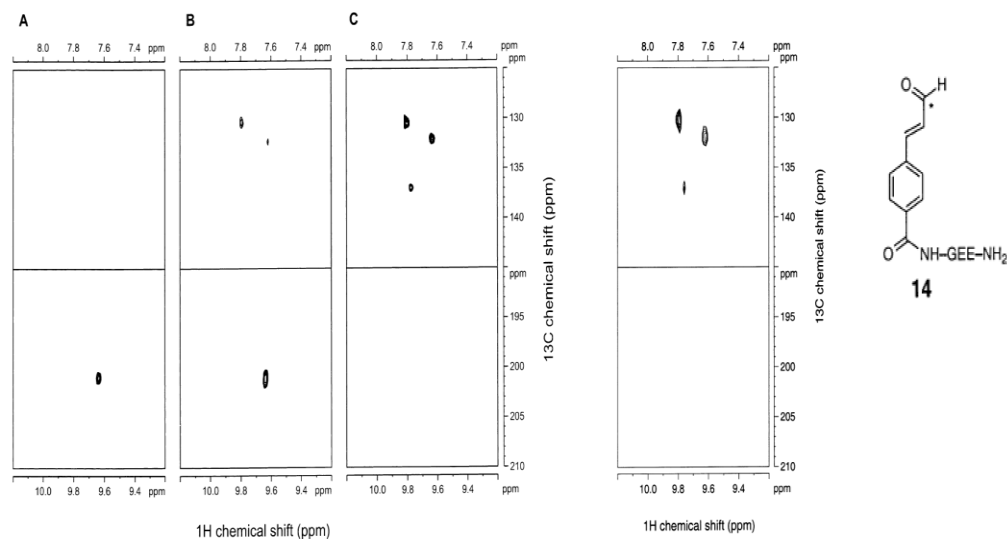
Figure 5. HSQC analysis of peptidyl cinnamaldehyde. A, compound 14 only; B, 1:1 of 14:PTP1B; C, 2:3 of 14:PTP1B. Spectra on the right, 2:5 of **14**: PTP1B mutant, C215A; Figure 5 and 6 from Fu, H. et al., 2002.[48]

Another unique example of inhibition was proposed for *trans*-β-nitrostyrene (TBNS) and its analogues by the same author that studied the cinnamyl aldehydes.[50] A nucleophilic addition reaction with the electrophilic β-carbon may be expected, but this seems not to be true. UV experiments were done to confirm the loss of its large nitroalkene peak at 320 nm with β-mercaptoethanol present. However, the same was observed when the experiment was repeated using PTP1B, although on a slower time scale. Again, HSQC experiments were performed, this time with the carbon attached to the nitro group labeled (Figure 6, compound 10). The reaction with β-mercaptoethanol has peaks moving very far upfield for both ^{1}H (~ 3 ppm shift) and ^{13}C (~ 100 ppm shift), from about δ 8 to 5 ppm and δ 145 to 45 ppm, respectively. When PTP1B is present, the HSQC upfield shifts for ^{1}H and ^{13}C are only about 1 ppm and 10–15 ppm respectively. In other words, the carbon-carbon double bond seems to remain intact when PTP1B is present, but a reaction or interaction with the inhibitor is occurring.
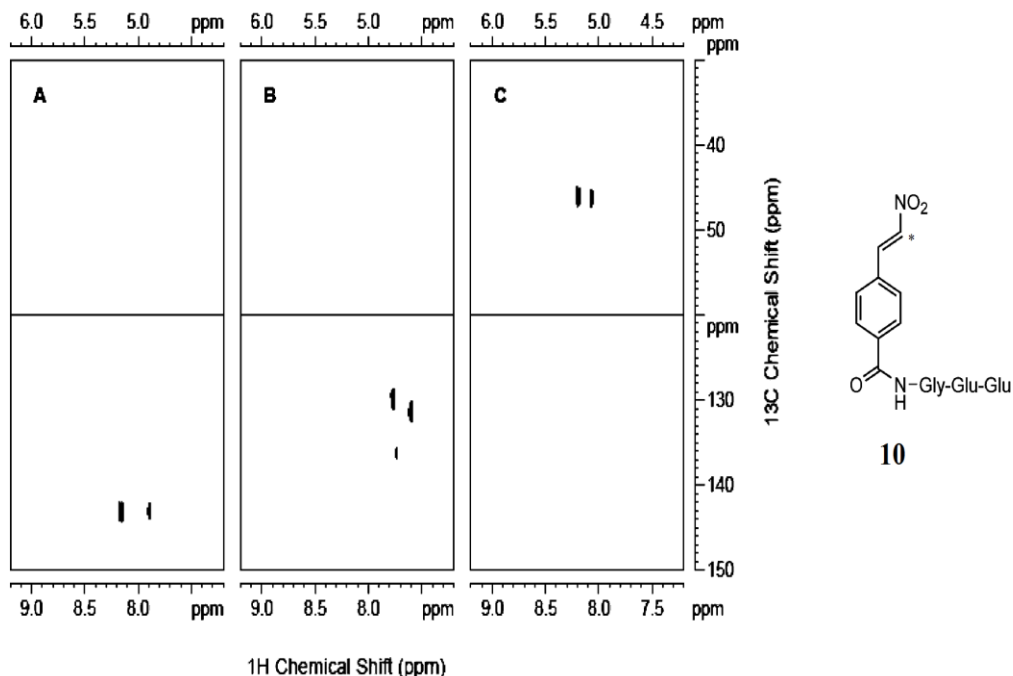
Figure 6. HSQC of peptidyl nitrostyrene. A, only compound 10; B, 1:2.4 of 10:PTP1B; C, 1:3.33 of 10:β-mercaptoethanol (from Park and Pei, 2004).[50]

Additionally, kinetic assay and mutation studies were done to verify the location of the binding at the catalytic cysteine. Mutation of C215S did not show peaks corresponding to the free inhibitor (i.e., compound 10 in Figure 6, A) or peaks indicating binding in any fashion. The authors state that ESI-MS was done on this mutant, and they found up to three TBNS additions. This led them to conclude that addition by surface residues occurred, which sufficiently scattered the NMR signal. However, a C215D mutation is known to be slightly catalytic toward pNPP. Another HSQC experiment returned similar plots as Figure 6, B; only the two peaks at about δ 7.5 ppm for ^{1}H and δ 130 ppm for ^{13}C were observed, however. This evidence led to the proposed slow-binding, reversible inhibition to the catalytic cysteine shown below (Figure 7).

19
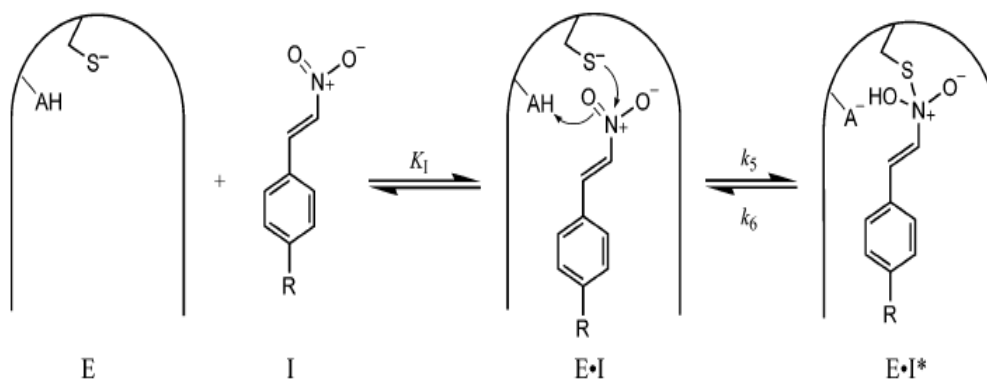
Figure 7. Proposed mechanism of inhibition for TBNS analogues (from Park and Pei, 2004).[50]

Nitrostyrene natural products and derivatives have previously generated interest as potential anti-cancer agents,[51] and they have received recent interest from drug development and marketing companies.[52] Several nitrostyrenes were designed and investigated for their ability to specifically inhibit PTPs. A mechanistic investigation for enzyme inhibition was not described, but there is evidence that these analogues may have a future as PTP inhibitors.

The inhibitor design has the potential to react with a nucleophilic cysteine thiol, which may form an episulfonium ion. While there is evidence for compounds that can create episulfonium ions intramolecularly,[53] there is only speculative evidence for this ion formation to be biologically relevant. However, a recent investigation of α-bromocyclopentenone possibly forming an episulfonium ion prior to being reactive has been reported (Scheme 2).[54] Some natural products contain this α-haloacrolyl group in their structure, and the authors were investigating a reason for their bioactivity.

A proposed mechanism was developed in which a cellular thiol reacted with the cyclopentenone, like a typical Michael acceptor. An episulfonium ion

formed upon displacement of bromide, which is followed by nucleophilic attack

by a DNA fragment. The α-bromocyclopentenone did not react with the DNA

fragment after extended pre-incubation with thiol, however. When α-

bromocyclopentenone was treated with only a DNA fragment, there was no

detectable reaction between them (by Maxam-Gilbert analysis). This and

additional evidence led the authors to conclude that the thiol is needed for

reaction. Episulfonium ion may be forming, but it is reacting immediately.

Extended incubation with the thiol is likely creating an inactive product (Scheme

2, far right structure).

Scheme 2. Proposed episulfonium ion from α-bromocyclopentenone
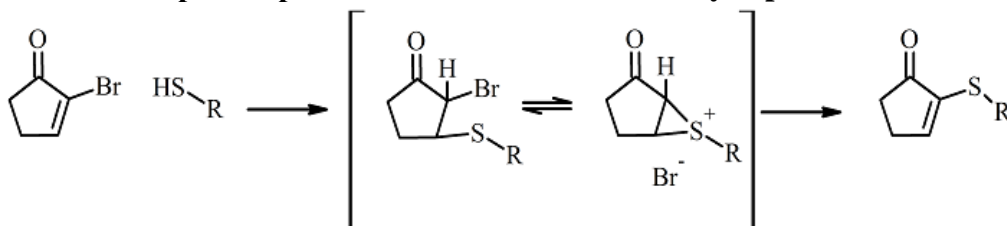
While this simple structure provides for the possibility of an episulfonium

ion forming under biological conditions, its targeting of DNA is not desirable for

the inhibitor design. Preferably, the designed inhibitors will selectively inhibit an

enzyme, like PTP, instead of damaging DNA. Most of the inhibitors to be

described either have halogenated alkyl groups or halogenated Michael-acceptor

functionality or something very similar. However, the reactivity of α-

bromocyclopentenone is just a simple example of a possible mechanism for more

complex structures. Thus, further investigations would be needed to elucidate

their inhibition toward enzymes or DNA.

2 DESIGN AND SYNTHESIS OF HALOGENATED COMPOUNDS

2.1 General Inhibitor Design

Design of the irreversible inhibitors incorporated the *o*-carboxyl group and modified the oxalylamino subsituent. The reversible binding of this group is modified to make a stable, irreversible bond with the catalytic cysteine of PTPs. Modifications of the starting material 2-carboxycinnamic acid (2-CCA) will involve adding or substituting halogens to the alkene and substitution on the aromatic ring. Occasionally, a halogenated lactone forms and lactone alkenes are also obtained from these substances. For clarity in discussing the variety of reactions with the 2-CCA analogues, a numbering scheme is provided (Figure 8) and will be referred to within the text. A similar numbering scheme will be used when describing the nitrolactones for consistency. It should be noted that the nitro group is in place of the first carbon of analogous 2-CCA compounds. However, the only relevant substitutions occur on the labeled carbons.
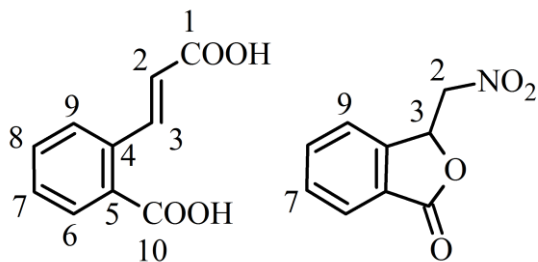
Figure 8. Numbering scheme for cinnamic and nitrolactone analogues. In the text, references to these structures will be made by simply stating relevant changes with respect to the carbon and the associated number, e.g., substitution of iodine at C7.

22

2.2 Halogen Addition to Analogues of Cinnamic Acid

Scheme 3. Synthesis of 2, 14 and 24

1, 13, 21
R = H, R^1 = COOMe (**1**)
R = H, R^1 = NO$_2$ (**13**)
R = I, R^1 = COOH (**21**)

2, 14, 24
R = H, R^1 = COOMe (**2**)
R = H, R^1 = NO$_2$ (**14**)
R = I, R^1 = COOH (**24**)
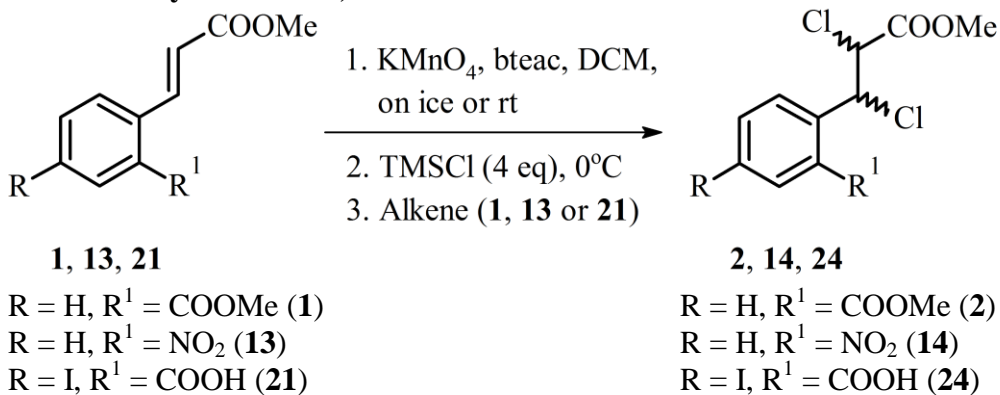
The first set of compounds was made by halogen additions to 2-carboxycinnamic acid (2-CCA). Chlorine and bromine are known to be good leaving groups in nucleophilic displacement reactions. Chlorine forms a stronger covalent bond to carbon in comparison to bromine, and that bond strength may make it a better candidate for future drugs. Problems arise for any potential inhibitors that are ambiguously active *in vivo* as opposed to active only upon entering the correct environment. In this case, the ideal reactivity would arise upon entering the catalytic-binding pocket of PTP and nowhere else.

Synthesizing the halogenated compounds without esterifying one of the acids of 2-CCA was problematic since it is not soluble in many organic solvents. The diester product **1** (Scheme 3) is soluble in organic solvents like dichloromethane (DCM). Standard methods used to add chlorine across an olefin rely on bubbling dangerous chlorine gas into an organic solution with the olefin dissolved. A new synthetic route was desirable to avoid excessive use and

exposure to this gas. Some reactions that generate radical chlorine or a small amount of chlorine gas *in situ* were attempted.

Two promising synthetic procedures failed to produce the desired addition. A hydrogen peroxide or organic peroxide solution was reported to add chlorine across an olefin when hydrochloric acid was present.[55] Another synthesis replaces the peroxide with an *N*-chloro organic reactant, Chloramine-T, to effect the same addition;[56] the conditions are similar to an Orton rearrangement. Both reactions supposedly generate a small amount of chlorine, *in situ*, that remains dissolved in the reaction solvent. No chlorine addition products were observed with 2-CCA (peroxide reaction attempted) or **1** (both reactions attempted).

A unique reaction mixture of potassium permanganate, organic chloride and trimethylsilyl chloride was the most successful reaction mixture, but it proceeds by an unknown route.[57] An oxidizing agent, potassium permanganate, is stirred in the presence of an organic ammonium chloride salt and a large amount of chlorotrimethylsilane to generate an emerald green solution capable of chlorine addition across a carbon-carbon double bond. Because DCM is used as the reaction medium, 2-CCA could not be used, as it is completely insoluble. The diester analogue **1** is soluble, and it afforded the desired addition of chlorine to the carbon-carbon double bond.

When **1** was added to the green solution, doublets appeared between δ 6.7 and 4.6 ppm in the NMR spectrum of the crude material. However, the progress of the reaction was not easy to monitor visually as the emerald green solution never seemed to fade or discharge its green color. This was reported to occur at

24

the end of some reactions, but it did not in this case.[57] A dark colored emulsion

typically formed as a lower layer, however. Thin-layer chromatography (TLC)

showed a few spots developing along with the remaining starting material at the

onset, but several spots appeared when lengthy (several hours) reaction periods

were allowed. The by-products that seemed to form were the lactone ester (**8** see

Scheme 5), possibly monochlorinated lactone ester (**11** and/or **12**, see Scheme 7),

and the diastereomer of **2**. These by-products are seen in NMR spectra of crude

material measured during the numerous syntheses, and confirmation of their

appearance is based on individual isolation in later syntheses.

The dichloro product **2** could form as 4 stereoisomers. These are from two

sets of enantiomers that would also be diastereomers of each other. Racemic

mixtures of each diastereomer form since the reaction does not have any chiral

solvents or reactants. The isolated product **2** forms as one set of doublets in the ^{1}H

NMR with $CDCl_3$ that are separated by almost 2 ppm (δ 6.62 and 4.75 ppm, $J =$

10.4 Hz). In comparison, addition of chlorine to cinnamic acid produces a set of

doublets separated by less than 0.5 ppm.[58] The doublets for **2** appeared in a 6:1

ratio, by integration, with another set of doublets near them. This less abundant

isomer (δ 6.67 and 5.12 ppm, $J = 4$ Hz) accounts for the bulk impurity.

When the carbon-carbon double bond was not adjacent to an aromatic

ring, anti addition of chlorine was said to occur exclusively.[57] In the one reported

case of a carbon-carbon double bond adjacent to an aromatic ring (*trans*-stilbene),

an equivalent mixture of anti-to-syn addition was found. One diastereomer

predominated during synthesis of **2**, but the stereochemistry, i.e. anti or syn

addition, was not determined. While **2** formed with this unique synthetic reagent, the isolated yield of pure product typically fell between 40–60%. The amount of green reagent solution was doubled and quintupled relative to **1**, but yields did not improve with the excess.

Scheme 4. Synthesis of 4 and 23

1, 20
R = H, R^1 and R^2 = Me (**1**)
R = I, R^1 = H, R^2 = Et (**20**)

4, 23
R = H, R^1 and R^2 = Me (**4**)
R = I, R^1 = H, R^2 = Et (**23**)
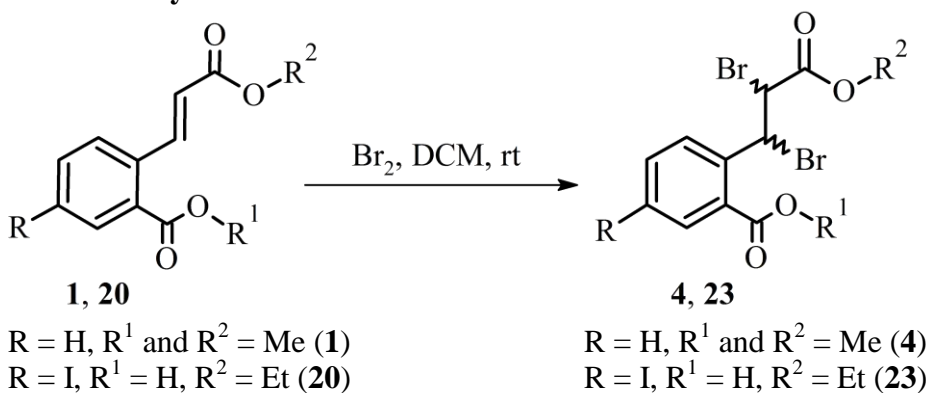
Addition of bromine to **1** in DCM produced **4**. While the diacid analogue of **4** has been reported (i.e. Scheme 4 if the product has R, R^1 and R^2 = H)[59], this diester was made for comparison purposes to **2**. Also, future substituents were going to be incorporated into the aromatic ring in the future, and a direct comparison to the unaltered ring was desired. Instead of the well-resolved doublets seen when **2** was isolated, broad peaks centered at δ 6.8 and 4.9 ppm appeared in the NMR spectrum of **4**. Elemental analysis did confirm that the bromine addition occurred, however. Side products rarely formed in these syntheses, and the product was acquired in very high yields.

Inhibitors with functionally useful carboxyl groups that are esterified are generally considered prodrugs. The esters can be hydrolyzed to their acid form by esterases *in vivo*. Then they may proceed to interact within the ionic binding-

pocket of PTPs more efficiently. Unfortunately, having only the prodrug for *in vitro* enzyme-only inhibition assays is not an ideal case as esterases are not present.

Synthetic procedures were devised to retain the phenyl carboxyl group while making an ester of the propenoate carboxyl group, C1 (Figure 8). A single ester should retain the solubility characteristics needed for synthetic transformations, and the phenyl carboxyl group was a noted feature for inhibitory activity in OBA. The *o*-carboxyl group's proximity to C3 of the propenoate chain allows for cyclization to a lactone when the compound is heated in acid. After cyclization, the free acid at C1 could be made into the ester, and the lactone could be reopened to free the *o*-carboxyl group.

Scheme 5. Synthesis of 7 followed by 8 and 9

R = Me (**8**), Et (**9**)
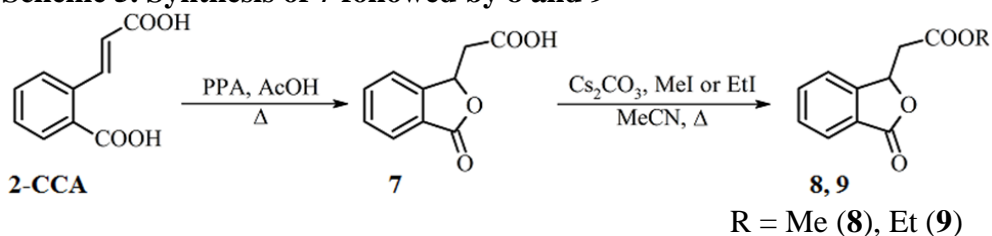
When 2-CCA was refluxed in polyphosphoric acid and acetic acid (Scheme 5), the lactone **7** formed in quantitative yield. A white solid precipitated from cold water and was collected by filtration. Esterification of the free carboxyl group proceeded in good yield as long as the cesium carbonate base was used sparingly. When using > 0.8 molar equivalents of cesium carbonate was used, the lactone would open and that resulted in the phenyl carboxylate being esterified too.

After esterification, reopening the lactone was usually done with triethylamine or DBU in suitable solvent (chloroform or DCM). Running the reaction neat with triethylamine provided the product. However, monitoring the reaction's progress by TLC was cumbersome without solvent. Some time was needed for either procedure, but typically yields were high. Also, any unreacted lactone was easily separated from product and could be reused with another procedure.

Aromatic substitution with iodine was also possible from **7**. This procedure, which is described later (see Scheme 8), provides compound **15**. Similar steps were taken to isolate the lactone ester analogues (**17** and **18**), and the subsequent alkenes (**20** and **21**) that were acquired prior to halogen addition (see Experimental).

The chlorination reaction that provided **2** was used to make **24** (see Scheme 3) after minor adjustments. Analysis of crude material from a room temperature reaction showed what may be two sets of ring closure doublets, similar to **11** and **12** (Scheme 7), that formed in a 1:1:2 ratio with the major product being **24**. The synthesis was repeated on an ice bath, which decreased lactone products and favored the desired chlorine-addition product. After purification by column chromatography and recrystallization, **24** was isolated in low yields, consistent with yields of **2** over several syntheses. Increasing the chlorinating reagents did not improve yields. In fact, doubling the chlorinating reagents at cold temperatures seemed to increase ring closure products.

Similar to the synthesis of **4**, simply adding bromine to a solution of **20** in DCM led to the previously unreported compound **23** (see Scheme 4). While the crude NMR spectrum did show signs of side products formation, they are in much smaller quantities when compared to the product. There were broad peaks in the ^{1}H NMR spectrum of **23** at δ 6.82 and 4.81 ppm instead of defined doublets, similar to what was observed with **4**. Elemental analysis confirmed that the desired product **23** formed.

A nitro group replacement of the *o*-carboxyl group, C10, was investigated with the chlorination reaction too (Scheme 3, **14**). The nitro group is isoelectronic to the carboxylate ion that is part of the oxalylamino benzoic acid, OBA. However, it is electronically neutral while still having partially charged oxygens capable of interacting with the binding pocket of enzymes. This will also allow the nitro compound to be more soluble when in aqueous solutions. While the carboxyl group does benefit similarly when in the ionic form, it is also less soluble in organic solvents needed to make necessary modifications of the structures. Esterification does alleviate this problem, but esterases are then necessary to hydrolyze these esters, *in vivo*, before the carboxylate becomes available.

Acid-catalyzed esterification of the lone carboxyl group (C1, Figure 8) provided the more soluble methyl ester **13** prior to submission to the chlorination reaction (Scheme 3). The chlorine-addition reaction was monitored by TLC, which showed starting material remaining with suspected product spots over long periods; additional spots did not appear as they did when **2** was made.

Furthermore, the emerald-green solution color did fade somewhat as the reaction progressed, along with accumulation of a brown precipitate. Addition of more TMSCl along with agitation of the reaction mixture by use of a pipet returned the solution to a greenish color. However, the reaction did not progress to completion, as judged by TLC. When a second equivalent of the chlorinating reagents was added, the reactant spot disappeared more quickly. The highest-yield procedure involved addition of 2.5 equivalents of the chlorinating reagents in portions before the starting material spot disappeared on TLC completely. ^{1}H NMR of the crude showed **14** had formed almost exclusively with a very small amount of unknown material. Unlike syntheses of **2** and **24**, this procedure yielded ~ 82% of the desired product as slightly impure crude prior to purification steps. The spots deemed to be product **14**, after separation by column chromatography, were recrystallized to yield 32% of pure product. Additional spots collected from the column were not analyzed further.

2.3 Halogenated Alkenes as Michael Acceptors

The susceptibility of an carbon-carbon double or triple bond to nucleophilic attack increases when it is conjugated to electron-withdrawing groups like carbonyls, nitro groups, cyano groups, etc. Nucleophiles favor reacting with C3 (Figure 8), the β-carbon from the withdrawing group, because electron density is removed from it via resonance. The carbon-carbon double bond of 2-CCA is already a weak Michael acceptor, but halogen addition removes the Michael acceptor functionality. Michael-acceptor molecules are known to be

30

good at forming covalent bonds and some have demonstrated an ability to react with a cysteine.[47] Reactive sulfhydryl groups of proteins have been probed by using Michael acceptors like *N*-ethylmaleimide, which forms a bond that is stable to hydrolysis.[60] Isolation of an alkene substituted with halogens could lead to novel inhibitors.

Scheme 6. Synthesis of 3 and 5

2, 4

X = Cl (**2**)
X = Br (**4**)

3, 5

X = Cl (**3**)
X = Br (**5**)
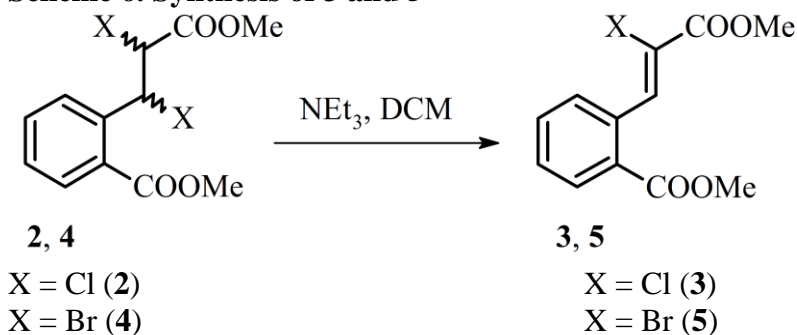
For compound **2**, there are two possible hydrogen chloride eliminations. The favored elimination involves the hydrogen on C2 and the chloride on C3 (See Figure 8). The hydrogen on C2, nearer to the carboxy ester, is more acidic and preferentially removed by basic solvent. Two unique singlet peaks are distinguishable in the NMR from olefinic protons, which are attributable to the *cis* or *trans* isomer forming. These two singlets are located at δ 8.47 and 7.80 ppm (in CDCl$_3$). The product with the singlet further downfield was the major isomer in every reaction, but the difference in the integration of the two singlets was smaller when using potassium carbonate as the base. When **2** was isolated and triethylamine used for the elimination reaction, the singlet located at δ 8.47 ppm appeared at much greater intensity. The reaction was run below 0°C and at room temperature, but both crude products' NMR spectra show nearly a 10:1 ratio of

31

the singlets at δ 8.47 to 7.80 ppm. After isolation of the major isomer **3**, X-ray

crystallography confirmed that the *Z*-alkene preferentially formed.[61]

The dibromo compound **4** was treated with base too, but unlike the

elimination seen with **2**, the dehydrobromination resulted in both *E*- and *Z*-alkene

products appearing in ratios less than 10:1. Attempts were made to isolate both

products for testing, but only **5** was isolated in sufficient purity to be cell tested,

whereas **6**, the other isomer, was only partially purified.

There are similarities when comparing **5** to **3** which leads to the

conclusion of **5** being in the Z configuration. The downfield singlet for the

olefinic proton of **5** is further downfield than the olefinic proton of **6** (δ 8.66 vs.

7.99 ppm). This is similar to **3** having the furthest downfield singlet from its

olefinic proton in comparison to the *E*-isomer. Furthermore, the two methyl ester

singlets for **3** and **5** appear almost as a doublet (about 0.015–0.019 ppm separation

vs > 0.3 ppm separation for the methyl esters of **6**) and both **3** and **5** were the low

spots on TLC.

2.4 Halogenated Lactones of Cinnamic Acid Analogues

While the chlorine-addition to alkenes was effective on both **1** and **21**

(Scheme 3), the same did not hold true when starting from **10** (Scheme 7).

Unfortunately, chlorine-addition to the alkene of **10** was not favored. NMR

analysis of crude reaction mixtures shows that the addition does not occur without

by-products forming equally or preferentially. Chlorine addition across the

carbon-carbon double bond was less favored than a single chlorine adding on the

propenoate, at C2, followed by ring closure to the lactone (Scheme 7). Overall this would be a substitution.

Scheme 7. Synthesis of diastereomers 11 and 12

1. KMnO$_4$, bteac, DCM, rt
2. TMSCl (4 eq), 0°C
3. Alkene, 0°C to RT

10

11, 12

11: (R^*, R^*), **12**: (R^*, S^*)
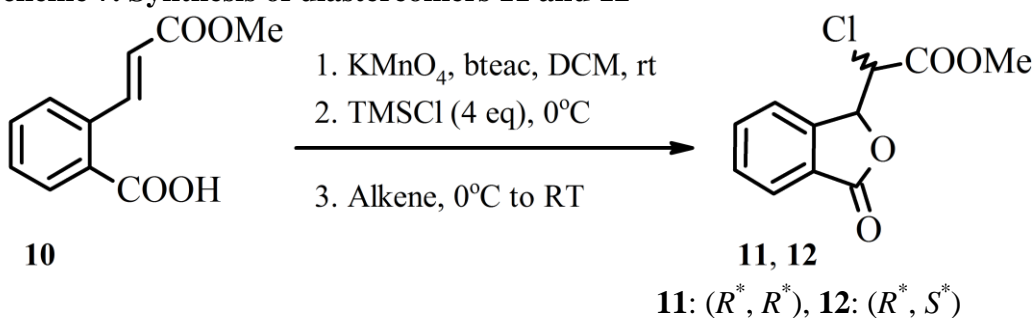
   This reaction was run similarly to the previous synthesis for **2**. The NMR of a crude reaction mixture after 1 hour showed evidence of 4 recognizable products, as follows: diastereomers **11** and **12**, the desired chlorine-olefin addition product and compound **8** (see Scheme 5). The small amount of compound **8** observed in the NMR spectrum may have already been present in the starting material and not generated from the reaction conditions. The formation of **11** and **12** causes the carboxylic acid proton to be lost to solution, making it available to generate **8**.

   Unfortunately, the crude masses acquired from these syntheses were substantially smaller than the starting material mass despite products forming with an added chlorine. Cold temperature reactions were utilized to investigate if chlorine-addition products to the alkene would increase; if chlorine addition precedes the formation of **11** and **12**, then it may be kinetically favored. A ^{1}H NMR spectrum of the cold reaction's crude material showed the suspected chloro lactone formed in either the same amount as the dichloro addition or in greater

amounts. The crude mass was still lower than the starting alkene's mass under colder conditions, too.

Complete separation of the two chloro lactone diastereomers **11** and **12** from one synthetic procedure was accomplished. Yield of each diastereomer was only 17% and 10% of the theoretical yield when calculations are based on their formation instead of the dichloro product. The doublets for the chloro lactones are usually closer together with a smaller coupling constant when compared to the non-lactone analogues, i.e. **2** and **24** (Figure 9). Additional confirmation by IR spectroscopy showed no evidence of a carboxylic acid. A fairly broad carbonyl peak centered at 1763 cm^{-1} is at a slightly higher energy because of the ring strain.
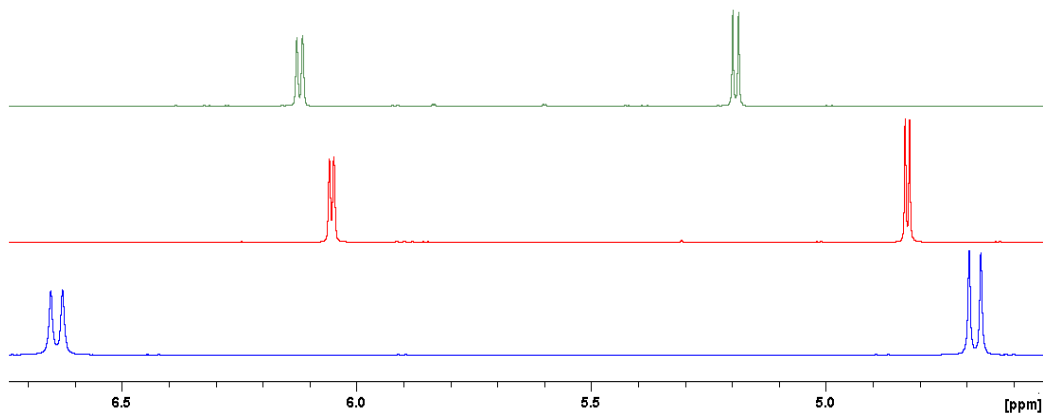
Figure 9. Doublets for chloro lactones, **11** and **12**, shown with **24** for comparison. Expanded on the region δ 6.7 to 4.0 ppm (top to bottom: **11**, **12** and **24**).

Because a mechanism for this green-colored, chlorination reaction has not been thoroughly investigated, chlorine addition across the carbon-carbon double bond prior to lactone ring formation cannot be ruled out. The carboxyl group (C10) is not expected to be a good nucleophile, at least not enough to displace a chloride. An initial addition of a single chlorine atom to the carbon-carbon double

34

bond may result in a resonance-stabilized benzyl cation intermediate (a chloronium intermediate is not expected). Competition between a second chloride attack or lactone ring formation at C3 would then occur, with the latter leading to the products seen in NMR analysis of crude material (Figure 9).

Substitution of a hydrogen by an iodine on the aromatic ring was first attempted with 2-CCA as the starting material. Because electrophilic iodine is created in the reacting solution, it would be expected to react with the carbon-carbon double bond, too. While 2-CCA was not soluble in organic solvents for chlorine and bromine reactions, it is soluble in the concentrated sulfuric acid solution used to generate the iodine electrophile. However, the reactivity of 2-CCA seemed greatly reduced in comparison to the reported compounds,[62] but one unique product was isolated that made this reagent worth further pursuit. A very small yield of one product had iodine substitution on the aromatic ring, in the desired *para* position, or C7 in Figure 8. Iodine was also added to the carbon-carbon double bond with subsequent ring closure as an overall substitution, similar to **11** and **12**. This is also similar to the polyphosphoric acid assisted reaction to form **7** (see Scheme 5), with electrophilic iodine instead of a Brønsted acid.

Unfortunately, the crude material resulting from 2-CCA reaction with the electrophilic-iodine reagent is insoluble in organic solvents making it difficult to analyze and separate. The entire reaction mixture was subjected to the esterification conditions used to make **1**, i.e., acetyl chloride in methanol to

35

generate HCl *in situ*, which allowed for easier separation and identification of the product, **26** (Scheme 9).

More careful procedures were devised to individually isolate the variety of products from this electrophilic iodine substitution reaction. Starting from **7** removes the double bond that competes with the aromatic ring for substitution. The acidic reaction mixture that creates the electrophilic iodine has a simple workup ("green") that involves dilution with water and filtration of the organic product that precipitates. The desired product **15** did precipitate but only in 30–50% of the theoretical yield (Scheme 8). On one occasion, excess reagent was made for the reaction that usually contained 110% total moles of I^+ coming from iodine and sodium iodate.[62] The amended procedure used 140% excess of I^+ in this example, and it yielded 61% of **15** upon purification. Extraction of the aqueous filtrate with organic solvent typically yielded another 30% of material in which the iodine was substituted in either the *para* or *ortho* position (C7 and C9, Figure 8) of the ring, along with a small amount of starting material, **7**. The *ortho*-substituted isomer was isolated, albeit in fairly low yields (see Experimental, **16**).

Scheme 8. Synthesis of 15
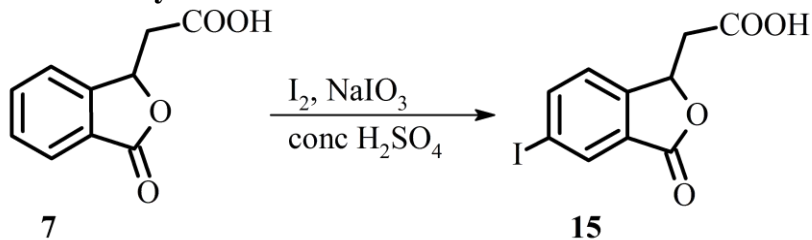
An attempt to force the equilibrium to favor products was also made by adjustment of the conditions and periodic analysis of reaction mixture aliquots by ^{1}H NMR. Regardless of the addition of more electrophilic-iodine reagent or gentle heating over several hours, starting material peaks always appeared in the spectrum from the seven aliquots, which were taken at various times during the reaction. While the peaks associated with compound **7** decreased with added reagent and heating, the reaction also became much darker black. In summary, a ^{1}H NMR of an aliquot showed ~ 20% of compound **7** present after the reaction was allowed to stir overnight. There was still between 14–17% of compound **7** present with excess reagent added. Heating the solution did not seem to reduce the amount of **7** any further, and it may have been causing the reactant, products or iodine reagent to decompose.

From **15**, the ethyl (**17**) and methyl ester (**18**) were made, similarly to what is shown in Scheme 5. Bulky amine bases were used to open the lactone and reform the alkene (ethyl ester **20** or methyl ester **21**) prior to making the dichloro and dibromo products, **23** and **24** respectively (see Schemes 3 and 4). However, treating the alkene (**20** or **21**) with the electrophilic-iodine reagent provided **26** (Scheme 9 with R = I).

Scheme 9. Synthesis of 25 and 26

R = H (**25**), I (**26**)

37
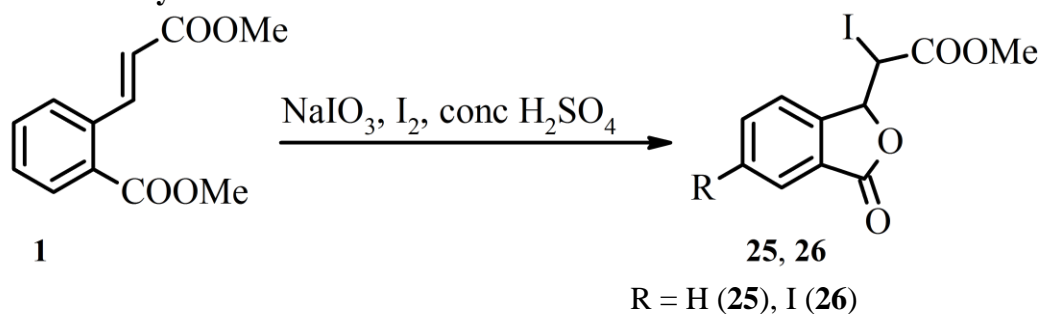
When treating **1** with the electrophilic-iodine reagent, **25** formed almost exclusively with very little aromatic iodine substitution (Scheme 9). The aryl ester is cleaved by the electrophilic-iodine reagent (C10 in Figure 8) to help form the lactone. Regardless of the amount of electrophilic-iodine reagent used, little to no aromatic iodine substitution occurred. Compound **1** was used in place of 2-CCA because working with the crude mixtures from the 2-CCA syntheses was problematic, and the crude products were typically esterified anyway to allow for easier separations.

Except for a few instances in which the molar equivalents of electrophilic-iodine reagent were increased, the reaction conditions were not varied greatly in an attempt to force a second substitution and acquire **26**. Heat and extended reaction times did not improve aromatic substitution when **15** was being synthesized, and the same result would be expected for **25** after it is formed *in situ* from **1** and the electrophilic-iodine reagent. Another route to the formation of **26** was found by simply resubmitting the recovered crude, i.e. mostly **25** and other aryl-iodo isomers, to fresh electrophilic-iodine reagent. Because of the ease of workup and good yields post-synthesis of **1** and **25**, this was the most used method to isolate **26** (see Experimental).

2.5 Lactone Alkenes of Cinnamic Acid Analogues

Scheme 10. Synthesis of 27, 28 and 29

25, 26	**27, 28, 29**
R = H (**25**)	R = H (**27**, *Z*; **28**, *E*)
R = I (**26**)	R = I (**29**, *E*; **30**, *Z*)
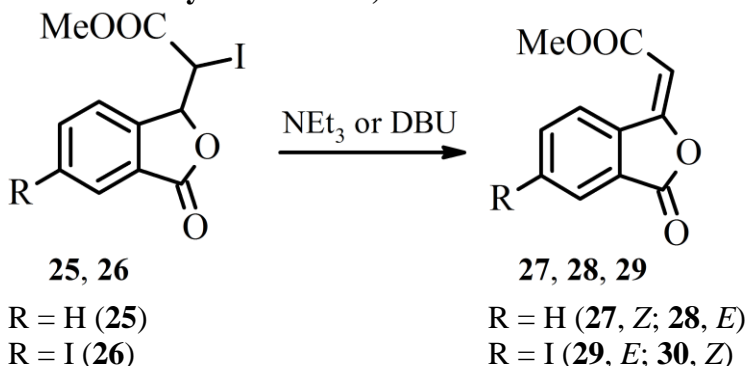
Because compound **25** could be recovered in high yields, it was tested first with bases under varying conditions to open the lactone to generate a halogenated Michael acceptor. If the lactone ring opened, a singlet peak was expected to appear in the aromatic region, similar to **3**. Furthermore, the doublet peaks seen in the ^{1}H NMR for **25** would disappear. Iodine's large size imparts a long bond length with carbon and allows it to stabilize the anionic iodide after bond breaking. This makes it a good leaving group. Therefore, dehydroiodination to form the lactone-alkene products, depicted in Scheme 10, was undesired but expected as a possibility as this same issue was encountered with a similar bromo lactone.[59]

Sodium methoxide in methanol and triethylamine in dichloromethane were tried first. Sodium methoxide is a small base that can deprotonate **25** if the large iodine and carbomethoxy crowded the hydrogen on C2. Triethylamine was used as a bulky base if the steric crowding was irrelevant. While both reactions were monitored by TLC until apparent completion, the sodium methoxide attempt

was still incomplete by NMR. It appears as though the doublets of **25** are present along with a new set of doublets right next to them. The doublets of **25** are at δ 5.65 and 4.78 ppm, and the new doublets are at δ 5.69 and 4.64 ppm. Methoxide was either reacting with **25** by substitution, S_N2, and replacing iodine with methoxy, or the alpha proton was being abstracted and replaced to form the previously unseen diastereomer of **25**. A peak for methoxy could not be confirmed as being present in NMR spectra of crude material, however. While only one product formed during the attempts to synthesize **25** (Scheme 9), another isomer is feasible. It is possible that only one diastereomer is favored after work up of the electrophilic-iodine reaction. Treating **25** with a small base allows for the other product to appear because reversible deprotonation does not favor one isomer.

There are small singlet peaks present in the spectrum, but one in particular is found around δ 8.56 ppm. This peak is very small, but it could be from the lactone ring opening to provide an iodine-substituted Michael acceptor product that was not isolated, i.e. elimination of the C2 hydrogen with subsequent lactone opening (similar to **3** and **5**). Between this singlet and the doublets for the starting material, **25** may be more stable or forming upon workup with acidic solutions. The singlet is less than 8% of the area of the smaller doublet arising from protons on C2 or C3 of **25** and its suspected diastereomer.

When triethylamine was used prior to distillation and being dried, the reaction mixture was allowed to stir overnight because TLC monitoring seemed to show no reaction occurring after a few hours. Only one spot appeared on TLC the

next day, but this time it was at lower R_f than the spot for **25**. Purification of the

crude material by column chromatography was followed by NMR examination of

the material of the corresponding spot, which was later purified and identified as

27 (*Z*-alkene). A smaller set of peaks appeared with the column-collected

material, too. Three peaks that integrate equivalently are as follows: a broad

peak/singlet located at δ 6.54 ppm, along with nearly equivalent doublets at δ 3.20

and 2.88 ppm ($J = 16$ Hz); the magnitude of the coupling constant points to these

signals arising from geminal protons. A large singlet that integrates as 3 protons is

also located at δ 3.82 ppm. A hypothesis is that this product could be a result of

hydroxide attack on C3 of **27** followed by proton transfer to the C2. The alcohol

either remains or forms a ketone (Figure 10), thereby opening the lactone. This

compound was collected by column chromatography in slightly pure form as the

material that came out right after **27**.

The TLC spot for **25** had a similar R_f as the *E*-alkene **28**. The *E*-alkene

may have been appearing immediately with appearance of the *Z*-alkene over time,

i.e. equilibration. NMR analysis of the reaction mixture was not done at the onset

because analysis of a previous sodium methoxide reaction showed the reaction

was incomplete. Hence, longer reaction times were thought to be needed, which

probably allowed for additional by-products to form.

Because **26** was more difficult to make and purify, fewer eliminations

were attempted with it. Distilled and dried triethylamine was used neat at room

temperature and with slight heating. Additionally, ethyl acetate was used once as

a reaction solvent with the thought that any lactone-opened product would be

insoluble in it and precipitate out of solution. Cesium carbonate in acetonitrile was used one time as well. Regardless, the desired lactone-opening reaction did not occur. Similar to **25**, reactions with compound **26** showed singlets appearing around δ 6 ppm (for **29** and the Z-isomer, **30**) along with several other peaks, indicating many side reactions.

One by-product was isolated, after use of cesium carbonate, that had the expected aromatic and methyl ester peaks for **26** without a singlet peak around δ 6 ppm due to the olefinic proton. Instead, two equivalent doublets located at δ 2.86 and 3.15 ppm appeared ($J = 16.4$ Hz for both). This is similar to the by-product of **25** except there is not an easily distinguishable broad peak near δ 6.5 ppm, expected for the alcohol proton (Figure 10). Regardless, these doublets are expected to be arising from two hydrogens located between the newly formed aromatic ketone and the terminal methyl ester (Figure 10) with either a hydroxyl attached at C3 or possibly iodide reattaching instead of hydroxide (not shown).
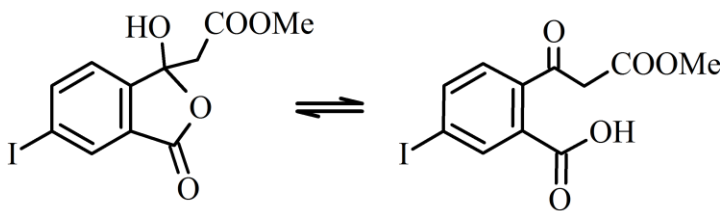
Figure 10. Possible by-products from elimination reactions with **26**.Tautomers are shown after HI elimination. The one on the right may be favored when C7 has an iodine, thereby extinguishing a broad alcohol peak at δ 6.5 ppm. The left may be favored when the iodine on C7 is replaced by hydrogen.

Although HI elimination resulted in a few products that were later cell tested, the elimination reactions were inefficient. More efficient synthesis of **27** and **28** have been described without requiring an iodo lactone.[63, 64, 65] The reaction

starting from **26** produces **29**, which is a novel compound, but the reaction

conditions were adjusted to push the reaction toward lactone opening. This

ultimately caused reduced yields. More careful control would be needed for a

future synthesis to prevent side reactions with **29** and its isomer. Unfortunately,

the Z-isomer (see Experimental, **30**) was not sufficiently purified to be cell tested

when the other compounds were submitted. A more suitable synthesis would

likely need to be devised for these compounds if additional transformations are

planned.

2.6 Synthesis of 3-Nitromethylphthalide Precursors

The last set of compounds synthesized replaced the carboxylic acid on the

alkyl chain with the isoelectronic nitro group. Nitro groups are also very strong

electron-withdrawing groups, which will make alpha hydrogens more acidic. This

is important because, in neutral and acidic solutions, the 3-nitromethylphthalide

(Scheme 11) prefers to cyclize into the five-membered lactone.[66, 67]

Scheme 11. Synthesis of 31

2-FA
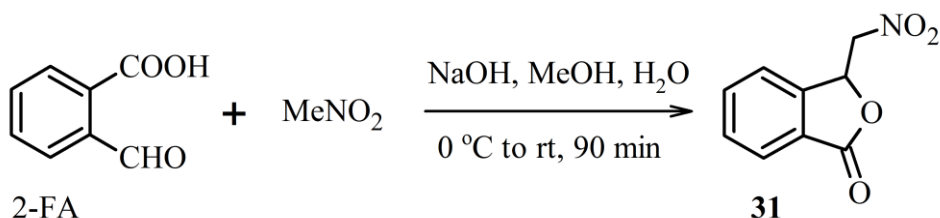
These reports corrected an assumption by Hashimoto, et al. (1960) that

provided for the possibility of acquiring an isomer of **31** that is in the open, or

non-lactone form.[68] While 2-CCA could be isolated as its lactone and readily

returned to the non-lactone, the nitrostyrene analogue will remain in the lactonized form unless it is in an alkaline solution. If *in vivo* conditions are neutral or acidic, then the reactive, Michael-acceptor olefin will essentially be hidden and thus unavailable to react with nucleophiles in unwanted side reactions.

Obtaining the lactone starting material, **31**, was planned as the first step with halogen substitution alpha to the nitro group (Figure 8, C2). The synthesis of these inhibitors utilized a Henry reaction with 2-formylbenzoic acid (2-FA) and nitromethane. This reaction is very similar to an aldol reaction in which a proton attached to the same carbon with an electron-withdrawing group is removed by base; the resulting carbanion reacts with the carbonyl carbon of an aldehyde. 2-FA has been investigated in a variety of reactions for its ability to react in fairly mild conditions.[69, 70] By starting from 2-FA and nitromethane, **31** forms readily and is isolated in high yields from an alkaline solution of aqueous alcohol.

Scheme 12. Synthesis of 32
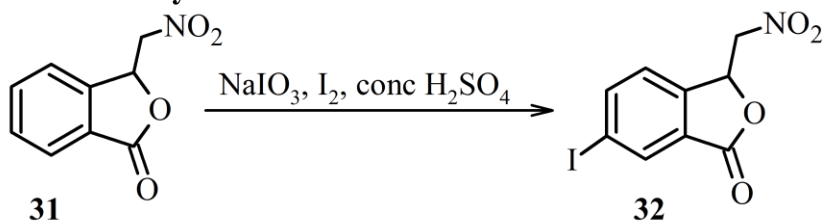
Substitution of the aromatic ring with iodine was also desired for this structure in order to make future analogues easier to substitute on the aromatic ring. Substitution of iodine starting from 2-FA was attempted but not very useful. Adding it to an iodinating solution resulted in the recovery of 2-FA along with many products that formed in small amounts. Ring closure of 2-FA in acetic acid

provided the acetate protected lactol,[69] which was subjected to the electrophilic-iodine reagent. Unfortunately, the acetate was removed *in situ*, and it provided many products along with 2-FA. The two dibrominated nitrolactones products, **33** and **35**, which are described later, were also individually subjected to the iodinating solution with minimal isolation of any iodoaryl products.

The procedure used to acquire acceptable yields of C7 (Figure 8) iodine substitution required addition of **31** to the electrophilic-iodine reagent (Scheme 12). Recovery of the desired C7 iodine product from solution was possible despite C9 substitution and formation of other minor products. All crude products also contained the reactant, **31**. A good amount of the C7-substituted product was obtained by precipitation when chlorinated solvent was added to the crude reaction product; it did co-precipitate with **31**, however. Both **31** and **32** spots do not separate greatly on TLC, and they could not be separated very easily with just column chromatography. Recrystallization from chloroform and hexanes or ethyl acetate and hexanes, however, effectively separated the iodide-substituted product.

2.7 Synthesis of Dibrominated Nitro Lactones

No suitable references were found that specified how to individually substitute a hydrogen alpha to a nitro group except under special or extreme conditions. Some methods require the organic nitro compound to be soluble in one equivalent of an alkaline solution while cold, typically –20 to 0 ºC.[71,72] This requires the organic compound to be soluble in a small or reasonably small

amount of the alkaline solution, which is not the case for **31**. Furthermore, some

literature techniques, e.g., Wohl-Ziegler reaction, that were used successfully to

monobrominate alpha to a carbonyl group did not work with the nitro group.[73, 74]

Regardless, dibromo substitution of the nitrolactone on C2 (Figure 8) was

relatively simple by use of a biphasic reaction mixture and bromine (Scheme 13).

This procedure did take 2 or more days to complete in good yields, however. It

was thought that **31** initially dissolved in DCM and would deprotonate to open the

lactone ring in slightly alkaline aqueous solution; the ionic intermediate would

preferentially dissolve in the aqueous solution. If an electrophile is present, such

as bromine, then the reversible ring closure would result in competitive reaction

between proton and bromine. After two bromine atoms attach to C2 however, the

new product would remain in the organic phase. While bromine is very soluble in

DCM, it is somewhat soluble in aqueous solution, too.

Scheme 13. Synthesis of 33
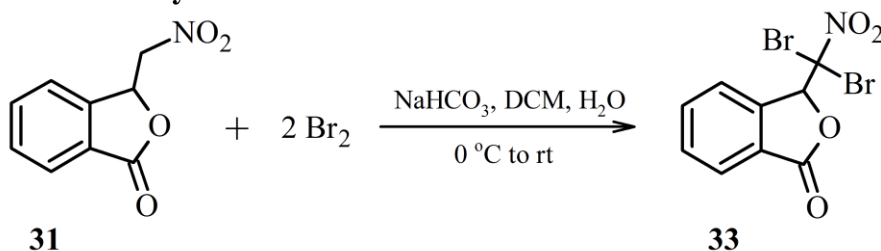
The reaction mixture was monitored by TLC, and it showed a minor spot

had appeared between those of **31** and **33**, when only one molar equivalent of

bromine was present. This implied that the intermediate product, i.e. a single

substitution of bromine at C2, favored reaction with bromine a second time, over

monobromination of **31**. In other words, the initial bromination is likely to be the rate-limiting step.

The biphasic reaction used to make **33** was not effective when **32** was the starting material. Also, it did not dissolve in DCM to the same extent as **31**. When the reaction was allowed to stir over long periods, it did appear to dissolve, but very low yields of **34** were isolated. Several organic bases (including pyridine, triethylamine and 2,6-lutidine) were used exclusively in organic solvents instead of biphasic reaction mixtures. Along with NBS and $Br_2(l)$, another brominating agent, pyridinium bromide perbromide (pBpB), was used as the source of bromine.[75] A reaction system with **32** and 2 equivalents each of pBpB and 2,6-lutidine in THF resulted in high yields of **34** (Scheme 14).

Scheme 14. Synthesis of 34
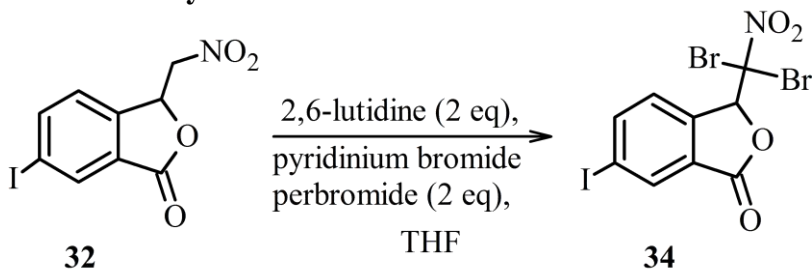
When only one equivalent of each reactant was added, the reaction was incomplete, as **32** and **34** were mainly recovered, i.e. single bromine substitution on C2 was also not favored in this system. Typically, one equivalent of base and pBpB were allowed to react until the reaction solution's red color had faded. At this point, the second equivalent of each was added. This same system was used on **31** to form **33** as well.

2.8 Synthesis of Monobrominated Nitro Lactones

Scheme 15. Synthesis of 35

33

35
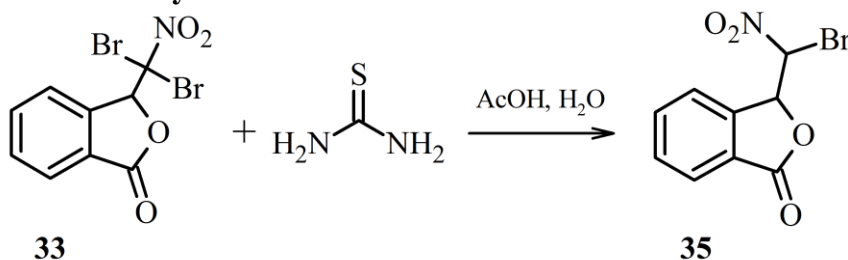
Because **33** was easy to make and isolate in the biphasic reaction, this product was acquired, and a synthesis to replace a single bromine with hydrogen was attempted. A couple of methods were found that could replace one of the bromines with hydrogen from readily available reagents. One method could not be tested sufficiently, though, as the lab reagent stannous chloride dihydrate was not sufficiently pure.[76] However, a reactant with very similar functional groups and characteristics as **33** had been found to be reduced with thiourea in an aqueous acetic acid solution.[77] When **33** was subjected to the same procedure (Scheme 15), a precipitate formed during the course of the reaction in very high yield and in large excess of one diastereomer.

For this reaction, **33** was first dissolved in acetic acid, and thiourea was separately dissolved in the same volume of water. The aqueous thiourea had to be slowly added to cause the desired precipitation in which one diastereomer formed and precipitated substantially from the solution. If the aqueous solution was added

in one portion, immediate formation of a precipitate resulted, as a lightly yellow colored solid, but it rapidly redissolved into solution. It is not known if this initial precipitate was **33** crashing out of the reaction mixture, or the desired product. However, precipitate formed after the solution was stirred for a few minutes, but the solid was darker yellow than the pale yellow solid obtained with slow addition of aqueous thiourea. Furthermore, this solid contained a larger proportion of **36**, the diastereomer of **35**, as evidenced by the increased intensity of doublets coupled with $J = 7.5$ Hz (Figure 13).

The TLC spot of **35** appeared at lower R_f than **33**, and another spot appeared at lower R_f still when excess thiourea was used (DCM developing solvent). The lowest spot appeared because of a double replacement of bromine with hydrogen to form **31**. The precipitated solid product was preferentially purified, in good yields, by immediate recrystallization from ethyl acetate and hexanes. The hydrogen on C2 is too labile when silica gel chromatography was attempted, and **35** could not be separated from **36**. The diastereomers **35** and **36** were recovered as a mixture in nearly equal quantities because of reversible deprotonation while moving through the column.

Scheme 16. Synthesis of 37
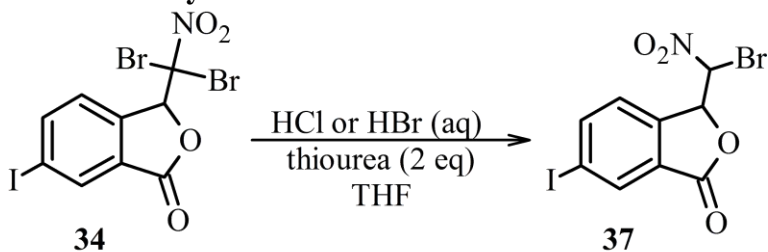
A small amount of the isolated **34** was briefly subjected to the same conditions described in Scheme 15. Unfortunately, **34** is only slightly soluble in acetic acid. The reaction was still attempted with what was soluble, however. Initially, the reaction seemed to proceed as expected, with some precipitate developing, but more precipitate formed that was orange to orange-red in color over time. Dissolving this precipitate after filtration was nearly impossible. A silica gel column was run to help separate any useful compounds from the insoluble orange-red material. However, **34** was recovered from the column, and very little of anything else. Small amounts of orange-red precipitate would form periodically from the original reaction filtrate (aqueous and acetic acid solution) left to stand. The orange-red precipitate was insoluble in many organic solvents. This material may be polymeric, but it is not clear how.

A change in solvent system was tried (Experimental, Table 8) from what had worked with **33**. While acetic acid was used in a few trials, it was replaced with another organic solvent that could completely dissolve **34**. An aqueous acid was used to replace the organic acid, too. Tetrahydrofuran (THF) was used since it is miscible with water, and **34** is soluble in it. Aqueous hydrochloric acid was also chosen as the acid replacement in most tests. Interestingly, initial tests revealed an incomplete reaction by TLC when only one equivalent of thiourea was used. Reactions with **33** showed evidence for replacement of both bromines when excess thiourea was used, and the referenced paper reports a similar double replacement with two equivalents of thiourea.[77] Thus, two equivalents of thiourea had to be used to effect the desired hydrogen substitution of a single bromine.

Slightly more than two thiourea equivalents did not cause two bromines to be replaced to any noticeable extent either, by TLC. This reaction system was varied to the point in which one diastereomer was slightly favored, but multiple recrystallizations were required to completely isolate **37** from its diastereomer.

2.9 Henry Reaction with Bromonitromethane and 2-Formylbenzoic acid

Scheme 17. Synthesis of Crude 36 by the Henry Reaction
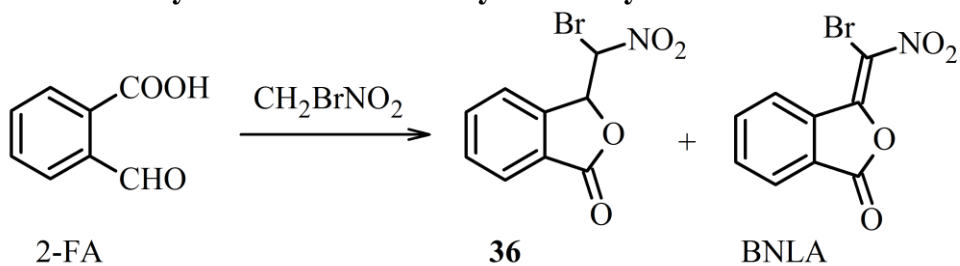
A separate Henry reaction was attempted with bromonitromethane. Nitromethane could be brominated once to bromonitromethane in high yields if done carefully and quickly.[71] As mentioned earlier, addition a single bromine alpha to a nitro group is possible and has been documented in cases of aqueous-soluble organics. The cited patent procedure was found to be very effective.[72] The desired bromonitromethane accounted for more than 80% of the product by ^{1}H NMR, with nitromethane and dibromonitromethane accounting for the rest in decreasing amounts (Experimental, Table 9). Distillation was only attempted one time to further purify the material, but the high boiling point and small amounts prepared resulted in low recovery with limited increase in purity (by NMR).

The Henry reaction with bromonitromethane utilized a procedure similar to one found in a patent too.[78] Methylamine and sodium carbonate were used in 0.1 equivalents to an aldehyde on a furan ring in the patented procedure.

However, one equivalent of sodium bicarbonate was included in the following procedure, unlike the patent. The first reaction in which this slightly amended procedure was employed led to recovery of a precipitate containing 2 products in ~ 1:6 ratio and a 42% yield based on formation of **35** or its isomer. The minor product, however, only showed peaks in the aromatic region of the ^{1}H NMR (Figure 11).
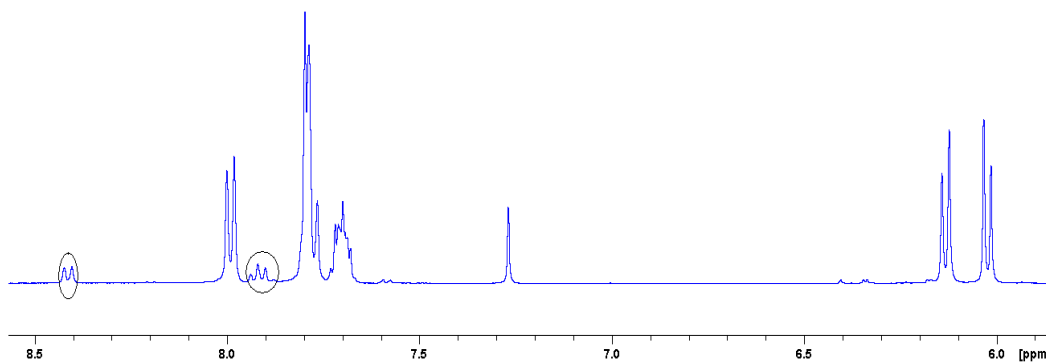
Figure 11. First Henry reaction with 2-FA and bromonitromethane. Impurity peaks are circled. Other peaks are from compound **36** with the doublet peaks, on the right, $J = 7.5$ Hz.

One of its most noticeable peaks is a doublet near δ 8.4 ppm, while a triplet also appears around δ 7.9 ppm. Other peaks for the minor product are expected to be in the aromatic region, but they are being overlapped by the major product **36**. The doublets around δ 6.0 and 6.1 ppm ($J = 7.5$ Hz for both) are attributed to the desired bromo lactone product **36**.

The unknown minor product, which has the furthest downfield doublet, could be from the reaction involving 2-FA and the small amount of dibromonitromethane present in the prepared bromonitromethane liquid (Figure

52

12). Formation of **33** is probably not the favored pathway to the boxed product, but a tiny peak in the above crude spectrum at δ 6.4 ppm may be a singlet. This is the typical location of the only non-aromatic hydrogen of **33**.
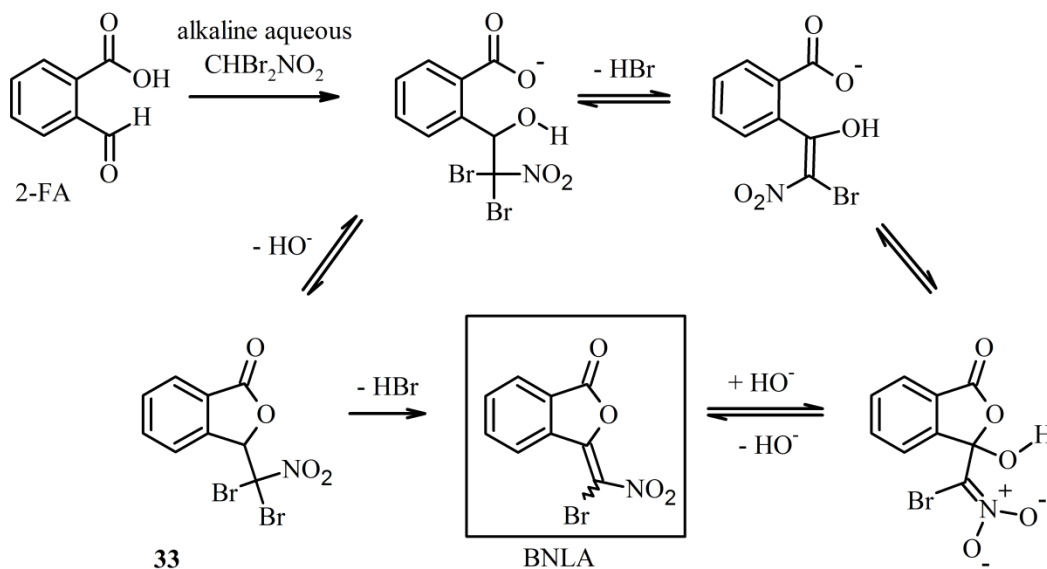
Figure 12. Possible pathway to unknown product, BNLA, the product proposed to be responsible for the doublet at δ 8.4 ppm appearing in Figure 11.

The major product in this precipitate had essentially only one set of doublets between δ 6.2 to 6.0 ppm ($J = 7.5$ Hz). Synthesis of **35**, from **33** and thiourea, also favored one product with a specific set of coupled doublets ($J = 3.6$ Hz, Figure 13). However, the diastereomer of **35** formed more favorably under the Henry reaction conditions based on the coupling of the doublets (Figure 13).
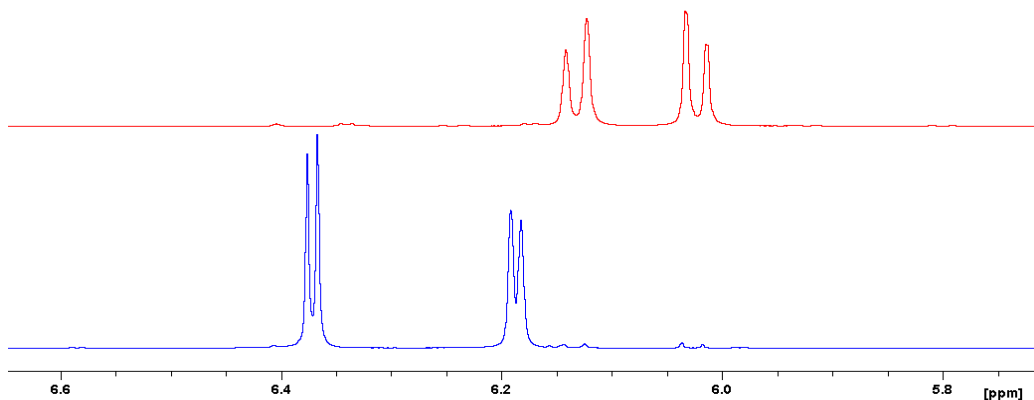
Figure 13. Comparison of doublets for **35** and its diastereomer **36**. ^{1}H NMR of doublets for **35** (bottom) and **36** (top), expanded on δ 6.7 to 5.7 ppm.

The low yield from this and subsequent reactions is probably from the reaction of water with intermediate products or with the minor product that was boxed in Figure 11. Additional discussion about this possible product and transformations can be found in Chapter 3.7 (see Figure 43).
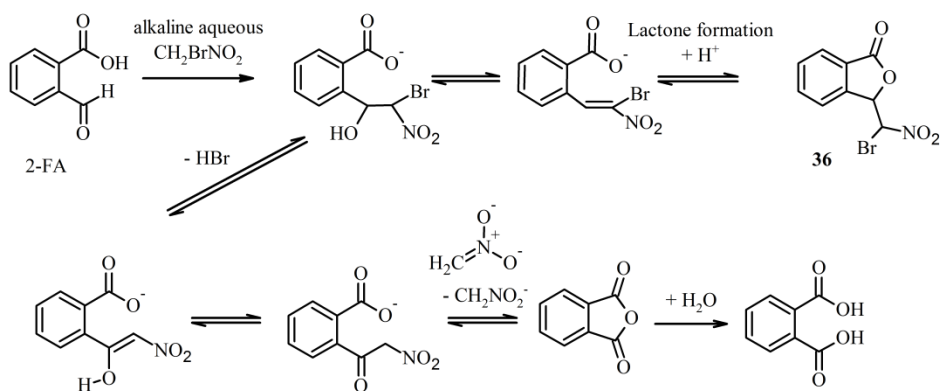
Figure 14. Pathway resulting in lost product from 2-FA reaction with bromonitromethane. Symmetric aromatic protons would appear from a phthalate analogue.

The solvents used in the initial reaction, water and ethanol, would likely keep the phthalic acid dissolved even upon acidification of the solution. If phthalic anhydride formed as an intermediate product, then it could also react

54

with bromonitromethane, as reactions with nitromethane are known, although

they occur under more forceful conditions (Figure 15).[79] This is another pathway

to the crude product seen in the spectrum as the furthest downfield doublet at ~

8.4 ppm. Unfortunately, only the first reaction using the procedure in Scheme 17

resulted in large amounts of precipitate during the workup. Several ^{1}H NMR

spectra of crude products from subsequent reactions showed evidence of the lactol

forming as well as the ethanol substituted lactol.[80]
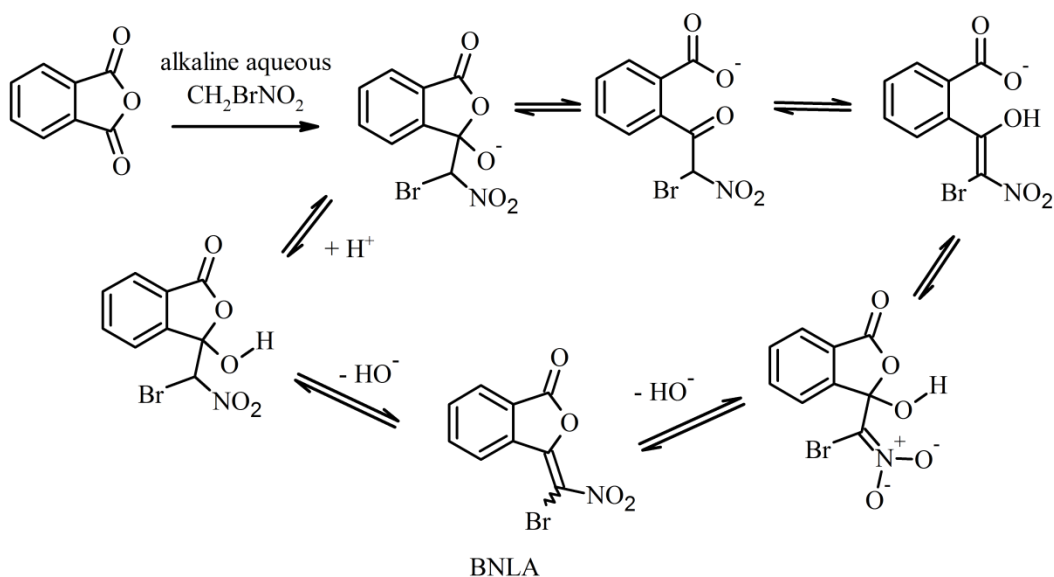
Figure 15. Phthalic anhydride pathway to BNLA product.

Attempts at a monobromination reaction starting from **31** of with *N*-

bromosuccinimide [NBS] employed two different procedures. The first was just

by heating in chlorinated solvent (both in the dark and in light), and the second

method utilized peroxides (*t*-butyl hydroperoxide) in an attempted radical

reaction.[74] Heating with NBS in both the dark and light provided only **33**, but it

was difficult to isolate in good yields, as an equilibrium seemed to form with the

starting material. Using peroxides did not cause any change except for some possible dibromination occuring in low yields.

One reaction mixture was allowed to stand for several days in a biphasic mixture of water and DCM with added bromine. After most of the DCM evaporated, solid crystals formed in the remaining aqueous solution. Collection of the crystals and analysis by TLC showed the appearance of an additional spot at much higher R_f than the starting material **31** and slightly higher than **33**. A ^{1}H NMR spectrum indicated bromine substituted for the benzyl hydrogen, on C3 (Figure 8). This results in doublets appearing between δ 5.52 and 5.35 ppm ($J =$ 14.4 Hz, Figure 16). A modification of the procedure, with either NBS or bromine in quartz tubes and chlorinated solvents only, did not provide the desired products (**35** or **36**).
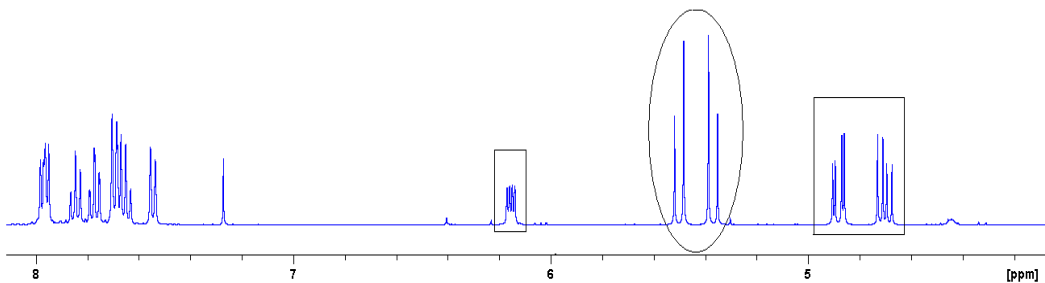
Figure 16. Bromination at C3 instead of C2 of **31**. Crude mixture of **31** (C2 and C3 protons in boxes) and the suspected bromo-substituted product on C3 (geminal protons on C2, $J =$ 14.5 Hz, circled).

3 RESULTS AND DISCUSSION

3.1 Cancer Cell Line Assay Background

The first analysis done on the inhibitors was a growth inhibition assay with three to six cancer cell lines. An absorbance measurement from either the sulphorhodamine B (SRB, Figure 17) or methylthiazolyldiphenyl-tetrazolium bromide (MTT, Figure 18) assay determined the effectiveness of an inhibitor. Cytostatic cell data are collected as an IC_{50} (or GI_{50}), which is the concentration of a compound that results in a 50% reduction of the net protein increase, and total growth inhibition (TGI), which is the concentration resulting in zero net protein increase. Cytotoxic data are collected as the LC_{50}, which is the concentration of compound that would result in a 50% reduction of the measured protein at the end of drug treatment when compared to the beginning. All values are compared to cell growth when no inhibitor is present.

The SRB and MTT assays provide comparable results when limited to IC_{50} data.[81] The SRB assay can provide additional data like TGI and LC_{50} that are not available with the MTT assay. The SRB assay utilizes a pink, negatively charged aminoxanthine dye. This is a protein-staining dye that binds to basic amino acids inside cells. The assay is run in a multi-well plate in which cells are allowed to grow in the presence or absence of an inhibitor. After fixing viable cells to the plate, the dye is added and taken up by the cells. Then the cells are lysed, and the absorbance is measured between 490–530 nm to determine the amount of dye that was taken into the cells.[82] The optical density of SRB is proportional to the cell number. A plot of optical density against inhibitor

concentration allows the IC_{50} (or GI_{50}) to be determined. Furthermore, this is the standard assay method used by the NCI in their 60-cell-line screen, and they provide simple equations to calculate the inhibition concentrations for the GI_{50}, TGI and LC_{50}.[83]
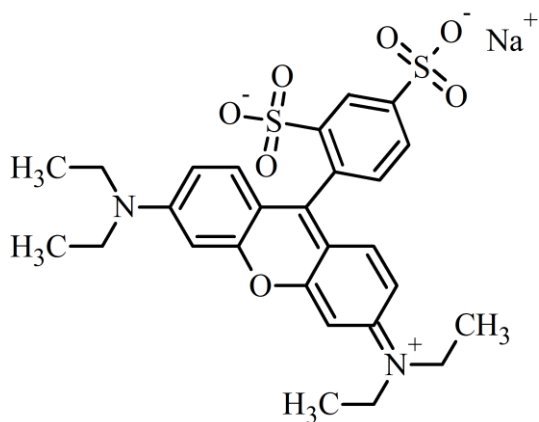
Figure 17. Sulphorhodamine B structure.

Unlike the SRB staining assay, the MTT assay relies upon a cellular conversion to an optically measurable product. Furthermore, the formazan product that forms is not soluble in the assay solution. Thus, an additional solubilizing step must be performed prior to measuring the optical density. The tetrazolium bromide is reduced in the mitochondria of a cell by intracellular NAD(P)H oxidoreductases during the cell growth period. This assay only provides GI_{50} data since it relies on viable cells to produce the optically detectable formazan.
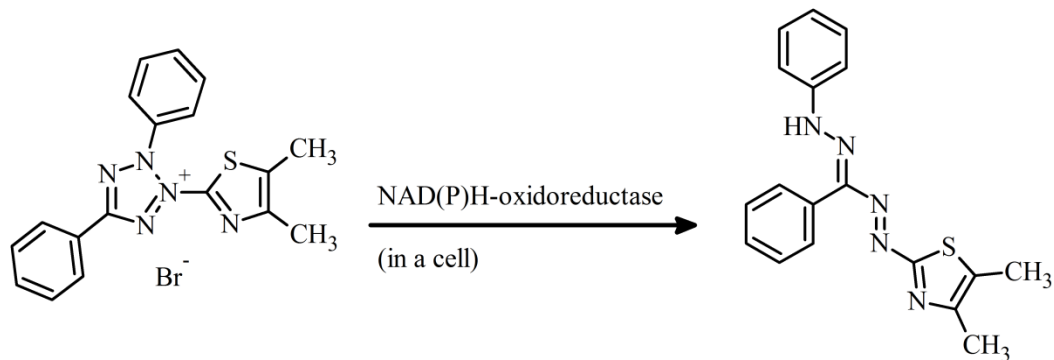
Figure 18. Methylthiazolyldiphenyl-tetrazolium bromide conversion to thiazolyl blue formazan.

3.2 Cancer Cell Growth Inhibition Results for Cinnamic Acid Analogues

The first set of compounds synthesized were the halogenated diesters of 2-carboxycinnamic acid (2-CCA). While the diacid form of the compounds would mimic the 2-(oxalylamino)-benzoic acid (OBA) more accurately, the diester form should enter cells better, whereupon esterases would liberate the corresponding acids. Furthermore, the reported OBA analogues are described in enzyme inhibition assays and not whole-cell assays.[34, 42] Unfortunately, this set of diester compounds did not significantly inhibit the cancer cell growth. Compound **4** did have a GI_{50} of 4.2 μM against the breast cancer cell line MCF-7. However, this was the only compound and cell line with a GI_{50} below 10 μM (Table 2). In general, the bromo compounds had greater inhibition than analogous chloro compounds. Both of the chloro compounds, **2** and **3**, showed relatively high GI_{50} values, and no measurable TGI or LC_{50} could be determined. In almost every case, the dihalogenated compound outperformed its corresponding dehydrohalogenated Michael-acceptor (i.e. **2** vs **3** and **4** vs **5**).

59

Table 2. Human Cancer Cell Line Growth Inhibition (SRB Assay) for **2–5**; values in µM

MeOOC Cl / Cl / COOMe   Cl COOMe / COOMe   MeOOC Br / Br / COOMe   Br COOMe / COOMe

2   **3**   **4**   **5**
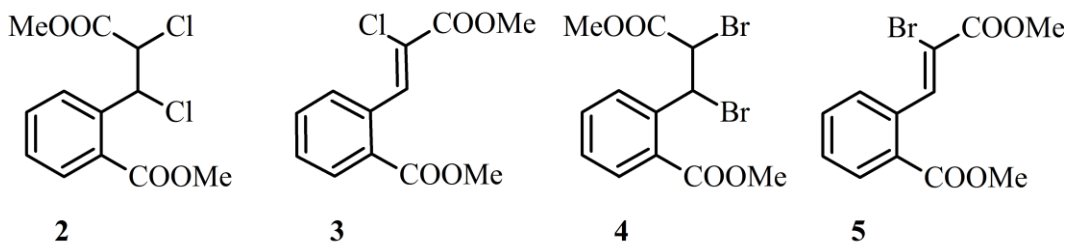
Compound		BXPC-3	MCF-7	SF-268	NCI-H460	KM20L2	DU-145
2 (343)	GI_{50}	110	105	122	110	134	125
	TGI	ND	ND	ND	ND	ND	ND
	LC_{50}	ND	ND	ND	ND	ND	ND
3 (392)	GI_{50}	127	179	155	126	182	156
	TGI	ND	ND	ND	ND	ND	ND
	LC_{50}	ND	ND	ND	ND	ND	ND
4 (263)	GI_{50}	41.6	4.2	46.3	51.3	29.7	36.6
	TGI	80.8	38.7	85.3	122	68.4	79.5
	LC_{50}	157	124	157	ND	157	173
5 (334)	GI_{50}	65.9	102	64.9	56.5	110	44.5
	TGI	129	290	139	132	ND	186
	LC_{50}	254	ND	298	310	ND	ND

BXPC-3 (pancreas adenocarcinoma), MCF-7 (breast adenocarcinoma), SF-268 (CNS glioblastoma), NCI-H460 (lung large cell), KM20L2 (colon adenocarcinoma), DU-145 (prostate carcinoma). The assay was carried out with a maximum dose of 100 µg/mL for each compound.
ND: No Detection of inhibition at the highest concentration tested as shown in micromolarity in parentheses below the compound number.

The X-ray structure of **3** was solved after the SRB assay and subsequent

PTP assays were complete (Figure 19). The π orbitals of aryl carboxylic ester and

the phenyl ring were essentially coplanar.[61] This forced the chloropropenoate

chain out of planarity with the benzene ring. The pi-orbital interaction between

the phenyl ring and the propenoate will not be as strong as it would if planarity

were intact. Without this extended conjugation, the beta carbon should be more

electrophilic, and hence, more capable of binding to a nucleophilic cysteine.

However, this low-energy alignment appears to have had no effect on its capacity

to inhibit cell growth.
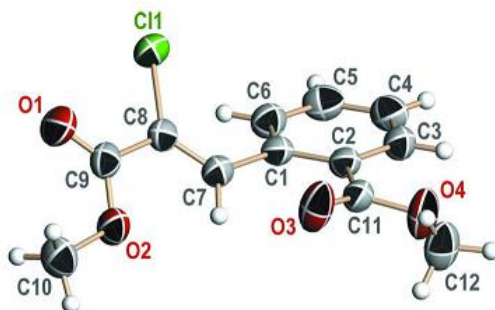
Figure 19. X-ray structure of **3**; the propenoate group is at an angle of 133.53°
with the benzene ring (C2-C1-C7-C8).[61]

The ring closures of halogenated cinnamic acids resulted in halogenated

lactones. The iodo lactone **26** was submitted for testing prior to the maximum

dosage in SRB assays being reduced from 100 µg/mL to 10 µg/mL.

Unfortunately, the two chloro lactones **11** and **12** were submitted and analyzed at

the lower maximum dosage, and none of the inhibition parameters were below the

maximum concentration employed in the assay. Since the chlorinated lactones are

diastereomers, they both share a maximum testing concentration of 41.6 µM,

which is far below the best cell-inhibition concentration for **26** (Table 3). The

dosage change prevented a more complete comparison of these three compounds

to each other. Furthermore, all subsequent SRB data were collected at the new,

lower dosage.

Table 3. Human Cancer Cell Line Growth Inhibition (SRB Assay) for **26**; values in µM
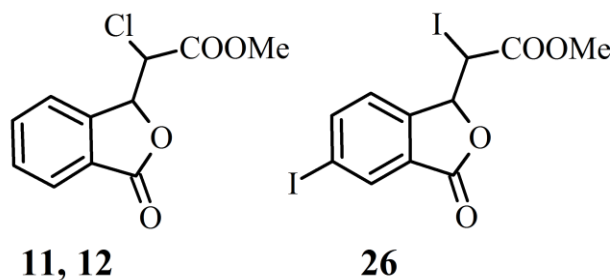
Compound		BXPC-3	MCF-7	SF-268	NCI-H460	KM20L2	DU-145
26 (218)	GI_{50}	94.5	73.4	71.0	88.6	ND	97.2
	TGI	ND	ND	ND	ND	ND	ND
	LC_{50}	ND	ND	ND	ND	ND	ND

BXPC-3 (pancreas adenocarcinoma), MCF-7 (breast adenocarcinoma), SF-268 (CNS glioblastoma), NCI-H460 (lung large cell), KM20L2 (colon adenocarcinoma), DU-145 (prostate carcinoma). The assay was carried out with a maximum dose of 100 µg/mL for each compound.
ND: No Detection of inhibition at the highest concentration tested as shown in micromolarity in parenthesis below the compound number. Diastereomers **11** and **12** were tested at $\leq$ 41.6 µM and no inhibition parameters could be determined.

For a brief period, the MTT assay was used in place of the SRB assay. A couple of cell lines were removed during the MTT assay period, but the 100 µg/mL dose was used in this assay for every compound against each cell line. Since the iodo-substituted aromatic compounds and lactone alkenes had been made at the time of the switch, they were subjected to the MTT assay (Table 4). While similar GI_{50} data can be expected between the two assays,[81] comparing potential inhibitors with differing assays and cell lines is not ideal. The MCF-7 and DU-145 cell lines were used in both assays, except for when compound **23** was submitted (Table 4). However, the MTT assay did include a nontumorigenic (but immortalized) breast cell line, MCF-10A, which acts as an initial test for

toxicity against normal cells. This may help determine if an inhibitor can

effectively target a cancer cell line over a normal one, or suggest the extent to

which a normal cell line would be harmed.

Table 4. Human Cancer Cell Line Growth Inhibition (MTT assay) results for **23**, **24**, **27**, **28** and **29**; GI_{50} values in µM
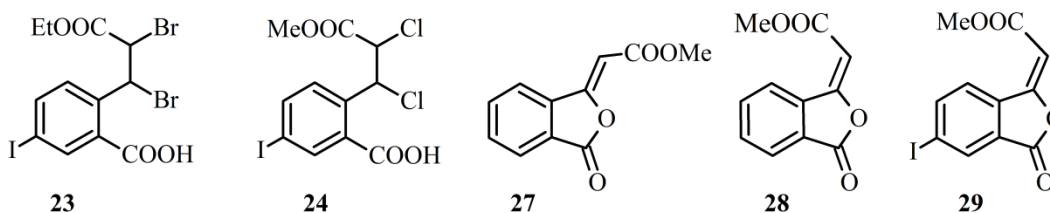
Compound	MCF-7	MCF-10A	A549	3LL[a] or DU-145
23 (197)[a]	ND	76.5	ND	ND
24 (248)	ND	18.9	21.1	19.9
27 (301)	ND	11.1	ND	ND
28 (301)	ND	ND	ND	ND
29 (218)	19.0	4.6	9.4	10.3

MCF-7 (breast adenocarcinoma), MCF-10A (non-tumor breast epithelial), A549 (lung adenocarcinoma), 3LL (Lewis lung carcinoma), DU-145 (prostate carcinoma).
The assay measured a maximum dose of 100 µg/mL, and the concentration corresponding to that dose for each compound is displayed in parentheses.
ND: No Detection of inhibition at the highest concentration tested as shown in micromolarity in parentheses next to the compound number.
[a] **23** was the only compound assayed with the 3LL cell line, and all others were assayed against the DU-145 cell line.

Compounds **23** and **24** are analogous, differing only in the type of halogen

substitution. The dibromo compound **23** was not active against any of the tested

cancer cell lines, while the dichloro analogue **24** did show some activity. Since

the GI_{50} can be compared between the MTT and SRB assays, the diester analogues **2** and **4** can be compared to ring-iodo monoesters **23** and **24** via the MCF-7 cell line. Notably, **23** does not inhibit MCF-7 cell growth, while the diester analogue **4** had micromolar activity (Table 2).

The aryl iodo substituent may have hindered the entry of **23** into the cells, or it was indiscriminately active prior to or after entry. The activity against the non-tumorigenic breast cell line, MCF-10A, make it appear as though **23** was entering cells during the assay period, however. If it was entering cancer cells too, then it was likely too reactive and not capable of reaching a vital enzyme or cellular component of the mutated cells. Neither **23** nor **24** were active against the breast cancer cell line, MCF-7, but they both inhibited the growth of MCF-10A. Compound **24** was active against the lung and prostate cancer cell lines, while **23** was not active against two separate lung cancer cell lines (A549 and 3LL). The SRB assay used a different lung cell line, NCI-H460, for inhibition data collected with **4**. Even though this is not the same cell line as either of those tested in the MTT assay, the lack of any inhibition against two lung cell lines for **23** was still unexpected. This was even more unexpected since **24** did inhibit A549, the lung cell line tested for both of these compounds.

Since other halogenated lactones, **11**, **12** and **26**, had limited or no observable activity from SRB assays, it is conceivable that **23** readily cyclized into a halogenated lactone, with loss of HBr, during the MTT assay period (Figure 20, **23a**). In general, bromide is a better leaving group than chloride, and **23** could favor lactone formation, whereas the dichloro analogue **24** may not. If HBr is

64

eliminated and the lactone forms, then the activity of **23** may be similar to the corresponding iodo lactone **26**. Cell-free experiments to open the lactone of **26** were unsuccessful, and the same would be expected for the bromo lactone.
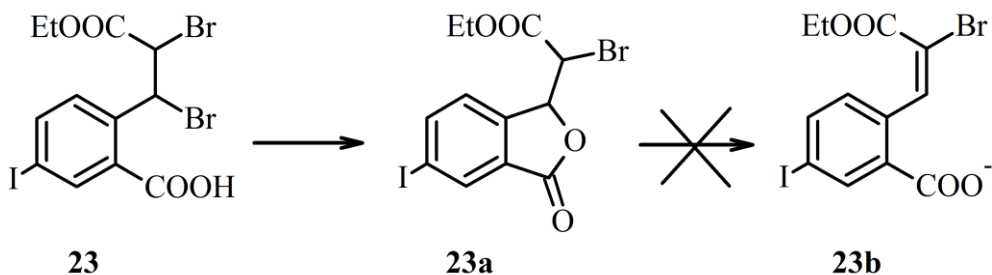
Figure 20. Possible formation of a bromo lactone **23a**. A reactive halogenated olefin **23b** is not expected to form *in situ* during the assay. Elimination of HBr (from C2 and C3 respectively) may precede lactone formation, or loss of H from the carboxylic acid with Br (from C3) may occur directly.

NMR and a preliminary X-ray analysis confirmed that hydrogen iodide had been eliminated from **26** to form the previously unreported **29**. The *cis-trans* isomers, **27** and **28**, were also obtained by elimination of HI from **25** and are known compounds.[64] The aromatic-iodine substitutent had a great effect on the inhibitory activity of this structure.

Despite the deviation from halogenated alkyl and alkenyl groups, the data collected on **29** provided a possible *in vitro* transformation to explain the limited cell-growth inhibition activity for **26**. This compound was not very active (Table 3), but its limited activity may come from *in situ* hydrogen-iodide elimination to form **29**. If the halogenated lactone compounds require dehydrohalogenation to become active, then **11** and **12** would eliminate HCl and produce **27** and/or **28**, which were both inactive in the MTT assay. If **23** forms **23a** (Figure 20) and HBr is subsequently eliminated, then the structure would match **29** or the untested isomer **30**. The activity of **23** would then be comparable to **29**, but it is not. This

can be explained by noting the limited activity of the iodo lactone, **26**.

Elimination of HI to make **29** provided some growth inhibition data (Table 3).

Since iodide is usually a better leaving group than bromide, **26** would be expected

to form **29** more readily than **23** would form **23a**. A similar bromo lactone would

eliminate HBr more slowly and not inhibit cell growth. For synthesis of an

analogous bromo lactone and subsequent HBr elimination see, Elvidge, et al.[59]

The formation of the **23a** is hypothetical. It would not be expected to form

and subsequently undergo dehydrobromination in assay buffer very easily.

Therefore, it is not likely to produce **29**. A mechanism-based activation of the

bromo lactone compound by an enzyme (or other cellular component) could

produce the brominated Michael-acceptor (Figure 20, **23b**), but this does not seem

to have occurred. The chloro analogue **24** may not favor forming a lactone at all,

as chloride displacement would be required *in situ*. Chloride is generally a poorer

leaving group in comparison to bromide. It is far more likely to inhibit cell growth

without transforming into a chloro-lactone (i.e. **11** or **12**) or alkene like **29**.

3.3 Protein Tyrosine Phosphatase Assay with Analogues of Cinnamic Acid and
para-Nitrophenyl Phosphate
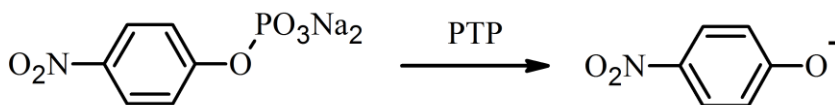
Figure 21. Dephosphorylation of pNPP to pNP by a tyrosine phosphatase. The
nitrophenolate product absorbs around 405 nm.

The first PTP assay used was a colorimetric assay that measured *para*-nitrophenyl phosphate (pNPP) conversion to *para*-nitrophenolate (pNP) by absorbance at 405 nm (Figure 21).[40,84,85] The pH of the assay buffer was between 7.0–7.4 as specified by the enzyme manufacturer (see Experimental), but several PTPs have been reported to display higher activity at lower pH.[44]

Several compounds (Figure 22) were used in this assay with an already described buffer.[40] They were individually dissolved in DMSO before being screened. The compounds were added to an enzyme in aqueous buffer (< 5% DMSO) and pre-incubated for 20–60 minutes. The reaction was started by addition pNPP and terminated by addition of a hydroxide solution after two or three minutes. The absorbance measurement was recorded at 405 nm, and a comparison was made between the compound wells and control wells (DMSO without a test compound dissolved into it). Regardless of the concentration used against PTP1B and PTPβ, none of the compounds (Figure 22) inhibited the activity of either enzyme.

Precipitation of some compounds from the assay buffer prevented testing at high concentrations, e.g., ≥ 100 μM. The DMSO-stock solutions of compounds were diluted into assay-buffer stock to their highest, visibly soluble concentration (see Experimental). These new stock solutions of the compounds were used in assays, but the enzymes were not inhibited. A known inhibitor of PTPases, sodium orthovanadate, was used during some assays, and enzyme activity was inhibited when it was used.[86]
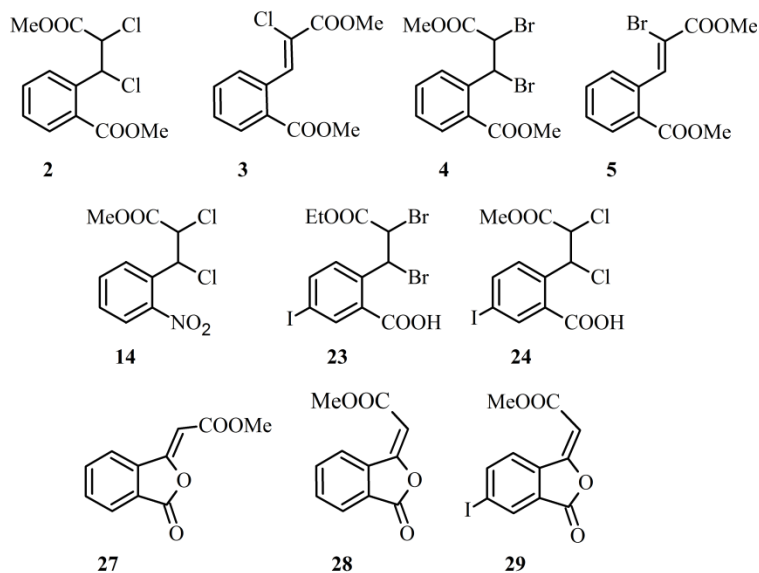
Figure 22. Compounds assayed against PTP1B and PTPβ with pNPP.

3.4 NMR Experiments with Alkenyl Analogues of Cinnamic Acid and Thiols

After several assay attempts with pNPP failed to show inhibition of the two PTP enzymes, a possible deactivating reaction between dithiotreitol (DTT) in the assay buffer and the compounds was considered. Two compounds were analyzed in NMR experiments for their ability to add a thiol. Compound **3** was separately run with DTT and *N*-acetylcysteamine (NAC), whereas **29** was studied with NAC only.

A mixture of **3** and DTT (1:1) in CDCl₃ was prepared, but there was no evidence of a reaction between the two. Since the enzyme assay is conducted between pH 7.0 and 7.4 with a pre-incubation step, a thiolate may be generated from DTT while in the assay buffer. Furthermore, DTT was present in millimolar concentrations, while inhibitors were in micromolar concentrations (i.e., between 100:1 and 1000:1 of DTT:**3**). Therefore, even a small amount of thiol-to-thiolate

conversion of DTT could result in reaction with an available electrophile. After an equivalent amount of DBU was added to the NMR tube with **3** and DTT, new peaks appeared in the aromatic region between δ 7.9 to 7.3 ppm (Figure 23). These new peaks are a clear indication of reaction of the thiolate of DTT with **3**.
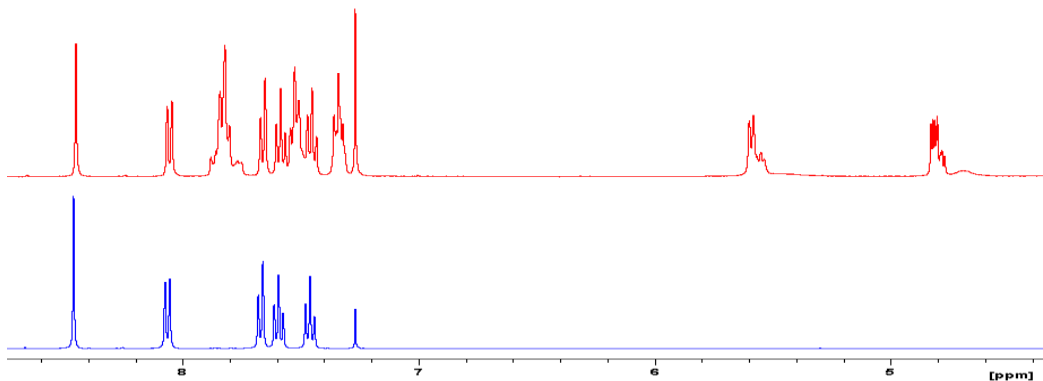
Figure 23. Observed NMR spectrum of **3** and DTT. Spectra are shown with (top) and without (bottom) DBU, between about δ 9–4 ppm in CDCl$_3$.

New peaks also appeared between δ 5.6 ppm and 4.8 ppm (Figure 23). Upon addition to the carbon-carbon double bond of **3** (Figure 24), this would be the expected location for the propanoate hydrogens. However, the splitting for these peaks is complex, and this is likely from more than one product being generated. The peaks around δ 4.8 ppm appear to be a large doublet of doublets partially overlapping a smaller doublet of doublets, while the peaks around δ 5.6 ppm appear to be a large doublet overlapping what may be a smaller triplet.

After this NMR reaction mixture was stored in the dark at about 4 °C for about one month, another spectrum was acquired. Several broad peaks still appeared in the region for aromatic protons and in the region between δ 6.5 ppm

69

to 4.8 ppm. One very distinct set of peaks separated from, or rose above, the noise. These appeared to be from an analogue of 2-CCA. Two doublets with equivalent integration appeared at δ 8.4 ppm and δ 6.3 ppm ($J = 16$ Hz). Additionally, a few peaks within the aromatic region separated from the other broad peaks, and they integrated equivalently with these doublets. The two coupling constants of 16 Hz and doublet locations of δ 8.4 ppm and δ 6.3 ppm are typical for the olefin protons of a structure like 2-CCA. Therefore, a hydrogen substitution of chloride occurred. If the initial Michael addition by the thiolate of DTT occurred as proposed, then this 2-CCA analogue could have arisen from an intramolecular disulfide formation with subsequent chloride elimination (Figure 24).
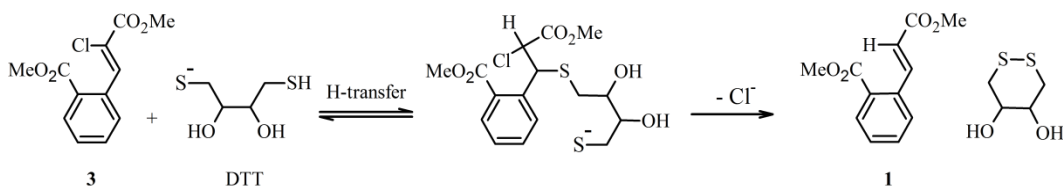
Figure 24. Thiolate of DTT reaction with **3**. Disulfide bond formed with expulsion of chloride to generate the olefin.

A different thiol, NAC, was used to investigation thiolate reaction and episulfonium ion formation. This thiol is a closer model for cysteine than DTT, and there is no possibility of intramolecular disulfide formation. Addition of the thiolate generated from NAC, proceeding to episulfonium ion, and elimination of HCl would generate a new product (Figure 25).
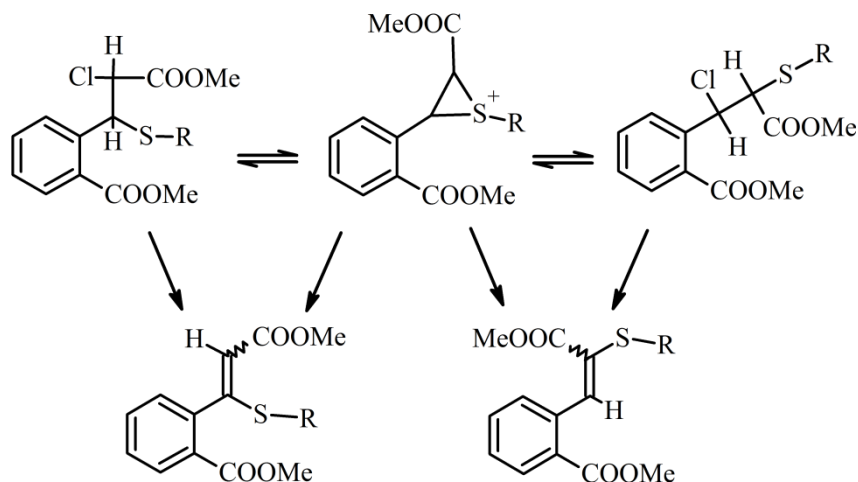
Figure 25. Thiol reaction with **3** and possible episulfonium pathway to a distinct product. Two potential routes to a new product are available. One of these products would provide preliminary evidence of an intermediate episulfonium ion formation (bottom right).
R, -CH₂CH₂NHC(O)CH₃

Similar to the DTT experiment, there was no reaction with **3** prior to the

addition of DBU (Figure 26, bottom). New aromatic peaks appeared along with

doublets between δ 5.7 to 4.7 ppm after DBU was added.
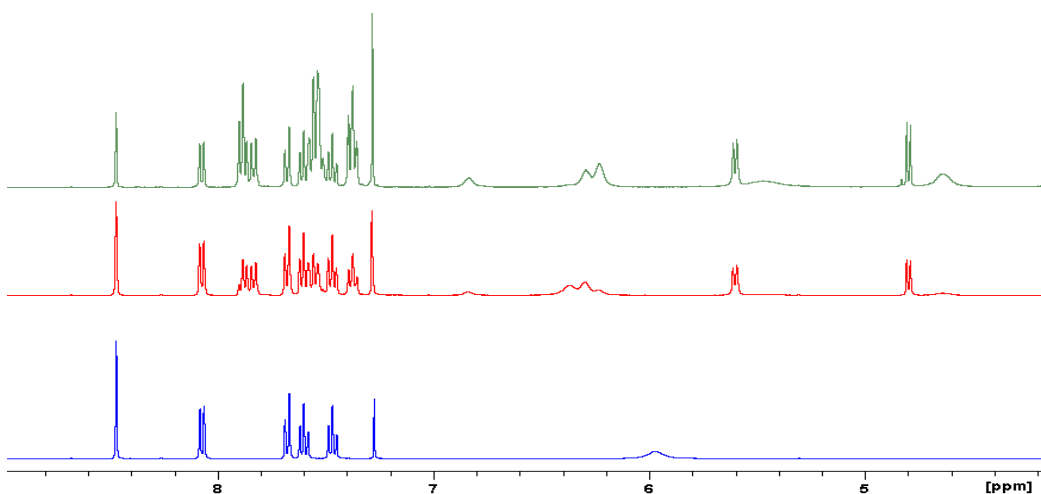
Figure 26. *N*-Acetylcysteamine NMR experiment with **3**. Equivalent amounts of **3** and NAC (bottom); 5 minutes after an equivalent amount of DBU was added (middle); 32 minutes after DBU addition (top). The solvent is CDCl₃.

Only one product may have formed based on the top two spectra in Figure 26. While broad peaks are seen near the doublets between δ 5.7 ppm to 4.7 ppm, there does not appear to be new aromatic or ester peaks that correlate with them. In addition to the two methyl ester singlets for **3**, there are three developing methyl ester singlets and not two, as may be expected from a single reaction product. However, two of these peaks (peaks 4 and 5, Figure 27) sum to the same value as the other, new singlet (peak 1, Figure 27).
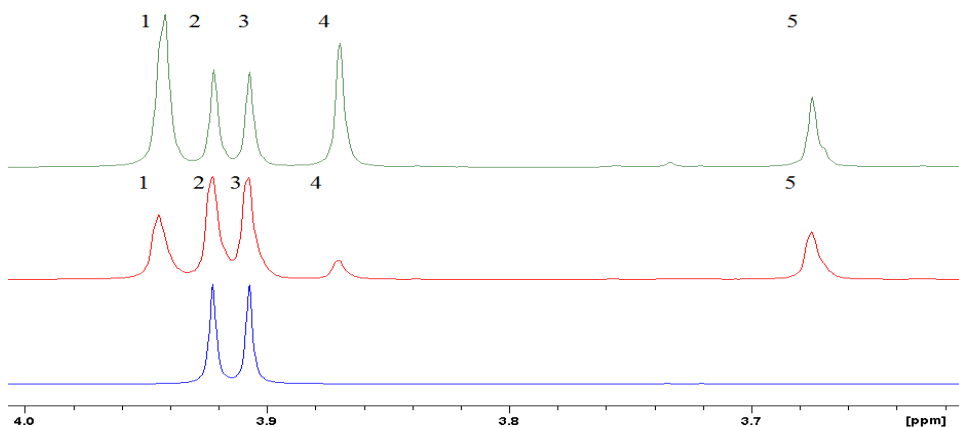
Figure 27. New methyl ester peaks from NAC and **3** reaction. Methyl esters for **3** (bottom), **3** + NAC + DBU after 5 minutes (middle), and again after 32 minutes (top) from Figure 26. The sum of the peaks labeled 4 and 5 integrate to the same value as peak 1.

The singlet peak labeled 1 is due to the phenyl ester, and the other peaks likely arise from an equilibrium between an intermediate carbanion and subsequent protonation (Figure 28).

72
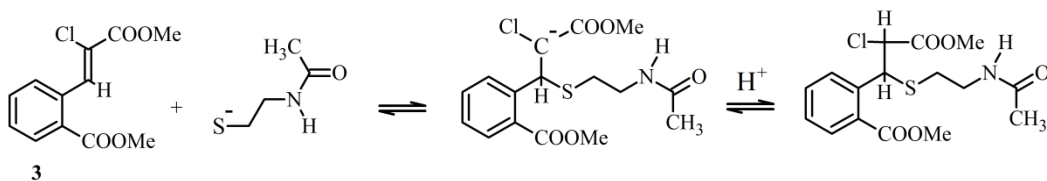
Figure 28. Proposed addition of NAC to **3**. The thiolate from NAC was generated after a reaction with DBU, and its proposed addition to **3**, based on ^{1}H NMR observation, is shown.

This NMR reaction mixture was stored in the dark at about 4 °C for 13 days, and another spectrum was acquired. Essentially only **3** was found and no addition products. A very small singlet was seen just to the right of the olefinic proton singlet from **3** (C2, Figure 8), along with some small aromatic peaks. There are small singlets near 3.7 ppm, but the most abundant one integrates to < 10% of the methyl ester singlets for **3**. The doublet peaks and N-H peak from NAC between δ 7.0 ppm to 4.7 ppm are no longer present either. There are two triplets at δ 3.54 ppm and 2.84 ppm and a singlet at δ 2.02 ppm that integrate to a 2:2:3 ratio. In addition to the missing N-H broad peak, the triplet peak that would be expected from the thiol proton at δ 1.35 ppm is no longer present. These observations indicate an intramolecular reaction of NAC to form 2-methyl-2-thiazoline (Figure 29). The locations of these new peaks differ slightly from what has been described in the literature,[87, 88] but that may be caused by the presence of DBU and water coming from dehydration of NAC. However, the NMR mixture was not separated or analyzed further to confirm the cyclization.
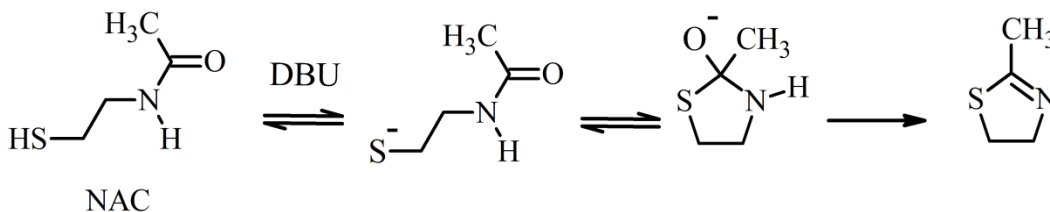
Figure 29. DBU proposed dehydration of NAC to 2-methyl-2-thiazoline.

The thiolate of NAC was undergoing an intramolecular cyclization and reacting with **3**. After 13 days, NAC may have generated 2-methyl-2-thiazoline. The initial interaction observed by NMR (Figure 26) was likely an association-disassociation equilibrium between the two. Formation of 2-methyl-2-thiazoline seems to be favored over the desired addition-to-episulfonium conversion that would form a new product from **3**.

After positive MTT assay results, **29** was subjected to a similar NMR experiment. If a nucleophile is added to the alkene bond, then it is possible for the double bond to isomerize to the Z-alkene upon elimination of said nucleophile. Addition of a nucleophile is the only step expected for this substance. If thiolate does add, future syntheses could be devised with the olefinic proton substituted by a halogen. Such a change would allow for an episulfonium ion to be generated.

The two spectra (Figure 30) show the starting material **29** and its Z-isomer **30** that was isolated with some minor impurities during synthesis. A spectrum with peaks matching the E- and Z-isomers **29** and **30** would be generated if NAC is added and eliminated from **29**. An NMR spectrum of just **29** and N-acetylcysteamine showed no addition had occurred. This is similar to NMR experiments with **3**, as these structures are not electrophilic enough to induce a

nucleophilic attack by thiol. Both require a base to generate the more nucleophilic

thiolate.
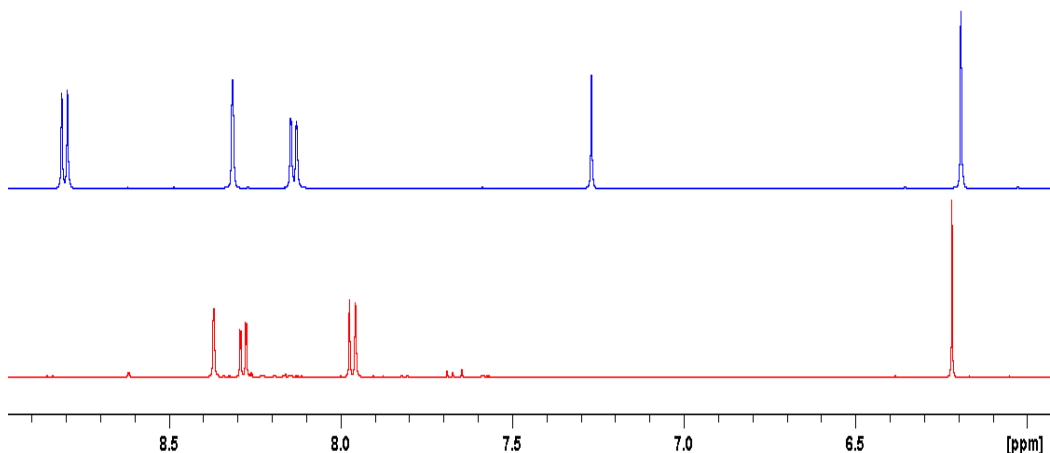
Figure 30. Spectra of **29** and its slightly impure *Z*-isomer **30** (top, in CDCl$_3$ and bottom, in acetone-*d$_6$* respectively), are shown from δ 9 to 6 ppm. There is a distinct downfield shift of the aromatic doublet for **29**, top, which is due to the ester carbonyl anisotropy.[64, 65]
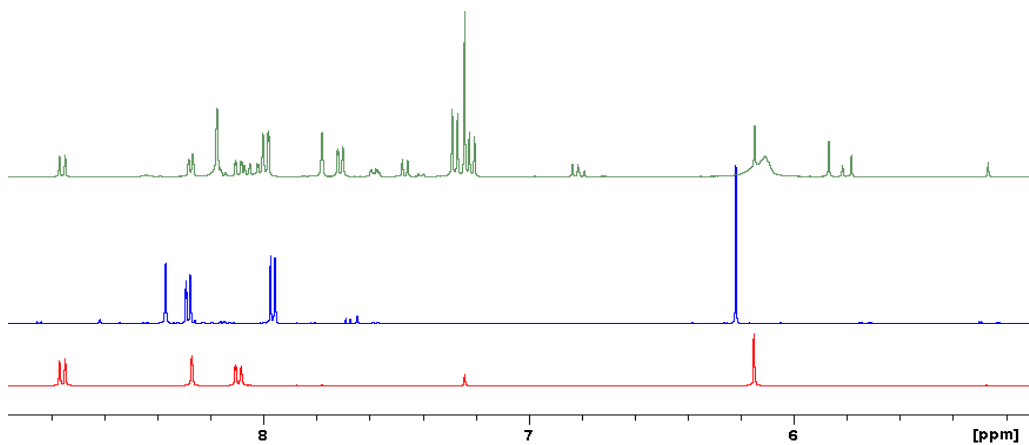
Figure 31. NMR spectra comparison for thiol reaction with **29**. Spectra of **29** (bottom, in CDCl$_3$), **30** (middle, in acetone-*d$_6$*) and the reaction mixture of NAC with **29** (top, in CDCl$_3$). A second NMR spectrum of the reaction mixture was acquired several minutes later, but it was identical to the one displayed at the top.

Several new peaks were found in the spectrum after DBU was added

(Figure 31, top). Since DBU and NAC do not have aromatic protons, only

reaction intermediates and products derived from **29** could produce the new

75

peaks. TLC of the NMR solution showed two noticeable spots, and a short silica gel column separated the materials responsible. This resulted in recovery of **29** as the high running spot, contaminated with a small amount of **30** and another unknown product (Figure 32). The small amount of contamination by **30** is readily apparent by the aromatic peaks, but the most notable peak is a second olefinic proton singlet near δ 5.8 ppm, which is just upfield of **29**'s olefinic proton singlet. The unknown impurity also has aromatic signals. Three singlets formed between δ 8.3 to 8.1 ppm (two of which come from **29** and **30**), and this would imply the unknown contains the aromatic ring. A previously unseen doublet has appeared just to the left of a known doublet for **30** at δ 7.4 ppm. Another peak is partially over lapped around δ 8.1 ppm too.
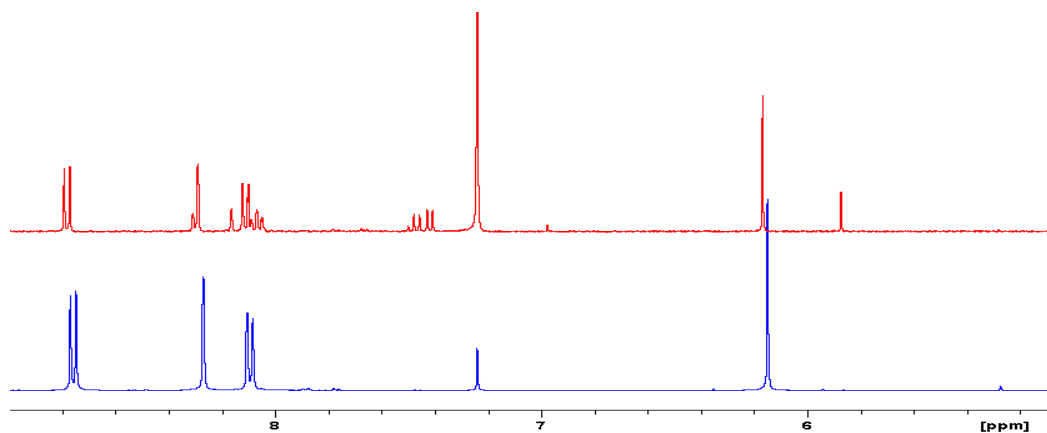
Figure 32. High spot column separated NMR reaction of thiol and **29**. NMR spectra of **29** (bottom) and high spot column separated material (top); both were measured in CDCl₃. Expanded in the region δ 9 to 5 ppm.

The lower spot material isolated from the column was composed mostly of compound **30**, but it contained the same unknown product, albeit in much smaller amount (Figure 33). The aromatic protons are almost unnoticeable, but a small

76

singlet peak is near δ 3.45 ppm. This peak is also present in the higher spot material.
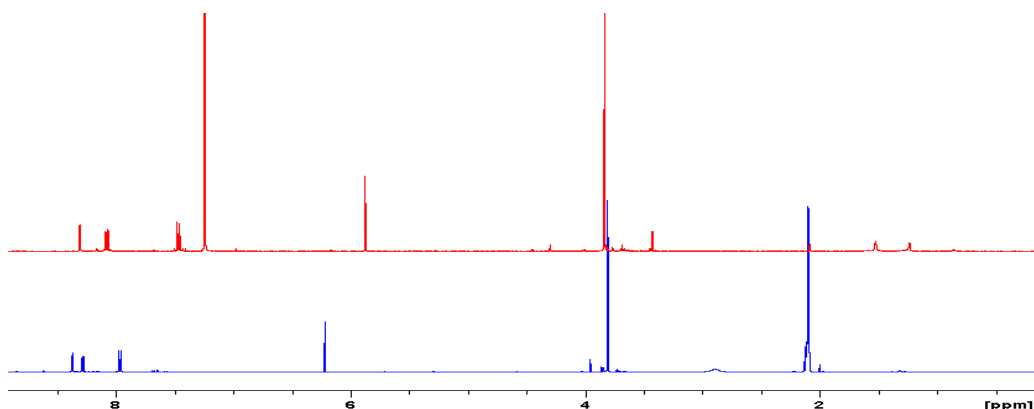
Figure 33. Low spot column separated NMR reaction of thiol and **29**. Spectra of **30** (bottom, in acetone-d_6) and column material (top, in CDCl$_3$).

An attempt was made to identify the impurity by subtraction of the known peaks, i.e. **29** and **30**, from the unknown material using features in Topspin, a tool for analyzing NMR spectra.[89] The following peak information was obtained: δ 8.15 ppm (s, 1H), 8.05 ppm (d, 1H), 7.42 ppm (d, 1H), 4.30 ppm (s, 1H), 3.45 ppm (s, 3H). An epoxide structure was reported from a reaction of **27** or **28** with dimethyldioxirane.[90] This epoxide product has similar non-aromatic peaks. A synthesis was attempted with dimethyldioxirane[91] and the analogous **29** to obtain the epoxide for direct comparison to the unknown. Unfortunately, the reaction appeared to form a polymer, as white solid precipitated out of a reaction solution of acetone and DCM. This solid was either not soluble or very slightly soluble in several other organic solvents, including DMSO.

The column-recovered materials support the addition-elimination reaction between **29** and NAC. This compound may be capable of binding to an enzyme, but irreversible inhibition is not likely. The carbanion that is generated upon

addition to the olefin would need to form a stable bond with an available

electrophile (Figure 34). Additionally, the carbanion could undergo lactone ring

opening instead of elimination of the thiolate nucleophile. That would trap the

nucleophile in a stronger alkenyl bond.
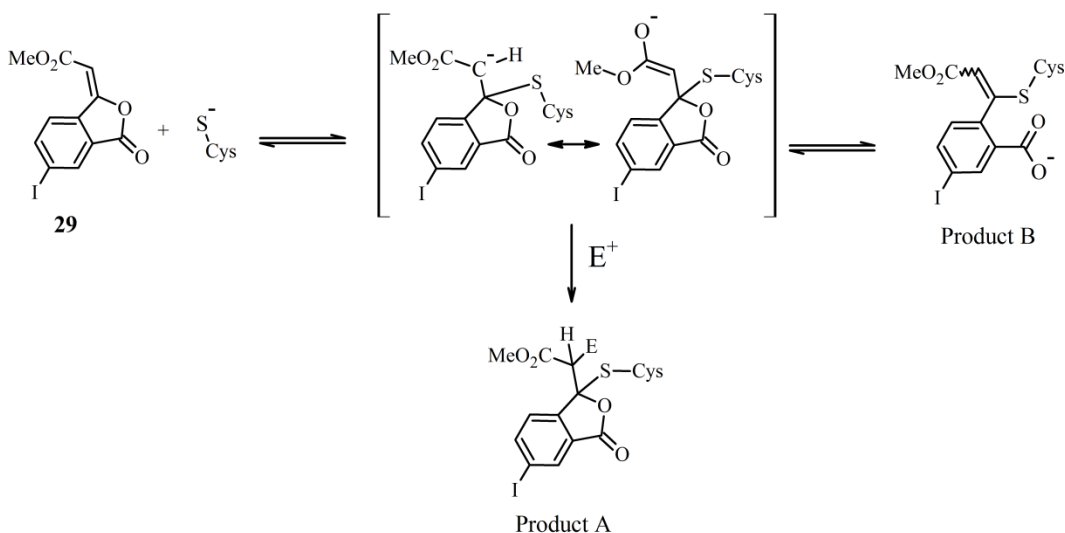
Figure 34. Two possible products from thiolate reaction with **29**. Product A is from the carbanion reaction with an electrophile, E^+. Product B could form if the lactone is opens, and the carboxylate is unable to react to reform it.

The mechanism proposed in Figure 34 is not the only pathway for addition

of a thiolate. Halo lactone alkenes have been proposed to inactivate serine

hydrolases with initial attack at the carbonyl carbon. Upon lactone opening, either

cysteine or another nucleophile would displace the halogen of the reported halo

lactone alkenes.[92] A reaction between the thiolate of NAC and the lactone

carbonyl of **29** (C10, Figure 8) would generate similar resonance structures

depicted in Figure 34. However, C3 would be a carbonyl carbon with a thiol ester

at C10.

Neither of the compounds examined by NMR was capable of adding a

thiol (DTT or NAC). Since the enzyme assays were run at or near neutral pH (7.0

to 7.4), inactivation by DTT is unlikely. Additional experiments observing the rate of the reaction by loss of the carbon-carbon double bond could be inspected by UV with these compounds (see Chapter 3.6). If the conjugated carbon-carbon double bond appears at a unique location in the UV spectrum, then its disappearance, or lack thereof, would determine if incubation with DTT buffer can inactivate these compounds.

Addition of a strongly basic amine produced the more reactive thiolate, which is the expected nucleophile in the catalytic pocket of PTPs. Both of these compounds showed evidence for addition of the thiolate. There was no evidence of an episulfonium ion from **3**. Compound **29** can add thiolate, but generation of an episulfonium ion was never expected. An addition-elimination reaction with **29** was confirmed by isomer isolation. An unknown product was also being generated, but confirmation of epoxide formation was not successful.

3.5 Cancer Cell and Protein Tyrosine Phosphatase Assays of Bromo Nitro Lactones

In contrast to the original cinnamic acid design, the nitro lactone analogues displayed much greater activity despite the lower dosage (10 µg/mL) used in SRB assays (Table 5). Compounds **11**, **12** and **26** are very similar to **33**, **34**, **35** and **37**. Furthermore, all of these lactones were tested in the SRB assay, so they can be compared directly. Presumably, the difference in activity for the lactones relies on the change to the nitro group from the carboxylic ester and not on the halogen. Unlike the hydrogen-iodide elimination products isolated when **26**

was treated with base, the bromo nitro lactones will preferentially be deprotonated alpha (C2) to the nitro group, for **35** and **37** to undergo opening of the lactone ring.

This lactone ring opening to generate a reactive Michael-acceptor in alkaline solution has been described for the non-halogenated precursor **31**.[66] This would generate the Michael-acceptor, which may be the actual inhibitor that forms from **35** and **37**. There are published reports that investigated the ability of several nitrostyrenes to inhibit cell growth in a couple of cancer-cell lines.[51] These cancer cell lines were generated by the Rous sarcoma virus infection of hamster fibroblasts.[93] Two cell lines were made with different levels of activity. The same cancer cell lines in a follow up study,[51] and **31** was found to be somewhat active around 50 μM. The authors proposed that nitrostyrene was generated and acted as the reactive compound (not experimentally supported).

Surprisingly, **33**, and to a lesser extent **34**, was active against some cell lines, too. Since no hydrogen is attached to the carbon with the nitro group, these compounds were not expected to undergo lactone opening that would create a reactive Michael-acceptor. However, there was a possibility of hydrogen-bromide elimination from C3 and C2. This is similar to the hydrogen-iodide elimination from **25** and **26** to form **27–30**. A lactone alkene would be generated, but bromine would be substituted on the olefin in place of the hydrogen (see BNLA in Figure 12). Evidence of this possible formation is discussed in Chapter 3.6.

After the promising SRB assay results, PTP assays were retried. However, more PTP targets were needed to determine the breadth of potential inhibition.

80

Millipore, Ltd., offered enzyme assays against ~ 21 PTPs. Five potential

inhibitors were assayed against five of these PTPs using the substrate 6,8-

difluoro-4-methylumbiliferyl phosphate, DIFMUP, which produces a fluorescent

molecule, 6,8-difluoro-7-hydroxy-4-methylcoumarin, DIFMU (Figure 35).[94]

Table 5. Human Cancer Cell Line Growth Inhibition (SRB Assay) for **33**, **34**, **35** and **37**; values in μM
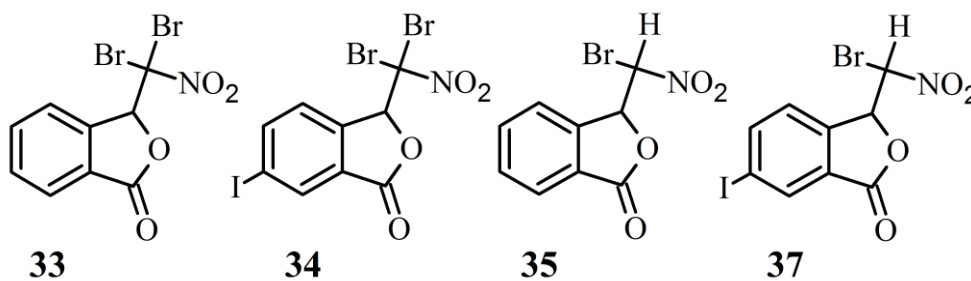
Compound		BXPC-3	MCF-7	SF-268[a]	NCI-H460	KM20L2	DU-145
33 (28.5)	GI_{50}	5.3	15.4	20.8	ND	12.1	ND
	TGI	11.1	ND	ND	ND	ND	ND
	LC_{50}	23.3	ND	ND	ND	ND	ND
34 (21.0)	GI_{50}	9.6	ND	2.8	ND	ND	ND
	TGI	ND	ND	ND	ND	ND	ND
	LC_{50}	ND	ND	ND	ND	ND	ND
35 (36.8)	GI_{50}	8.1	8.9	13.9	12.9	8.1	11.9
	TGI	15.8	18.7	ND	ND	15.3	34.1
	LC_{50}	32.9	ND	ND	ND	32.7	ND
37 (25.3)	GI_{50}	5.5	22.2	2.2	13.6	16.9	ND
	TGI	12.0	ND	ND	ND	ND	ND
	LC_{50}	ND	ND	ND	ND	ND	ND

BXPC-3 (pancreas adenocarcinoma), MCF-7 (breast adenocarcinoma), SF-268
(CNS glioblastoma), NCI-H460 (lung large cell), KM20L2 (colon
adenocarcinoma), DU-145 (prostate carcinoma).
[a] The SF-268 cell line was unstable. Thus the results displayed may not be
accurate.
The assay employed a maximum dose of 10 μg/mL, and the concentration
corresponding to that dose is displayed in parentheses below each compound
ND: No Detection of inhibition at the highest concentration tested as shown in
micromolarity below the compound number.
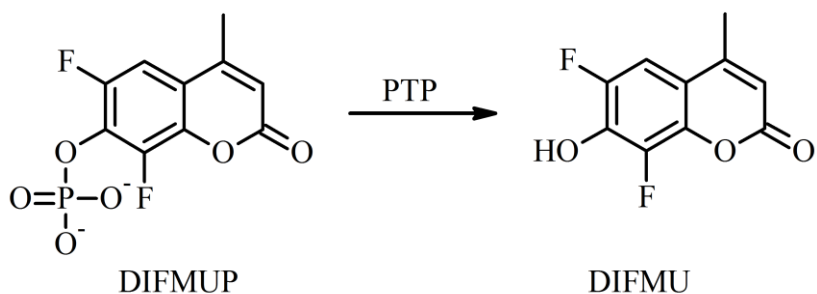
Figure 35. Dephosphorylation of DIFMUP to DIFMU by a tyrosine phosphatase. The DIFMU product is excited at 358 nm and emission read at 455 nm.[95]

The five compounds that were tested included **24** and **29** along with **33**, **35** and **37**. A DMSO stock solution of each compound was prepared. The solubility of all but **29** was confirmed to be at least 100 μM in phosphate-buffered saline, pH 7.4 (see Experimental). Therefore, they were tested at 100 μM, except **29** was tested at the lower concentration of 50 μM, at which it was soluble (Table 6). There was no pre-incubation step during this assay, which was run at a pH 7.2 with a DTT concentration of 0.1 mM. A buffer suitable for each PTP was also selected for the assay (correspondence with Millipore).

The DIFMUP assay supports the results of the pNPP assay in that **24** and **29** are not active against PTP1B. The only enzyme inhibited by **24** and **29** was SHP-2, but the inhibition was minimal given the high inhibitor concentration. Repeating this assay with pre-incubation of these compounds with enzyme may lead to improved inhibition. As of now, there is no evidence to imply that their ability to inhibit cell-growth was a result of targeting PTPs.

Table 6. PTP activity (% of control) with **24**, **29**, **33**, **35** and **37**
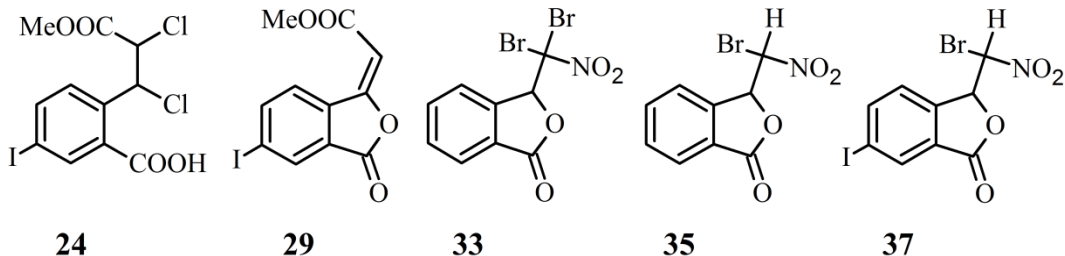
PTP Human origin	24 (100 μM)	29 (50 μM)	33 (100 μM)	35 (100 μM)	37 (100 μM)
CD45	85	102	0	3	4
PTP1B	118	102	39	15	16
TCPTP	112	115	0	6	9
SHP-1	102	103	0	7	8
SHP-2	63	77	0	1	1

Displayed in each column is the % activity of a particular PTP enzyme, all human origin, with a test compound present. In parentheses is the assay concentration of test compound. The % activity is calculated from the enzyme's ability to dephosphorylate DIFMUP without test compound present.

The superior performance of the bromo nitro lactones in the SRB assay was also observed in the DIFMUP enzyme assay. Even lacking a pre-incubation step, they proceeded to dramatically reduce the activity of all the PTPs. Interestingly, the ubiquitous PTP1B enzyme seemed to be the most resistant to inhibition in each case. Unfortunately, PTP selectivity cannot be evaluated from this initial examination of a single concentration of applied test compound. Surprisingly, **33** inhibited four of the five enzymes essentially completely. Its activity was thought to arise from elimination of HBr that produced a bromo nitro lactone alkene (BNLA). This possibility was further investigated and supported.

3.6 Characterization of Bromo Nitro Lactones by Ultraviolet Spectroscopy

The UV spectra of **33**, **35** and **37** were collected in phosphate-buffered saline. Only **33** showed variation over the course of one hour while in a phosphate-buffered saline solution (Figure 36). The UV spectra for both **35** and **37** remained essentially constant for over one hour (not shown).
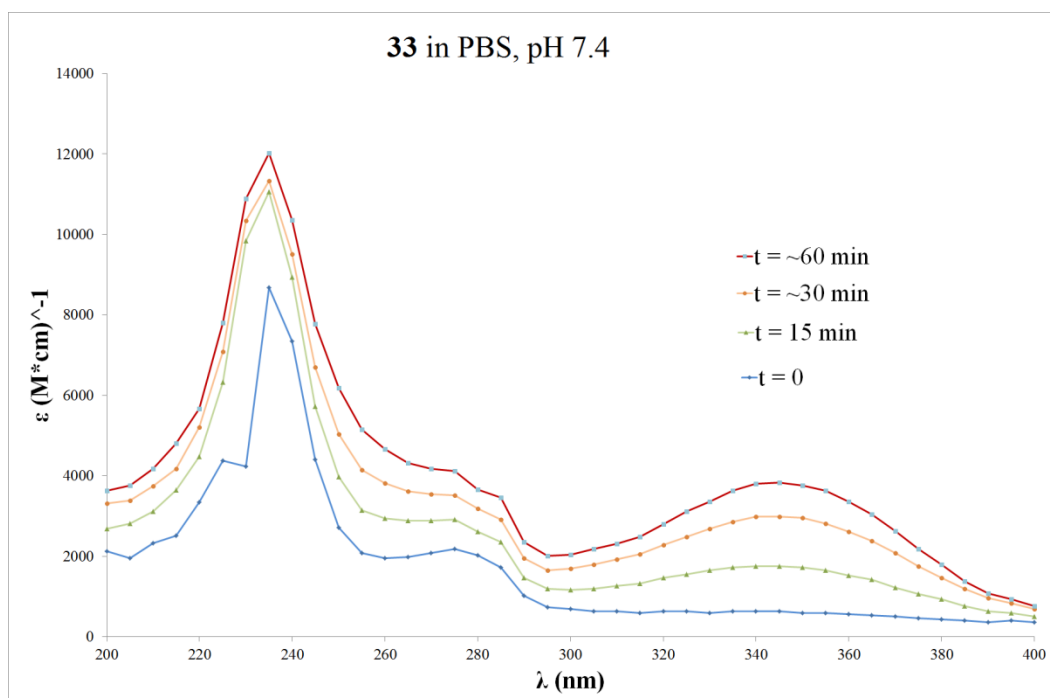
Figure 36. UV spectra of **33** in phosphate-buffered saline for 1 hour. Compound **33** was dissolved in DMSO, then diluted into PBS, pH 7.4, to 100 μM and monitored in a Costar UV multi-well plate with a final volume of 100 μL (2% DMSO) for 1 hour at room temperature.

Given its structure, **33** is not expected to absorb in the region from 300–400 nm. However, elimination of hydrogen bromide would generate a carbon-carbon double bond that has extended conjugation from the aromatic ring to the nitro group. In general, nitrostyrenes have a distinct absorption maximum between 300 and 350 nm,[96] and the UV spectrum of the C2-bromo substituted

nitrostyrene has been reported to have a λ_{max} at 324 nm.[97] When **33** was allowed

to stand in phosphate-buffered saline, pH 7.4, a λ_{max} at 345 nm with $\varepsilon = 3.8 \times 10^3$

$M^{-1}cm^{-1}$ developed. The elimination is likely favored due to the conjugation

between the nitro group and the aromatic ring to form BNLA (Figure 37).
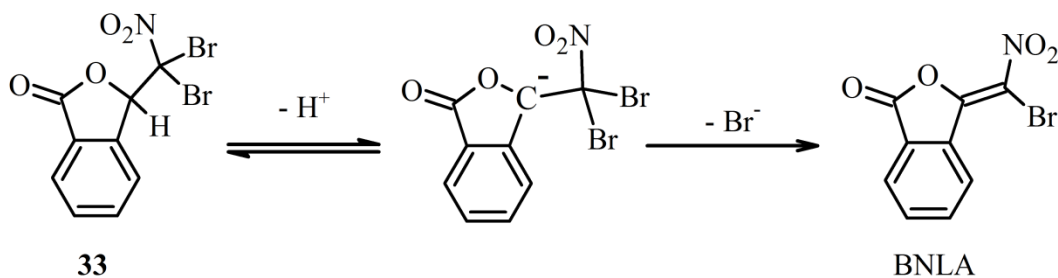
Figure 37. Dehydrobromination of **33** to produce bromo nitro lactone alkene, BNLA. The *E*-alkene is shown, but the *Z*-configuration is also possible. A stepwise elimination is shown, but the reaction may be concerted (E2).

The product BNLA may further hydrolyze to produce an enol that can

tautomerize to a ketone in a subsequent step (Figure 38). It is currently unknown

if this occurred in the PBS solvent. If hydroxide does add, then the enol may be

preferred in alkaline solution, as extended conjugation from the aromatic ring to

the nitro group would remain intact.
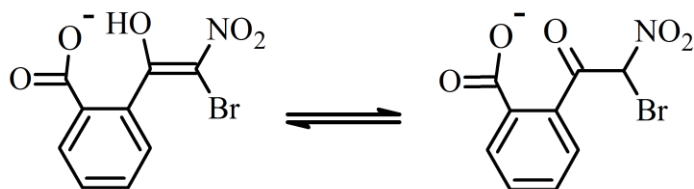
Figure 38. The tautomers of BNLA after addition of hydroxide.

The above enol may not be the source of the large peak that is generated

around 345 nm in Figure 36. A nitrostyrene with two bromines substituted on the

carbon-carbon double bond in place of hydrogens has been reported as not having

any absorption in this region.[98] An X-ray structure confirmed that the olefin and aromatic ring were not in the same plane. The authors believed this was due to the steric strain caused by the presence of the olefinic bromine nearer to the phenyl ring. Thus, the enol double bond may not be coplanar with the aromatic ring if the steric strain between the hydroxyl and carboxylate is greater than the electrostatic interaction between the carboxylate and the partially charged proton of the hydroxyl group. In other words, BNLA may form in the buffer as a stable but still reactive product.

Compound **31** reportedly generated a small hump at 319 nm from the conjugated alkene that forms upon opening of the lactone when it is dissolved in aqueous alkaline solution.[66] This peak decreased significantly in a few minutes as a new peak at 248 nm appeared. This was attributed to the nitronate that formed after hydroxide added to the carbon-carbon double bond. A large hump for **35** and **37** was not present in water, but it was immediately generated when the solutions were made more alkaline (Figure 39).

Unlike the reported UV spectra of **31**, the peak appearing around 340 nm for **35** and **37** does not decrease after 5 minutes in solution (not shown). A hyperchromic effect is noted for **35** with addition of NaOH. For **37**, this effect is not as great, but the sharp spike at 235 nm and the small shoulder at 270 nm have combined. Regardless of these slight differences, the appearance of the hump around 340 nm is still believed to arise from opening of the lactone (Figure 40).

86
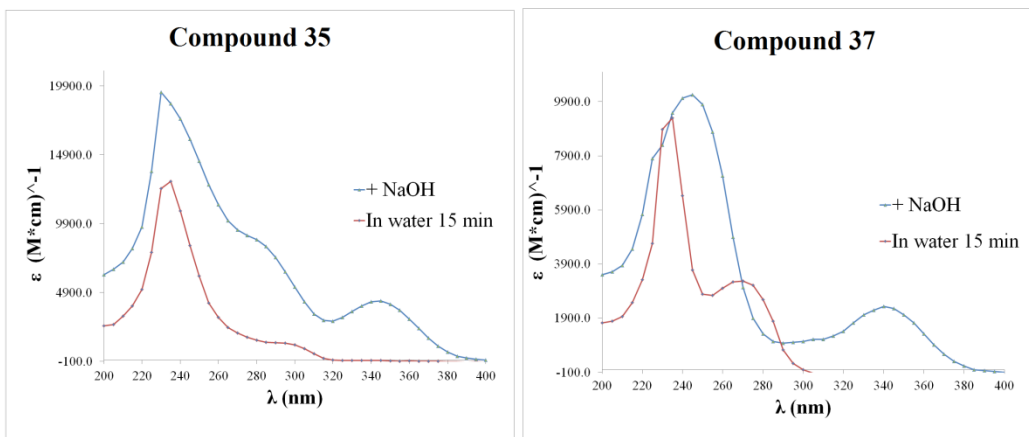
Figure 39. UV spectra of **35** and **37** in water and with sodium hydroxide. Collected in a Costar UV multi-well plate with a final volume of 100 µL (2% DMSO). Proposed nitro olefin peaks appearing at 345 nm ($\varepsilon = 4.3 \times 10^3$ M^{-1}cm^{-1}) for **35** and 340 nm ($\varepsilon = 2.3 \times 10^3$ M^{-1}cm^{-1}) for **37**.
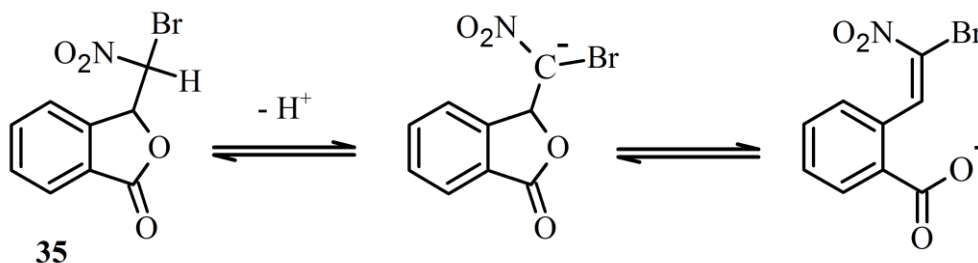
Figure 40. Loss of a proton and generation of a conjugated bromo nitro alkene from **35**. The same mechanism can be extended to **37**.

Both **35** and **37** appear to be stable in buffered solution, but the opened lactones are halogenated Michael acceptors that are the suspected inhibitory compounds. Additional UV spectra were collected for **35** a few months after the spectra in Figure 39 were collected. The original DMSO-stock solution was diluted into PBS buffer and stored for 19 hours at room temperature prior to acquisition of the UV spectrum (Figure 41). When the 19-h solution is compared to immediate addition of **35**, a small hump has noticeably developed at 340 nm ($\varepsilon = 2.1 \times 10^3$ M^{-1}cm^{-1}) for the 19 h solution. There is a possibility **35** is slowly generating the reactive olefin as shown in Figure 40.
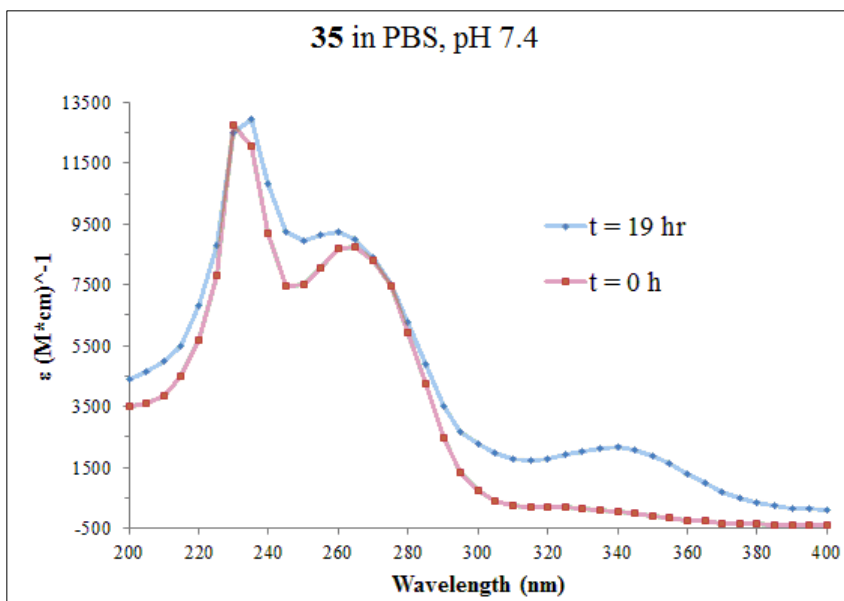
Figure 41. UV spectra of **35** in phosphate-buffered saline, 0 and 19 h. Two spectra were acquired for each time, and the average of the two spectra are plotted. The hump is centered at 340 nm ($\varepsilon = 2.2 \times 10^{-3}$ M^{-1}cm^{-1}).

3.7 Experiments with Bromo Nitro Lactones and Thiols

An NMR experiment with **33** and triethylamine in CDCl$_3$ was carried out to investigate the potential dehydrobromination reaction (Figure 36). As noted, during the Henry reaction between bromonitromethane and 2-formylbenzoic acid (Chapter 2.9), a by-product formed along with compound **36** (the diastereomer of **35**). This by-product had an aromatic doublet shifted downfield to about δ 8.4 ppm, and no other distinguishable peaks were seen outside of the aromatic region (see Figure 11). The lack of peaks appearing outside of the aromatic region and the downfield shifted doublet were rationalized as arising because of the formation of BNLA (Figure 36). The NMR experiment with **33** and triethylamine showed two doublets downfield between δ 8.6 and 8.3 ppm (Figure 42).
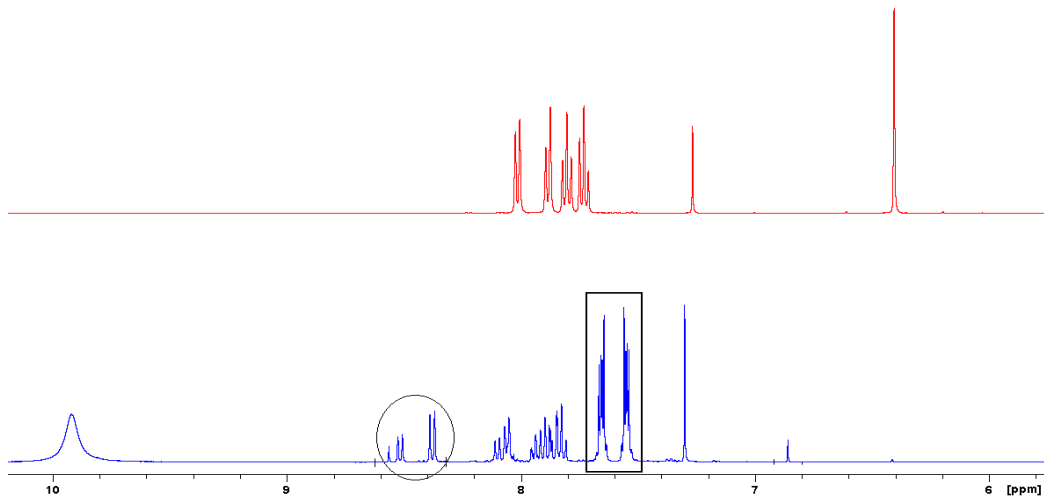
Figure 42. NMR experiment with 33 and triethylamine. ^{1}H NMR of **33** (top) and **33** + NEt$_3$ (bottom) in CDCl$_3$. Circled, doublets from suspected formation of E and Z isomers of BNLA. Boxed, symmetric peaks from suspected phthalate analogue.

The singlet peak for the lone, non-aromatic proton of **33** (on C3) that is located at about δ 6.4 ppm was gone in less than 15 minutes. Surprisingly, two nearly symmetric aromatic multiplets appeared as the preeminent peaks. The doublets between δ 8.5 to 8.4 ppm are likely due to anisotropy from the bromine or nitro group upon formation of E or Z alkene (BNLA).[79] Two low-integrating singlets are present, too (δ 8.55 and 6.85 ppm), and they could be from intermediates. The symmetric multiplets between δ 7.5 and 7.7 ppm formed in preference to anything else.

The newly generated lactone alkene (BNLA) is a Michael acceptor that is the expected reactive molecule in assays. It did not appear to be too reactive in UV experiments using PBS, as the proposed nitro-alkene hump did not vanish over time. However, there is a possibility that it may be too reactive in this NMR experiment with NEt$_3$. A subsequent transformation is occurring in the NMR experiment, and this product may be responsible for the enzyme and cell-growth

89

inhbition. The CDCl$_3$ solvent used does have a small amount of water present.

Thus, hydroxide formation from water and triethylamine would occur, and

addition of the hydroxide to the alkene could result in further transformations that

produce a phthalate or similar analogue (Figure 43).
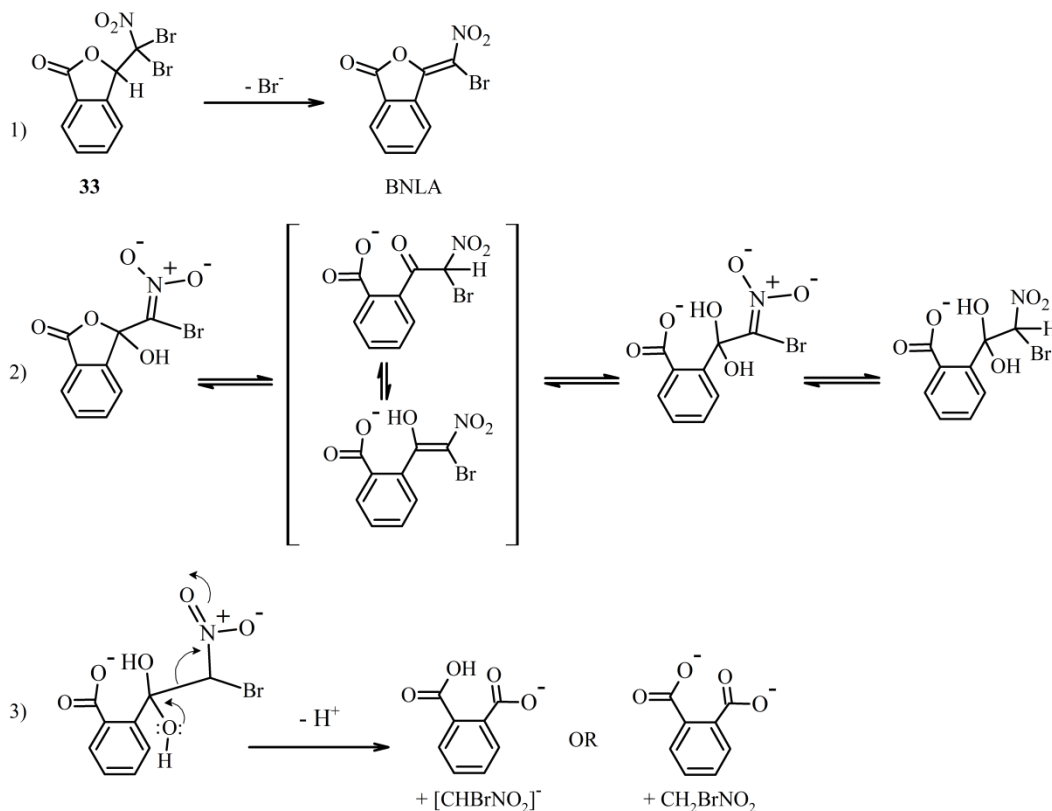
Figure 43. The proposed transformation from **33** to phthalate. Upon loss of HBr (step 1), hydroxide can add at two places; only addition to the conjugated nitro alkene is shown (step 2). Loss of bromonitromethane produces phthalate (step 3).

Thus, the singlets that appeared in the NMR spectrum during the reaction,

at δ 8.55 and 6.85 ppm, may be from an intermediate. Only addition of hydroxide

to the conjugated nitro alkene is shown in Figure 43, but it may add to the

carbonyl carbon too. Analogous compounds have been proposed to react with

hydroxide or methoxide via the carbonyl carbon prior to undergoing

rearrangements (i.e., dibromobenzalphthalide).[99] Similar rearrangements would

90

generate additional intermediates and products that are not shown. Regardless, NMR experiments indicated fast transformations with BNLA that seemed to be produce phthalate analogues.

Isolation of BNLA was attempted, but phthalic acid formation seems to occur even when dry reaction conditions were used. A reaction with *t*-butoxide in *t*-butyl alcohol under nitrogen was attempted, but it was very slow. The crude product NMR spectrum had signals for unreacted **33** with a small symmetric peak. The ^{13}C NMR spectrum of this crude material was acquired, and thirteen peaks appeared. Nine of the peaks belong to unreacted **33**, and the other four peaks were from the formation of the symmetric product believed to be a phthalate analogue (in DMSO-d_6, 400 MHz, δ 169.1, 168.2, 144.1, 135.8, 133.2, 132.0, 131.2, 128.7, 126.5, 126.3, 124.5, 87.5, 83.2).

If a rearrangement of **33** can occur similarly to what was described by Alexander, et al.[79] or Shchukina,[99] then a compound like 2-nitro-1,3-indandione or a similar structure may form. Five carbon peaks would be expected to appear in ^{13}C NMR, but only four were found for 2-nitro-1,3-indandione.[100] However, the furthest downfield peak for that compound is located at δ 181.6 ppm in the same solvent as the reaction product with **33**. Therefore, elimination of bromonitromethane, which can polarize the carbon-carbon bond and stabilize the resulting charge, seems to be the most plausible pathway. Similarly, phenylnitromethane has been proposed as a good leaving group for *o*-[nitro(phenyl)acetyl]benzoic acid (a hydrogen substituted at C2 by phenyl and C3

by hydroxyl, Figure 8) coming apart in alkaline solution with formation of phthalic anhydride.[101]

Triethylamine and DCM were separately dried and distilled before storage over Molecular Sieves, and subsequent reactions with **33** were run under a nitrogen atmosphere. A crude product from a reaction of **33** with NEt$_3$ in DCM was isolated when the reaction was run very cold (Figure 44). From the ^{1}H NMR spectrum, the crude product consisted of unreacted **33** and the two lactone alkene products. There is evidence of small, symmetric peaks, too (δ 8.2 ppm and the corresponding symmetric peak is likely masked by other aromatic protons), which would mean a phthalate analogue formed again. However, this lone peak is small and shifted downfield from what was seen previously (Figure 42). The reduced intensity of this peak from this reaction run at lower temperature supports initial formation of BNLA prior to any phthalate. The downfield shift is possibly from the lack of an amine base being present like in the NMR experiment.
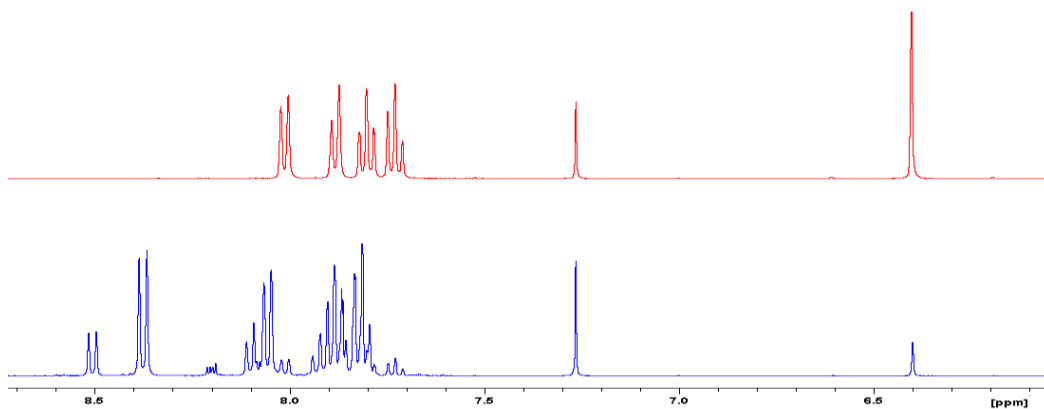
Figure 44. Crude material from a low reaction between **33** and triethylamine. ^{1}H NMR of **33** (top) and crude material from reaction of **33** with NEt$_3$ between -20 and 0 °C (bottom); both in CDCl$_3$.

92

Attempts were also made to isolate a product from reaction of **35** with a base-generated thiolate, similar to Fekry, et al.[54] An initial ^{1}H NMR reaction mixture of β-mercaptoethanol and NEt$_3$ showed some promise (Figure 45).
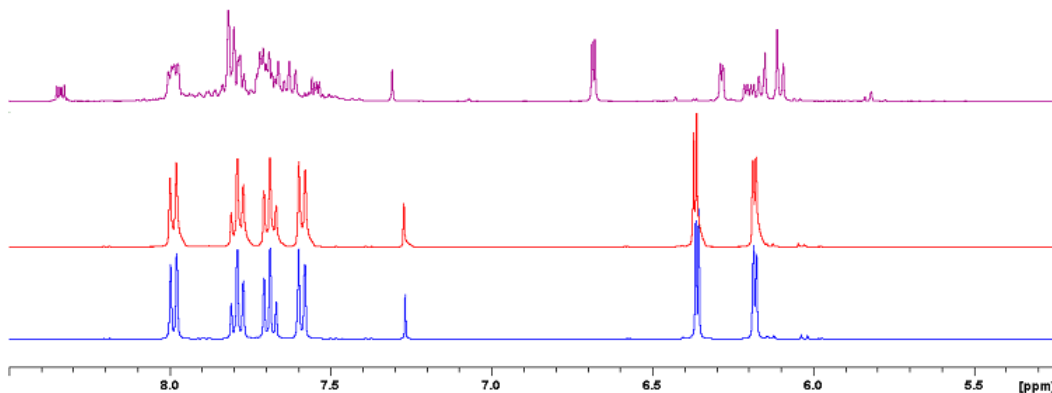
Figure 45. Reaction of **35** with β-mercaptoethanol and triethylamine. Bottom: **35**; middle: **35** + β-mercaptoethanol; top: **35** + β-mercaptoethanol + NEt$_3$; in CDCl$_3$.

As the bottom two spectra in Figure 45 are almost identical, compound **35** does not react with just β-mercaptoethanol. Addition of NEt$_3$ resulted in several new doublets, and two multiplets, at δ 8.35 and 6.20 ppm. The latter multiplet is commonly seen with **31**, and there are two more multiplets upfield (not shown) between δ 5.0 and 4.7 ppm. These peaks are also from **31**. The new doublets were initially thought to be from thiolate addition. Unfortunately, the same peaks developed when **35** was treated with only NEt$_3$ (Figure 46).

The NMR reaction mixture was treated with acetic acid, in an amount equivalent to NEt$_3$, to check for any changes and to neutralize the amine base (Figure 46, top). It also helped resolve certain peaks. The NMR spectrum of **33** was included because a singlet was formed in the location normally seen for its non-aromatic proton (C3). While a dehydrobromination reaction occurred when

NEt$_3$ and **33** were combined, the same elimination was not expected for **35** (i.e., HBr elimination between C2 and C3 in Figure 8). A downfield doublet would be expected to form very far downfield (from the proton on C9) if that were the case, but a multiplet formed instead.
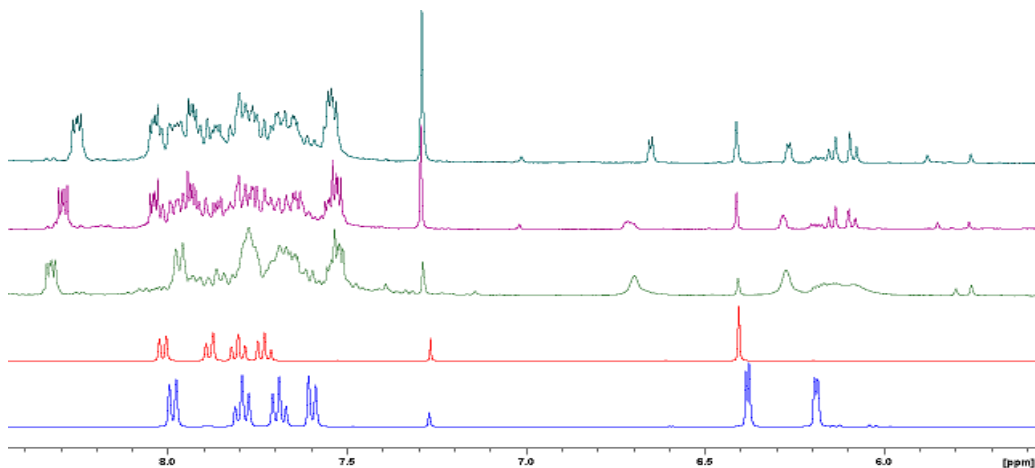
Figure 46. Reaction of **35** with triethylamine. Bottom to top: compound **35**, compound **33**, **35** + NEt$_3$ at 10 min, then 48 hours and finally with an added equivalent of AcOH. All spectra were measured in CDCl$_3$.

A dehydrobromination from **35** would result in a lactone-alkene structure similar to **29**, and the singlet near δ 6.4 ppm may be attributed to that olefinic proton. However, NEt$_3$ appears to have removed either the proton, or possibly the bromine, next to the nitro group (Figure 47). Two sets of doublets appeared between δ 6.7 to 6.0 ppm after acetic acid was added to the NMR mixture (Figure 46, top). At about δ 6.1 ppm, one set of doublets appear ($J = 7.5$ Hz), which are in the same location as the doublets for **36** (the diastereomer of **35**). The doublets for **35**, which were separated by 0.2 ppm prior to the reaction, also resolved ($J = 3.2$ Hz), but one of the proton peaks (C2) has shifted about 0.3 ppm downfield. Also, this set of doublets is now about 0.4 ppm apart. The appearance of doublets for **36**

94

was expected, as the proton on C2 is exchangeable, and a base should scramble any initial stereochemistry at that carbon.

Triethylamine was not expected to be act as a reducing agent capable of removing a bromine, but reactions between amines and organobromides or amines and bromine are known.[102, 103] Peaks for **31** are still observed when only the amine base was used (Figure 46). The singlet at δ 6.4 ppm is attributed to the generation of **33**. This singlet is not present when a thiol is in the reaction mixture, though (Figure 45). In this case, formation of **31** is either preferred or **33** forms and reacts quickly.
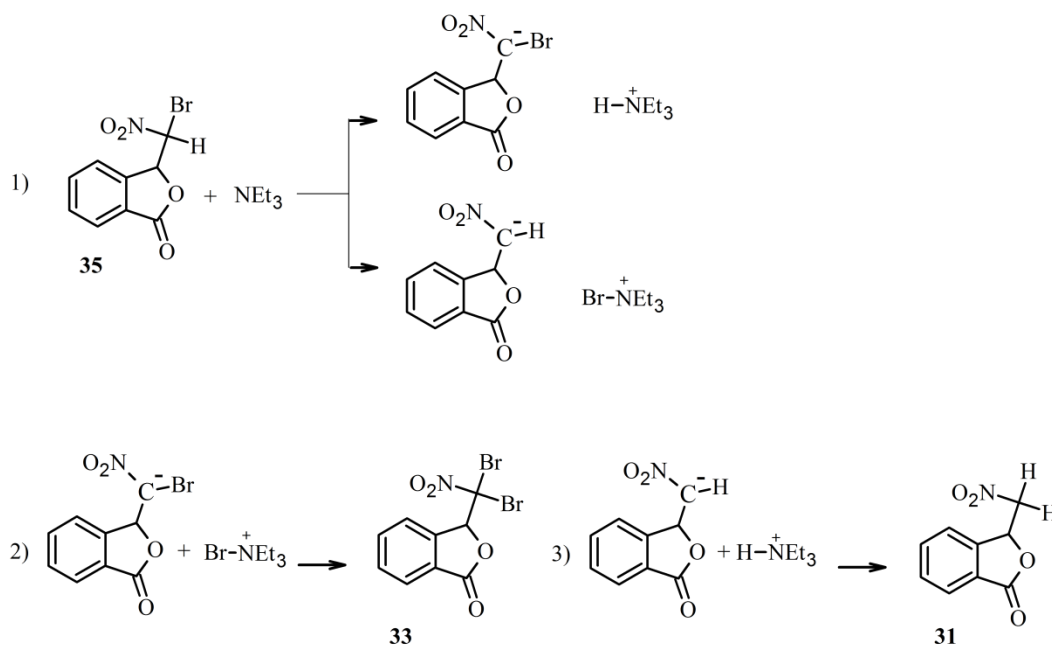
Figure 47. Reduction or oxidation of **35** by triethylamine. NEt$_3$ either deprotonates or debrominates **35** (reaction 1). Both carbanions are formed reversibly, which would result in **35** or **36** being formed. Additionally, the carbanions can react to form **33** (reaction 2) or **31** (reaction 3).

Additional experiments were done with **35** in various systems, and the crude material analyzed by NMR spectroscopy (Table 7). Several experiments were done with PBS, pH 7.4, being used. A new thiol was also used, the sodium salt of β-mercaptoethanesulfonate (MESNA). In every reaction with an amine base or thiol present, **31** was recovered in majority. When **35** was stirred in PBS buffer without base or thiol added, only **35** and **36** were recovered. Only reversible deprotonation of **35** would afford both isomers. In other words, the buffered solution could deprotonate **35** and possibly generate a reactive alkene (Figure 40), but there is no loss of bromide in solutions of only buffer. Regardless, no thiol-addition products could be isolated from any reaction mixtures to confirm the existence of this reactive alkene. Even when a slightly acidic buffer was used, pH 6.81, the reduction to **31** occurred as long as MESNA was in the reaction mixture. This indicates deprotonation, or even lactone opening, is unnecessary for removal of the bromine, i.e. it is removed directly from **35**.

A biphasic reaction mixture was also employed (Table 7). Compound **35** is soluble in DCM and deprotonation, with potential lactone opening in a subsequent step, would result in an intermediate that is soluble in the aqueous phase. MESNA is ionic and not likely to transfer into DCM; it would only be in the aqueous phase. The attempted generation of the reactive alkene prior to coming into contact with a thiol did not produce a new product, though.

Table 7. Reaction of **35** with Thiols in Various Systems.

Thiol (eq)	Base (eq)	Solvent(s)	**35:36:31**
MESNA (1.2)	Pyridine (3.7)	Pyridine	Only **31**
MESNA (1.1)	-	PBS	1.00:0.07:0.58
-	-	PBS	1.00:0.53:0
MESNA (1)	-	PBS[a]	1.00:0.22:0.79
MESNA (1.1)	-	DCM and PBS	1.00:0.52:1.40
DTT (1)	-	PBS	1.00:0.07:2.60

All reactions started with **35**. PBS, pH 7.4, served as the base and solvent in most experiments. Only one reaction did not include a thiol. The molar equivalents of thiol or base in comparison to **35** are in parentheses.
[a] PBS, pH 6.81.

4 EXPERIMENTAL

All melting points were taken in an Electrothermal® melting point apparatus and are uncorrected. ^{1}H and ^{13}C NMR were acquired with the solvent and radio frequency (in MHz) listed. When TMS was included in the solvent, the peak locations are listed downfield from TMS. If TMS is not listed, spectra were referenced to the solvent residual peak ± 0.01 ppm.[104] Solvents used in reaction mixtures were distilled and dried over Molecular Sieves prior to use unless specified. All reactants were used as purchased without purification unless noted. Safety information (MSDS) is provided by the chemical supplier and is available free of charge on their website (ex. http://www.sigmaaldrich.com/safety-center.html). Elemental analysis were performed by Atlantic Microlabs, Inc. (Norcross, Georgia). Measurements for the UV spectra of compounds and the pNPP assay were done on a BioTek Synergy 2 Multi-mode Microplate Reader using a SQ Xenon Flash light source.

Methyl (E)-(2-methoxycarbonylphenyl)prop-2-enoate (1):
Acetyl chloride (1 mL) was slowly added to 25 mL of methanol in a 100-mL round-bottom flask while on ice. The reaction mixture was refluxed for 10 min prior to addition of 2-carboxycinnamic acid (381 mg, 2 mmol). After refluxing 2 h, the reaction mixture was concentrated by vacuum rotoevaporation and passed through a short silica gel column with DCM as the eluting solvent. A viscous clear oil of **1** was recovered upon evaporation of DCM (420 mg, ~ 95%). ^{1}H NMR (300

MHz in CDCl$_3$) δ 8.48 (d, 1H, *J* = 15.9 Hz), 7.98 (d, 1H, *J* = 7.8 Hz), 7.57 (m,

2H), 7.44 (t, 1H), 6.34 (d, 1H, *J* = 15.9 Hz), 3.94 (s, 3H), 3.82 (s, 3H).

Methyl 2,3-dichloro-3-(2-methoxycarbonylphenyl)propanoate (2):

KMnO$_4$ (0.73 g, 4.62 mmol) and benzyltriethylammonium chloride (bteac, 1.04 g,

4.57 mmol) were stirred in 20 mL of dry DCM. The resulting dark purple solution

was cooled on ice for 20 min. Four equivalents of distilled TMSCl (2.00 g, 18.4

mmol) was slowly added to the stirred solution, which gradually took on a dark

green color. The reaction mixture was allowed to warm to room temperature

before **1** (1.00 g, 4.55 mmol) was added. The reaction was terminated, as multiple

spots appeared on TLC, by addition of 0.1 M sodium thiosulfate to the organic

phase. After extraction of the organic phase, it was washed with brine prior to

being dried over anhydrous sodium sulfate. A silica gel column was used to

separate the mixture (elution with 1:1 hexanes–chloroform). Recrystallization

from DCM–hexanes yielded **2** (640 mg, 48%) as a white solid, mp 70.5–72 °C.

^{1}H NMR (400 MHz in CDCl$_3$) δ 7.97 (d, 1H, *J* = 8.0 Hz), 7.69 (d, 1H, *J* = 7.6

Hz), 7.60 (t, 1H, *J* = 7.6, 7.6 Hz), 7.44 (t, 1H, *J* = 7.6, 8.0 Hz), 6.62 (d, 1H, *J* =

10.4 Hz), 4.75 (d, 1H, *J* = 10.4 Hz), 3.95 (s, 3H), 3.88 (s, 3H); ^{13}C NMR (100

MHz in CDCl$_3$) δ 167.5, 167.0, 137.7, 132.6, 130.6, 130.0, 128.9, 128.6, 59.2,

55.8, 53.4, 52.6. Anal. Calcd (%) for C$_{12}$H$_{12}$Cl$_2$O$_4$: C, 49.51; H, 4.15. Found: C,

49.30; H, 4.11.

Methyl (*Z*)-2-chloro-3-(2-methoxycarbonylphenyl)prop-2-enoate (3):

In 2 mL of DCM was dissolved **2** (300 mg, 1.03 mmol). Triethylamine was then

added (110 mg, 1.10 mmol), and the reaction was monitored by TLC. The mixture

was washed successively with ~ 5 mL of 1.0 M HCl and brine and dried with

sodium sulfate. The crude product was crystallized multiple times from

DCM-hexanes to yield **3** (90 mg, 36%) as a white solid, mp 85.5–87.5 °C. [1]H

NMR (500 MHz in CDCl$_3$) δ 8.45 (s, 1H), 8.05 (d, 1H, *J* = 12.5 Hz), 7.66 (d, 1H,

J = 8.0 Hz), 7.57 (t, 1H, *J* = 8.0, 12.5 Hz), 7.44 (t, 1H, *J* = 7.5, 8.0 Hz), 3.90 (s,

3H), 3.88 (s, 3H).

Methyl 2,3-dibromo-3-(2-methoxycarbonylphenyl)propanoate (4):

Bromine (0.1 mL) and **1** (250 mg, 1.14 mmol) were stirred in DCM until the

reaction was judged to be complete by TLC. The excess bromine was evaporated,

and the crude material was applied to a silica gel column with DCM. Collection

of the product spots and evaporation of DCM provided **4** as a colorless solid in

quantitative yield, mp 94–97 °C. ^{1}H NMR (300 MHz in CDCl$_3$) δ 7.95 (d, 1H, *J* =

7.8 Hz), 7.62 (m, 2H), 7.60 (t, 1H, *J* = 7.6 Hz), 6.80 (br s, 1H), 4.90 (br s, 1H),

3.98 (s, 3H), 3.91 (s, 3H). Anal. Calcd (%) for C$_{12}$H$_{12}$Br$_2$O$_4$: C, 37.93; H, 3.18.

Found: C, 37.91; H, 3.13.

Methyl (*Z*)-2-bromo-3-(2-methoxycarbonylphenyl)prop-2-enoate (5) and

Methyl (*E*)-2-bromo-3-(2-methoxycarbonylphenyl)prop-2-enoate (6):

Triethylamine (30 mg, 0.30 mmol) and **4** (100 mg, 0.26 mmol) were combined

and stirred overnight. Two TLC spots developed below the spot for **4** with the

lower of the two spots being **5**. The products were separated by silica gel

chromatography using DCM and hexanes and recrystallized from DCM and

hexanes to yield pure **5** (10 mg, 13%) as a colorless solid, mp 79–80 °C. Isolation

of **6** yielded an oil that was slightly contaminated with **5**.

(**5**) ^{1}H NMR (500 MHz in CDCl$_3$) δ 8.66 (s, 1H), 8.07 (d, 1H, J = 7.3 Hz), 7.60

(d, 2H, J = 7.7 Hz), 7.47 (m, 1H), 3.92 (s, 3H), 3.90 (s, 3H). Anal. Calcd (%) for

C$_{12}$H$_{11}$BrO$_4$: C, 48.18; H, 3.71. Found: C, 48.30; H, 3.62.

(**6**) ^{1}H NMR (500 MHz in CDCl$_3$) δ 8.04 (d, 1H, J = 7.8 Hz), 8.00 (s, 1H), 7.50 (t,

1H, J = 7.5 Hz), 7.42 (t, 1H, J = 7.5 Hz), 7.23 (d, 1H, J = 7.6 Hz), 3.91 (s, 3H),

3.51 (s, 3H).

(3-Oxo-1,3-dihydro-2-benzofuran-1-yl)acetic acid (7):

2-Carboxycinnamic acid (0.95 g, 4.99 mmol) was refluxed in 10 mL acetic acid

and 0.92 g polyphosphoric acid for 2 h before pouring into an Erlenmeyer flask

with 50 mL ice water. After stirring for 1 h, the white precipitate was vacuum

filtered and washed with water. After drying, **7** was recovered (958 mg, 100%) as

a white solid, mp 151–153.5 °C. ^{1}H NMR (500 MHz in acetone-d_6 and TMS) δ

7.85 (d, 1H, J = 7.7 Hz), 7.77 (m, 2H), 7.62 (t, 1H, J = 7.3 Hz), 5.92 (dd, 1H, J =

5.1, 7.5 Hz), 3.15 (dd, 1H, 4.75, 16.8 Hz), 2.87 (dd, 1H, 7.8, 16.8 Hz).

Methyl (3-oxo-1,3-dihydro-2-benzofuran-1-yl)acetate (8):

In a RBF were dissolved **7** (1.146 g, 5.96 mmol) and cesium carbonate (flame

dried prior to using, 1.90 g, 5.83 mmol) in 8 mL of MeCN. After being stirred at

room temperature for about 5 min, a salt precipitated. Iodomethane (3.70 g, 26.1

mmol) was dissolved in 17 mL of MeCN and added to the salt. The reaction

mixture was refluxed on a sand bath for about 1 h, whereupon the reaction was

complete as judged by TLC. MeCN was almost completely evaporated, and

EtOAc was added to the solid. The mixture was filtered, and the filtrate was

evaporated to yield a pale yellow oil (1 g). The oil crystallized upon dissolving in

hot EtOAC and hexanes followed by cooling. This initial precipitate was

repeatedly recrystallized from EtOAc and hexanes to yield **8** as small white

needles in two crops (820 mg and 140 mg, total 960 mg, 78%).

Ethyl (3-oxo-1,3-dihydro-2-benzofuran-1-yl)acetate (9):

7 (198 mg, 1.03 mmol) was dissolved in 12 mL MeCN with cesium carbonate

(338 mg, 1.04 mmol) and stirred at room temperature for 5 min as the milky white

solution turned into a salt-like mixture. Iodoethane (730 mg, 4.67 mmol) was

added, and the mixture was stirred for 1 h at room temperature. The reaction

mixture was then heated at about 60 °C for 1 h and stirring was continued at rt for

2 h. The reaction mixture was filtered, and the filtrate evaporated and collected in

a large volume of chloroform (60 mL). The organic solvent was washed with 2%

aq $NaHCO_3$ (3 × 10 mL), then brine before being dried with sodium sulfate and

rotary evaporation of the solvent to yield **9** (189 mg, 83%) as a white solid. ^{1}H

NMR (500 MHz, $CDCl_3$) δ 7.89 (d, 1H, J = 7.7 Hz), 7.68 (t, 1H, J = 7.5 Hz),

7.54 (t, 1H, J = 7.5 Hz), 7.50 (d, 1H, J = 7.7 Hz), 5.87 (t, 1H, J = 6.6 Hz), 4.19 (t,

2H, J = 7.2 Hz), 2.89 (dd, 2H, J = 3.6, 6.5 Hz), 1.25 (t, 3H, J = 7.2 Hz). This

product was not used in a future synthesis.

2-[(1*E*)-3-methoxy-3-oxoprop-1-en-1-yl]benzoic acid (10):

In a RBF was dissolved **8** (820 mg, 3.98 mmol) in 2 mL DCM. Triethylamine (448 mg, 4.44 mmol) was added, and the reaction mixture was stirred at room temperature while being monitored by TLC. More triethylamine (155 mg, 1.53 mmol) was added as TLC showed starting material present after being stirred overnight. Upon completion of the reaction judged by TLC, 5 mL of 1 M HCl (aq) was slowly added while a precipitate formed. After being stirred for more than 30 min, water (20 mL) was added prior to filtration of the solid, which was washed with more water (460 mg **10**, 56%). Extraction of the aqueous filtrate with EtOAc (3 × 12 mL) yielded additional **10** as an impure, light yellow oil (317 mg, 39%). ^{1}H NMR (400 MHz in acetone-d_6) δ 8.55 (d, 1H, J = 16.0 Hz), 8.02 (d, 1H, J = 8.0 Hz), 7.80 (d, 1H, J = 8.0 Hz), 7.62 (t, 1H, J = 7.6 Hz), 7.52 (t, 1H, J = 7.6 Hz), 6.41 (d, 1H, J = 16.0 Hz), 3.74 (s, 3H).

(*R**, *R**)-Methyl chloro(3-oxo-1,3-dihydro-2-benzofuran-1-yl)acetate (11) and **(*R**, *S**)-Methyl chloro(3-oxo-1,3-dihydro-2-benzofuran-1-yl)acetate (12)**:

Benzyltriethylammonium chloride (511 mg, 2.24 mmol) and potassium permanganate (343 mg, 2.17 mmol) were stirred in 8 mL of DCM. Chlorotrimethylsilane (990 mg, 9.17 mmol) was added, and the solution turned dark green. **10** (420 mg, 2.03 mmol) was not entirely soluble in DCM (10 mL), but an attempt was made to carry out the reaction with TLC monitoring. After being stirred 7 h on ice, the reaction mixture was poured into 30 mL of 0.1 M sodium thiosulfate (aq), and the organic layer was extracted. The aqueous layer was also extracted with EtOAc (3 × 15 mL). A viscous brown oil was recovered

(394 mg) and ^{1}H NMR of this crude material showed mostly ring closure with chlorine addition and a very small amount of chlorine-olefin addition. In TLC with EtOAc:hexanes (1:4) with 1% EtOH, a spot moving with the solvent front was seen, along with two other spots (R_f 0.33 and 0.20). Silica gel chromatography with 10 to 20% EtOAc in hexanes to isolate the two spots resulted in recovery of **11** (85 mg, 17%, > 95% by ^{1}H NMR) as a light yellow oil and **12** (49 mg, 10%) as a colorless solid.

11 ^{1}H NMR (400 MHz, acetone-d_6): δ 7.87 (1H, d, J = 8 Hz), 7.79 (1H, t, J = 8 Hz), 7.69 (2H, m), 6.12 (1H, d, J = 4.8 Hz), 5.19 (1H, d, J = 4.8 Hz), 3.85 (3H, s). IR peaks $\tilde{v}$ (cm^{-1}): small, sharp peaks: 3033, 2955, 1612 and 1597; medium intense peaks: 1466, 1436, 1354, 1110, 895, 865, 838, 798; intense peak 1763, 1281, 1198, 1169, 1060, 997, 687.

12 ^{1}H NMR (400 MHz, CDCl$_3$ and TMS): δ 7.93 (1H, d, J = 7.6 Hz), 7.74 (1H, t, J = 7.6 Hz), 7.57 (2H, m), 6.05 (1H, d, J = 3.6 Hz), 4.83 (1H, d, J = 3.6 Hz), 3.85 (3H, s).

Methyl (2*E*)-3-(2-nitrophenyl)prop-2-enoate (13):

In a 250-mL RBF in ice was added 2-nitrocinnamic acid (950 mg, 4.92 mmol) with 100 mL of MeOH. Acetyl chloride (5 mL) was added slowly, and the solution was refluxed for 90 min. MeOH was evaporated, and the crude was dissolved in DCM, which was washed with water and brine to yield **13** (1.0 g, 98%) as a slightly tan-colored solid. This was used without further purification to make **14**. ^{1}H NMR (400 MHz in CDCl$_3$) δ 8.12 (d, 1H, J = 16.0 Hz), 8.04 (d, 1H,

J = 8.0 Hz), 7.64 (m, 2H), 7.55 (t, 1H, J = 6.8, 8.0 Hz), 6.37 (d, 1H, J = 16.0 Hz), 3.83 (s, 3H).

Methyl 2,3-dichloro-3-(2-nitrophenyl)propanoate (14):

KMnO$_4$ (0.62 g, 3.93 mmol) and benzyltriethylammonium chloride (0.88 g, 3.89 mmol) were stirred in DCM (10 mL). The resulting dark purple solution was cooled, and cold TMSCl (~ 1.68 g, 15.57 mmol) was added. To the now green solution was added **13** (0.81 g, 3.90 mmol). After several hours, the color faded, and TLC showed the reaction to be incomplete. KMnO$_4$ (0.62 g, 3.93 mmol), benzyltriethylammonium chloride (0.89 g, 3.90 mmol) and TMSCl (~ 1.67 g, 15.5 mmol) were prepared as above and added to the reaction mixture. After several more hours, the color faded and TLC showed incomplete reaction. Additional chlorinating reagent was prepared with KMnO$_4$ (0.35 g, 2.19 mmol), benzyltriethylammonium chloride (0.44 g, 1.95 mmol) and TMSCl (0.87 g, 8.06 mmol) in DCM (~ 5 mL) and added to the reaction mixture. After several hours, TLC showed no starting material. The organic layer was washed with 0.1 M sodium thiosulfate and brine before being dried with magnesium sulfate. Evaporation of the solvent left a yellow solid (0.89 g) that had minor impurities by ^{1}H NMR. A silica gel column was run with DCM to collect **14** (0.35 g, 32%) as a faintly yellow-white solid, mp 64–66 °C (chloroform-hexanes). ^{1}H NMR (400 MHz in CDCl$_3$) δ 7.96 (d, 1H, J = 8.0 Hz), 7.74 (m, 2H), 7.56 (t, 1H, J = 7.6 Hz), 6.10 (d, 1H, J = 10.4 Hz), 4.70 (d, 1H, J = 10.4 Hz) 3.89 (s, 3H).

(5-Iodo-3-oxo-1,3-dihydro-2-benzofuran-1-yl)acetic acid (15) and

(7-Iodo-3-oxo-1,3-dihydro-2-benzofuran-1-yl)acetic acid (16):

The electrophilic-iodine reagent was made by crushing iodine (185 mg, 0.73

mmol) in 5 mL 98% sulfuric acid and addition of sodium iodate (153 mg, 0.77

mmol), along with an additional 5 mL sulfuric acid (total moles of iodine, 2.23

mmol). The electrophilic-iodine solution was allowed to stir for 30 min. **7** (400

mg, 2.08 mmol) was dissolved in 5 mL of 98% sulfuric acid, and the

electrophilic-iodine reagent was added dropwise over 20–25 min. The original

reagent flask was rinsed with a small amount of sulfuric acid that was

subsequently added to the reaction mixture, and the combined mixtures were

allowed to stir for 3.5 h at rt. The reaction mixture was poured into an Erlenmeyer

flask containing ice water (150 mL), and the reaction flask was rinsed with water

(50 mL) that was subsequently added to the Erlenmeyer flask. The precipitate that

formed was filtered and washed with water to yield **15** (210 mg, 32%) as an off-

white solid with a slight pink hue to it, mp 188–192 °C. The aqueous filtrate was

extracted with EtOAc to yield about 300 mg of a crude, solid mixture. This was

recrystallized with chloroform to yield an additional 55 mg of product with the

same melting point as above. The remaining material was partially separated by

silica gel cyclograph chromatography (2×) using 10–20% EtOAc in hexanes with

< 2% acetic acid. The first band that eluted (~ 80 mg) was analyzed by ^{1}H NMR,

and the isolated material was identified as the *ortho*-substituted isomer **16** (~ 84%

by NMR); < 30 mg of **15** was recovered from the cyclograph.

15 ^{1}H NMR (500 MHz in acetone-d_6 and TMS) δ 11.13 (br s, 1H), 8.16 (s, 1H),

8.12 (d, 1H, J = 8.1 Hz), 7.60 (d, 1H, J = 8.1 Hz), 5.89 (dd, 1H, J = 5.1, 7.3 Hz),

3.16 (dd, 1H, J = 4.95, 17.0 Hz), 2.93 (dd, 1H, J = 7.5, 17.0 Hz).

16 ^{1}H NMR (500 MHz in acetone-d_6 and TMS) δ 11.11 (br s, 1H), 8.20 (d, 1H, J

= 7.8 Hz), 7.88 (d, 1H, J = 7.6 Hz), 7.43 (t, 1H, J = 7.6 Hz), 5.78 (dd, 1H, J =

2.3, 8.1 Hz), 3.54 (dd, 1H, J = 2.5, 17.0 Hz), 2.90 (dd, 1H, J = 8.2, 17.0 Hz).

Ethyl (5-iodo-3-oxo-1,3-dihydro-2-benzofuran-1-yl)acetate (17):

15 (698 mg, 2.19 mmol) was placed in a 50-mL RBF with 8 mL of MeCN. A brief

reflux dissolved the solid prior to addition of cesium carbonate (1.71 g, 5.25

mmol). Iodoethane (1.74 g, 11.1 mmol) was dissolved in 20 mL of MeCN and

added to the salt mixture before the mixture was refluxed for 2 h. TLC in EtOAc

and hexanes (1:2) showed two product spots forming, the higher of which was

from opening of the lactone, causing the ethyl ester analogue of **1** to form. The

reaction mixture was filtered to remove cesium salts, and the organic filtrate was

evaporated. As much solid as would dissolve in 5 mL chloroform was collected,

and the solution was washed successively with 5 mL of 5% aq NaHCO$_3$ and brine

prior to being dried with sodium sulfate. The solvent was evaporated to yield a

viscous yellow oil (650 mg) as **17** with some diester impurity. This crude material

was used without further purification to make **20**. ^{1}H NMR (400 MHz in CDCl$_3$) δ

8.24 (s, 1H), 7.99 (d, 1H, J = 8.0 Hz), 7.29 (d, 1H, J = 8.0 Hz, partial overlap

with chloroform signal), 5.83 (app t, 1H, J = 6.4, 6.8 Hz), 4.21 (q, 2H, J = 7.2

Hz), 2.95 (dd, 1H, J = 6.6, 16.6 Hz), 2.84 (dd, 1H, J = 6.4, 16.4 Hz), 1.27 (t, 3H,

7.0 Hz).

Methyl (5-iodo-3-oxo-1,3-dihydro-2-benzofuran-1-yl)acetate (18):

15 (270 mg, 0.85 mmol) and cesium carbonate (260 mg, 0.82 mmol) were stirred in a 2-mL RBF with 3 mL of MeCN, which turned to a milky white salt solution in ~ 3 min. Iodomethane (518 mg, 3.65 mmol) was dissolved in 2 mL MeCN and added to the reaction mixture. After stirring for 30 min at room temperature, the RBF was connected to a water condenser and gently heated (< 70 °C). TLC after 50 min of heating showed no more starting material, with a small amount of **1** appearing as a higher spot. The MeCN was evaporated, and chloroform was added with subsequent filtration. The solid salt was dissolved in water and extracted with chloroform (3 × 20 mL). The organic extracts were combined with the filtrate and washed with brine before being dried with sodium sulfate. Rotoevaporation yielded a white oil (243 mg), and silica gel chromatography with 30% EtOAc in hexanes isolated **18** (210 mg, 75%) from unreacted starting material. This material was immediately used to make **21**.

Ethyl (7-iodo-3-oxo-1,3-dihydro-2-benzofuran-1-yl)acetate (19):

16 (500 mg, 1.57 mmol) and cesium carbonate (677 mg, 2.08 mmol) were stirred in MeCN (23 mL) at rt for 3 h. In that time, the initially yellow, sticky solid had broken apart into a cloudy, salt-like suspension. Ethyl iodide (1.07 g, 6.84 mmol) was dissolved in MeCN (2 mL) before being added to the reaction mixture, and the mixture was gently heated (< 65 °C) and stirred magnetically for 1 h. The stir bar stopped when the mixture became sticky and turned orange-yellow. The flask was removed from the heat source and stirred manually until the stir bar was freed. After an additional 1 h of stirring at rt, TLC showed no more reactant. A

similar work up used to isolate **18** was employed. A brown tinted solid was obtained upon solvent evaporation (350 mg, 64%). This material was contaminated by the diester that formed due to the lactone opening and by impurities in the starting material. ^{1}H NMR (400 MHz in CDCl$_3$) δ 8.06 (d, 1H, J = 7.7 Hz), 7.91 (d, 1H, J = 7.6 Hz), 7.31 (t, 1H, J = 7.7 Hz), 5.72 (dd, 1H, J = 2.8, 8.4 Hz), 4.17 (q, 2H, J = 7.2 Hz), 3.52 (dd, 1H, J = 2.8, 16.6 Hz), 2.78 (dd, 1H, J = 8.4, 16.6 Hz), 1.24 (t, 3H, J = 7.1 Hz).

5-iodo-2-[(1*E*)-3-ethoxy-3-oxoprop-1-en-1-yl]benzoic acid (20):

17 (350 mg, 1.01 mmol) and triethylamine (102 mg, 1.01 mmol) were stirred in a RBF in 5 mL MeCN at room temperature overnight. There was no change as judged by TLC. The volume of MeCN was reduced to 1 mL and more triethylamine (539 mg, 5.34 mmol) was added before the reaction mixture was gently heated (sand bath, ~ 60 °C). The reaction mixture was stirred until it was judged complete by TLC. EtOAc was added to the reaction material, and it was acidified with 3 M HCl (aq). The organic was removed and washed with brine before being dried with sodium sulfate. The organic solvent was rotary evaporated off. The residue was subjected to silica gel chromatography using EtOAc–hexanes (2:3) with < 2% AcOH to isolate **20** (280 mg, 80%) as an off-white solid contaminated with about 6% of the ethyl ester analogue of **22** by NMR. ^{1}H NMR (400 MHz in acetone-d_6) δ 8.47 (d, 1H, J = 16.0 Hz), 8.33 (s, 1H), 7.98 (d, 1H, J = 8.3 Hz), 7.61 (d, 1H, J = 8.3 Hz), 6.45 (d, 1H, J = 16.0 Hz), 4.21 (q, 2H, J = 7.1 Hz), 1.29 (t, 3H, 7.1 Hz).

5-Iodo-2-[(1E)-3-methoxy-3-oxoprop-1-en-1-yl]benzoic acid (21):

To **18** (210 mg, 0.63 mmol) was added triethylamine (130 mg, 1.29 mmol), which was stirred at rt before being gently heated in a warm water bath (~ 50 °C). More triethylamine (120 mg, 1.19 mmol) was added before the reaction was judged complete by TLC. Addition of 3.5 mL of 1 M HCl (aq) was followed by chloroform extraction (3 × 2 mL). The organic layer was dried with sodium sulfate and evaporated to yield 200 mg of crude white solid which was recrystallized (CHCl₃–hexanes) to yield **21** (105 mg, 50%) that was immediately used to make **24**.

3-Iodo-2-[(1E)-3-methoxy-3-oxoprop-1-en-1-yl]benzoic acid (22):

The crude **19** (350 mg, 1.01 mmol) from an incomplete reaction with triethylamine was stirred in MeOH (5 mL) with NaOMe (50 mg, 0.93 mmol) for 1 h at rt and monitored by TLC. The solution was heated by sand (45–75 °C) for 2 nights (~ 40 h), and a ^{1}H NMR spectrum of an aliquot showed the lactone opened with the ethyl ester replaced by a methyl ester (transesterification). Additional NaOMe (70 mg, 1.30 mmol) was added, and the reaction mixture heated until the reaction was complete by TLC. MeOH was evaporated before addition of water (10 mL), and the mixture was extracted with EtOAc (4 × 10 mL). The combined organics were washed with brine before being dried with sodium sulfate. Evaporation of the solvent yielded a solid (300 mg) that was recrystallized (DCM-hexanes) to give **22** (120 mg, 36%). ^{1}H NMR (400 MHz in CDCl₃) δ 10.72 (br s, 1H), 8.11 (d, 1H, J = 7.9 Hz), 7.98 (d, 1H, J = 7.3 Hz), 7.92 (d, 1H, J = 16.2

Hz), 7.13 (d, 1H, J = 7.9 Hz), 5.99 (d, 1H, J = 16.2 Hz), 3.85 (s, 3H). Peaks

corresponding to DCM and hexanes were present, too.

2-(1,2-Dibromo-3-ethoxy-3-oxopropyl)-5-iodobenzoic acid (23):

In 5 mL DCM were dissolved **20** (293 mg, 0.847 mmol) and bromine (140 mg,

0.875 mmol). The reaction mixture was stirred at room temperature until the

reaction was judged complete by TLC. The solvent and excess bromine were

evaporated. The solid residue was redissolved in DCM prior to being washed with

water and brine and dried with sodium sulfate to yield 350 mg of crude solid

material. Repeated recrystallizations from DCM-hexanes yielded **23** (275 mg,

64%) as a white solid, mp 162–165 °C. ^{1}H NMR (500 MHz in CDCl$_3$) δ 8.46 (s,

1H), 7.99 (d, 1H, J = 8.5 Hz), 7.41 (d, 1H, J = 8.5 Hz), 6.83 (br s, 1H), 4.81 (br s,

1H), 4.39 (q, 2H, J = 7.0 Hz), 1.39 (t, 3H, J = 7.0 Hz); Anal. Calcd (%) for

$C_{12}H_{11}Br_2IO_4$: C, 28.49; H, 2.19. Found: C, 28.58; H, 2.15.

2-(1,2-Dichloro-3-methoxy-3-oxopropyl)-5-iodobenzoic acid (24):

Potassium permanganate (47.5 mg, 0.30 mmol) and benzyltriethylammonium

chloride (69 mg, 0.30 mmol) were stirred in 2 mL of DCM for 20 min before

addition of TMSCl (198 mg, 1.82 mmol) in 5 mL of DCM while on ice. To the

reaction mixture was added **21** (95 mg, 0.29 mmol) with stirring. TLC of the

reaction mixture showed product formation stopped without multiple spots having

appeared (reactant/product degradation), but the green reaction mixture color had

faded. A second equivalent of chlorinating reagent, as described above with

KMnO$_4$, benzyltriethylammonium chloride and TMSCl, was added, which

resulted in the starting alkene spot vanishing by TLC. Addition of 1 M sodium thiosulfate (aq) to quench the permanganate was followed by extraction of the organic layer with additional DCM. The combined organics were washed with brine before being dried by sodium sulfate. Purification by silica gel chromatography (EtOAc-hexanes) along with recrystallization (chloroform-hexanes) yielded **24** (61 mg, 52.9%) as a white solid, mp 159–162.5 °C. ^{1}H NMR (400 MHz in CDCl$_3$) δ 8.47 (s, 1H), 8.00 (d, 1H, J = 8.4 Hz), 7.46 (d, 1H, J = 8.4 Hz), 6.64 (d, 1H, J = 10.0 Hz), 4.68 (d, 1H, J = 10.0 Hz), 3.90 (s, 3H).

Methyl iodo(3-oxo-1,3-dihydro-2-benzofuran-1-yl)acetate (25):

Iodine (472 mg, 1.86 mmol), sodium iodate (194 mg, 0.98 mmol) and 98% sulfuric acid (8 mL) were combined and stirred for about 30 min. This solution was added to **1** and stirred at rt for 95 min. The reaction mixture was poured into ice water (60 mL) and extracted with EtOAc (3 × 40 mL). The combined organics were washed with brine and dried with sodium sulfate. Evaporation of the solvent yielded a crude off-white solid (1.26 g, 89%). Recrystallization from DCM and hexanes yielded **25** (1.12 g, 72%) as a white solid, mp 121.5–126.5 °C. This material was used in syntheses (**26**, **27**, and **28**) without extensive purification. ^{1}H NMR (400 MHz, CDCl$_3$): 7.94 (m, 2H), 7.72 (t, 1H, J = 7.6 Hz), 7.62 (t, 1H, 7.6 Hz), 5.67 (d, 1H, J = 6.4 Hz), 4.79 (d, 1H, J = 6.0 Hz), 3.86 (s, 3H).

Methyl iodo(5-iodo-3-oxo-1,3-dihydro-2-benzofuran-1-yl)acetate (26):

Electrophilic-iodine reagent was prepared in a 50-mL RBF from iodine (480 mg,

1.89 mmol), sodium iodate (190 mg, 0.96 mmol) and 98% sulfuric acid (25 mL) with stirring for about 30 min. The dark red-black solution was added to **1** (940 mg, 4.27 mmol). After being stirred for 1 h, the reaction mixture was poured into 300 mL of cold water that was in an ice bath. The reaction flask was rinsed with 50 mL of cold water that was added to the aqueous solution. Viscous black semi-solid precipitated, and it was filtered after 1 h (the next day for some procedures) and rinsed with water. The black solid was dissolved in EtOAc that was washed with sodium bisulfite and brine prior to being dried with sodium sulfate and evaporated to provide a yellow oil. Additionally, the aqueous filtrate was extracted with EtOAc (3 × 300 mL), and washed and dried as above, to yield additional crude material. All the crude was subjected to another round of electrophilic-iodine reagent as described in the beginning of this procedure with similar workup steps. Silica gel chromatography (EtOAc-hexanes) and recrystallization (CHCl$_3$–hexanes) were used to isolate **26** (650 mg, 33% from **1**) as a white solid, mp 134–135.5 °C. ^{1}H NMR (500 MHz, CDCl$_3$): δ 8.27 (s, 1H), 8.02 (d, 1H, J = 8.0 Hz), 7.71 (d, 1H, J = 8.5 Hz), 5.57 (d, 1H, J = 5.5 Hz), 4.84 (d, 1H, J = 6.0 Hz), 3.86 (s, 3H).

Methyl (2Z)-(3-oxo-2-benzofuran-1(3H)-ylidene)ethanoate (27) and
methyl (2E)-(3-oxo-2-benzofuran-1(3H)-ylidene)ethanoate (28):
25 (115 mg, 0.35 mmol) was stirred in 0.5 mL of DCM with 180 mg triethylamine overnight. An additional 206 mg of triethylamine was added over the course of another day until the starting material spot disappeared by TLC (321 mg NEt$_3$ total, 3.18 mmol). The reaction mixture was acidified and extracted with EtOAc

to yield 90 mg of crude. Silica gel column chromatography with EtOAc-hexanes (7:3) was used to isolate **28** (15 mg, 21%) as the first material off the column and **27** (12.5 mg, 17.5%) as the second material off the column. *E*-alkene, **28**: ^{1}H NMR (500 MHz, CDCl$_3$): δ 9.06 (d, 1H, *J* = 8.0 Hz), 7.98 (d, 1H, d, *J* = 7.5 Hz), 7.84 (t, 1H), 7.72 (t, 1H), 6.17 (s, 1H), 3.85 (s, 3H). *Z*-alkene, **27**: ^{1}H NMR (400 MHz, CDCl$_3$): δ 7.99 (d, 1H, *J* = 6.4 Hz), 7.78 (m, 2H), 7.70 (t, 1H), 5.90 (s, 1H), 3.86 (s, 3H).

Methyl (2*E*)-(5-iodo-3-oxo-2-benzofuran-1(3H)-ylidene)ethanoate (29) and methyl (2*Z*)-(5-iodo-3-oxo-2-benzofuran-1(3H)-ylidene)ethanoate (30): **26** (140 mg, 0.31 mmol) was treated with distilled and dried triethylamine (75 mg, 0.74 mmol) in < 0.5 mL of CHCl$_3$ in a conical vial. The reaction mixture turned yellow immediately, and some solid precipitated. An air condenser and drying tube were attached, and the reaction mixture warmed to about 45 °C on a sand bath. After 2 h, TLC showed starting material still present. Additional triethylamine (65 mg, 0.64 mmol) was added, and the reaction mixture was stirred at ~ 45 °C overnight. The next day, chloroform and 1 M HCl (aq) were added to the now red reaction solution, which faded to a clear yellow color once stirred. The solution was extracted with CHCl$_3$ (3 × 4 mL), the organics combined and washed with brine before drying with sodium sulfate to yield 93 mg of crude yellow oil. The aqueous was also extracted with EtOAc (2 × 8 mL), which was similarly washed and dried to yield 93 mg of yellow solid. The two extracted materials were combined and subjected to column chromatography with EtOAc and hexanes, and **29** eluted first. A white solid was obtained upon recrystallization

114

with DCM and hexanes (60 mg, 60%), mp 170.5–172.5 °C. A small amount of the

Z-isomer **30** was isolated but slightly impure (20 mg, <20%). **29**: ^{1}H NMR (500

MHz, CDCl$_3$): δ 8.81 (d, 1H, J = 8.5 Hz), 8.31 (s, 1H), 8.13 (d, 1H, J = 8.0 Hz),

6.19 (s, 1H), 3.85 (s, 3H).

30: ^{1}H NMR (500 MHz, acetone-d_6): δ 8.37 (s, 1H), 8.28 (d, 1H, J = 8.0 Hz),

7.96 (d, 1H, J = 8.0 Hz), 6.22 (s, 1H), 3.81 (s, 3H).

3-(Nitromethyl)-2-benzofuran-1(3H)-one, "3-nitromethylphthalide," (**31**):

Nitromethane (4.27 g, 66.5 mmol) and 2-formylbenzoic acid (10 g, 66.7 mmol)

were stirred in a 250-mL RBF with MeOH (40 mL) while on an ice-water bath.

Sodium hydroxide (6.43 g, 156 mmol), dissolved in water (22 mL), was cooled on

ice then added to the RBF. After 80 min of being stirred on ice, 40 mL of 5 N HCl

(aq) was added to the stirred solution. A few color changes occurred but faded

quickly before the solution became pale yellow and then colorless. In about 5

min, a white precipitate developed. The solution was stirred 4.5 h (or overnight in

some procedures) on a fresh ice bath before filtration. The filtered solid was

washed with about 150 mL water and dried on a vacuum filter. Additional drying

on dry filter paper and vacuum-oven drying yielded **31** (12.0 g, 93%) as a white

solid, mp 129.5–131.5 °C that could be optionally recrystallized (MeOH) to yield

colorless blocks with a similar melting point.

^{1}H NMR (400 MHz, acetone-d_6): δ 7.89 (d, 2H, J = 7.7 Hz), 7.84 (d, 2H, J = 4.3

Hz), 7.69 (m, 1H), 6.29 (dd, 1H, J = 2.9, 8.3 Hz), 5.44 (dd, 1H, J = 2.8, 14.5 Hz),

4.98 (dd, 1H, J = 8.4, 14.5 Hz).

6-Iodo-3-(nitromethyl)-2-benzofuran-1(3H)-one (32):

Iodine (6.23 g, 24.5 mmol) was partially crushed in 113 mL of 98% sulfuric acid.

Sodium iodate (2.45 g, 12.4 mmol) was added with an additional 40 mL of 98%

sulfuric acid. The electrophilic-iodine reagent was stirred 40 min before the

solution turned a dark, brown-red color. **31** (9.64 g, 49.9 mmol) was added to the

solution and stirred 140 min before the reaction mixture was poured into 1000 g

of ice. The reaction flask was rinsed with water that was also poured into the same

ice flask. The flask was placed in an ice bath and stirred overnight. The solution

was vacuum filtered and washed with more water before the filtered solid was

dissolved in EtOAc (150 mL). The organic solution was washed with saturated

sodium bisulfite (turning the solution from dark red to orange-yellow) and brine

before being dried with sodium sulfate. About 12.5 g of sticky, yellow solid was

recovered after evaporation of the EtOAc. About 40 mL of DCM was added to the

crude material and everything dissolved except 4.1 g of pink-yellow solid. The

solid was filtered and collected, and the DCM filtrate was placed in the freezer

overnight to precipitate additional solid. The initially insoluble solid (4.1 g) and

precipitate from overnight freezing, which was collected by filtration, totaled 5.5–

6 g. Recrystallization yielded **32** (4.6 g, 28.8%), as a white solid (CHCl$_3$) or white

needles (EtOH), mp 126–129 °C for both. ^{1}H NMR (400 MHz, acetone-d_6) δ 8.23

ppm (s, 1H), 8.20 ppm (d, 1H, J = 8.0 Hz), 7.70 ppm (d, 1H, J = 8.0 Hz), 6.30

ppm (dd, 1H, J = 3.2, 8.2 Hz), 5.44 ppm (dd, 1H, J = 2.8, 14.8 Hz), 5.04 ppm (dd,

1H, J = 8.2, 14.7 Hz). ^{1}H NMR (400 MHz, CDCl$_3$ and TMS) δ 8.31 ppm (s, 1H),

8.06 ppm (d, 1H, J = 8.0 Hz), 7.30 ppm (d, 1H, J = 8.0 Hz), 6.08 ppm (dd, 1H, J

= 4.6, 7.4 Hz), 4.81 ppm (dd, 1H, J = 4.5, 14.1 Hz), 4.73 ppm (dd, 1H, J = 7.5, 14.1 Hz).

3-[Dibromo(nitro)methyl]-2-benzofuran-1(3H) (33):

31 (1.922 g, 9.96 mmol) was dissolved in DCM (5 mL). NaHCO$_3$ (919 mg, 10.9 mmol) dissolved in water (10 mL) was added to the organic phase and stirred vigorously while on an ice-water bath. Bromine (1.6 g, 10.0 mmol) was dissolved in 5 mL DCM and added to the biphasic mixture. The reaction was stirred on ice for 2.5 h before the reaction material was allowed to warm to rt. Optionally added was sodium bromide (200 mg, 1.94 mmol; for some reactions). After the red color faded (~ 5 h), a second equivalent of bromine (1.6 g, 10 mmol) dissolved in DCM (5 mL) was added. The reaction mixture was placed back on ice before addition of the second equivalent of NaHCO$_3$ (0.870 g, 10.4 mmol) with 3 mL of water. The reaction mixture was again warmed to room temperature and stirred until the reaction mixture was complete by TLC (48–72 h). The organic solution was extracted before being washed with brine and dried with sodium sulfate. Rotoevaporation yielded **33** (2.68g, 76.7%) as a white solid (mp 95–99 °C) and colorless blocks upon recrystallization, mp 98.5–101.5 °C (EtOAc-hexanes). ^{1}H NMR (400 MHz, CDCl$_3$ and TMS) δ 8.00 ppm (d, 1H, J = 7.6 Hz), 7.88 ppm (d, 1H, J = 7.8 Hz), 7.81 ppm (t, 1H, J = 7.4, 7.6 Hz), 7.73 ppm (t, 1H, J = 7.5 Hz), 6.40 ppm (s, 1H).

3-[Bromo(nitro)methyl]-2-benzofuran-1(3H)-one (34):

32 (1.187 g, 3.72 mmol) was stirred in chloroform (5 mL) on an ice bath.

Pyridiniumbromide perbromide (2.69 g, 7.57 mmol) was added as a solid, and

2,6-lutidine (841 mg, 7.86 mmol) was dissolved in chloroform (5 mL) before

being added one molar equivalent at a time. The second equivalent of each was

added after the red solution color faded to orange (< 3 h). The flask was allowed

to warm to about 15 °C until the reaction was complete by TLC (~ 7 h). The

organic solution was washed with 1 M HCl (3 × 25 mL) and brine before being

dried with sodium sulfate. Evaporation of the organic yielded a yellow solid after

vacuum drying (1.46 g). Silica gel chromatography with DCM yielded a yellow

solid, too (1.3 g). Recrystallization provided **34** (0.880 g, 49.7%) as a white

powder, mp 117–122 °C (EtOAc-hexanes). White needles (120 mg) were

recovered from the mother liquor, and the residual crude from evaporation of the

mother liquor was recrystallized again to yield a lightly yellowed solid (162 mg)

and light needles (130 mg), mp 117–122 °C. ^{1}H NMR (400 MHz, CDCl$_3$ and

TMS) δ 8.32 ppm (s, 1H), 8.12 ppm (d, 1H, J = 8.4 Hz), 7.66 ppm (d, 1H, J = 8.0

Hz), 6.36 ppm (s, 1H). ^{13}C NMR (100 MHz) δ 165.7, 143.7, 142.7, 135.4, 128.9,

125.4, 97.2, 87.2, 83.1 ppm.

(R*, S*)-3-[Bromo(nitro)methyl]-2-benzofuran-1(3H)-one (35):

33 (1.792 g, 5.11 mmol) was dissolved in AcOH (10.5 mL). Thiourea (0.390 g,

5.12 mmol) was dissolved in water (11 mL) and added dropwise over 4–5 min to

the AcOH solution while being magnetically stirred. As the aqueous thiourea

solution was added, the reaction mixture turned yellow, and precipitate

continually developed after half of the aqueous-thiourea solution was added. The reaction mixture was vacuum filtered 40 min after the initial aqueous solution addition, and the solid was washed with about 100 mL of water. The light yellow crude material (1.067 g, 76.8%) was dried on vacuum filter. Additional precipitate formed in the filtrate and was collected (0.100 g orange-yellow solid). The original precipitate was recrystallized with EtOAc and hexanes to yield **35** (0.660 g, 47.5 %) as white needles, mp 127–129.5 °C (~ 45:1 diastereomer ratio of **35**:**36** by NMR comparison of the doublets between δ 6.4 and 6.0 ppm; presumably reacemic). ^{1}H NMR (400 MHz, CDCl$_3$ and TMS) δ 7.99 ppm (d, 1H, 7.6 Hz), 7.79 ppm (t, 1H, J = 7.6 Hz), 7.69 ppm (t, 1H, J = 7.6 Hz), 7.60 ppm (d, 1H, J = 7.6 Hz), 6.36 ppm (d, 1H, J = 4.0 Hz), 6.19 ppm (d, 1H, J = 3.6 Hz); ^{13}C NMR (100 MHz) δ 168.1, 143.1, 135.1, 131.1, 126.6, 126.3, 122.5, 80.5, and 78.7 ppm; Anal. Calcd (%) for C$_9$H$_6$BrNO$_4$: C 39.73, H 2.22, N 5.15. Found: C 39.66, H 2.24, N 5.11.

(*R**, *R**)-3-[Bromo(nitro)methyl]-6-iodo-2-benzofuran-1(3H)-one (37):
34 (153 mg, 0.32 mmol) was dissolved in 0.5 mL THF and stirred in an ice bath. Thiourea (52 mg, 0.68 mmol) was dissolved in 0.3 mL THF and 0.7 mL 1 M HCl and cooled on ice prior to being added. The thiourea solution was added dropwise over about 3.5 min, however the rate of addition was later determined to not be important. The lower layer was immediately removed, and the aqueous was extracted with DCM. The THF layer and DCM extract were combined and evaporated. The residue was taken up in DCM, which was washed with 1 M HCl (aq) and brine before being dried with sodium sulfate. Evaporation of the organic

left a faintly tan oil (116 mg). Several recrystallizations from EtOAc and hexanes

yielded **37** (26 mg, 20%) as colorless blocks of one diastereomer (presumably

racemic) by ^{1}H NMR, mp 107–110 °C. ^{1}H NMR (400 MHz, CDCl$_3$ and TMS) δ

8.31 ppm (s, 1H), 8.09 ppm (d, 1H, J = 8.0 Hz), 7.35 (d, 1H, J = 8.0 Hz), 6.33

ppm (d, 1H, J = 3.6 Hz), 6.10 ppm (d, 1H, J = 3.6 Hz); ^{13}C NMR (100 MHz) δ =

166.2, 143.8, 142.4, 135.6, 128.3, 124.0, 95.5, 79.7, and 78.7 ppm; Anal. Calcd

(%) for C$_9$H$_5$BrINO$_4$: C 27.16, H 1.27, N 3.52. Found C 27.29, H 1.12, N 3.54.

Table 8. Reduction of **34** by Thiourea in Various Systems

Composition[a]	Thiourea, HCl[b]	Diastereomer Doublets (3.6 Hz, 7.2 Hz)[c]
THF, H$_2$O (5:1)	0.99[d]	3, 1
THF, AcOH (1:1)	1	2, 1[e]
THF, HCl (3:1)	1, ~ 3	~ 3, 1
THF, H$_2$O (1:2)	2.13[d]	~ 1.28, 1
THF, HCl (3:1)	2, 0.19	~ 2.4, 1
THF, HCl (2.2:1)[f]	1, 1	~ 5, 1
THF, NaHCO$_3$ (2:1)[g]	~ 1, 1[g]	~ 2.25, 1

[a] Ratio displayed is by volume.
[b] In molar equivalents for each substance in comparison to **34**.
[c] Doublet ratio is from crude ^{1}H NMR, with 3.6 Hz attributed to **34** and 7.2 Hz the unisolated diastereomer (*R**, *S**).
[d] Only thiourea was used and no acid.
[e] About 25% of the material remaining is **34**, by ^{1}H NMR.
[f] Experimental for this reaction is described above.
[g] Sodium bicarbonate used in place of HCl.

SRB Assay[105]

Inhibition of human cancer cell line growth was performed by Dr J. C. Chapuis and determined using the NCI's sulforhodamine B assay as previously described. In summary, cells in a 5% fetal bovine serum/RPMI 1640 medium were inoculated in 96-well plates and incubated for 24 h. The compounds were added as serial dilutions. After 48 h, the plates were fixed with trichloroacetic acid, stained with sulforhodamine B and read with an automated microplate reader. Growth inhibition data (GI_{50} and TGI) and cell death data (LC_{50}) were calculated from optical density with Immunosoft software.

MTT Assay[106]

Inhibition of human cancer cell line growth was performed by Dr J. C. Chapuis. Cells were treated with a range of concentrations of each compound and seeded in 96-well plates with 200 µL/well and five wells per sample concentration at a density of between $1–4 \times 10^4$ cells/mL. Control cells were treated with 0.1% DMSO and blank wells were loaded with medium only. After 5 days, 50 µL 1.0 mg/ml MTT was added to each well and the plates were incubated for 4 h at 37 °C prior to dissolution of fomazan crystals in 200 µL DMSO. Absorbance at 570 nm was determined for each well, and the survival fraction for each was calculated from the following ratio: (mean A_{570} treated cells – mean A_{570} blank wells) / (mean A_{570} control – mean A_{570} blank). The IC_{50} was determined using CalcuSyn software (Biosoft, Cambridge, UK).

Synthesis of bromonitromethane from nitromethane (essentially as described by Slagh[72]):

Water (120 mL) was added to an Erlenmeyer flask and cooled on ice prior to addition of NaOH pellets (4.178 g, 101.3 mmol). After the solid dissolved, nitromethane (6.510 g, 101.3 mmol), previously cooled on ice, was poured into the aqueous solution. The mixture was swirled for 1 min and immediately poured into a 500 mL RBF that was placed in a salt-ice bath with a stir bar and bromine (16.32 g, 101.5 mmol). Initially, the mixture was swirled vigorously by hand, and then it was stirred magnetically for 25 min. The red bromine color faded and a yellow-white oil developed. The mixture was distilled to collect the products and water in a Dean-Stark trap. Upon cooling, the products separated from water as the lower layer and were transfered to a vial prior to being stored in a freezer (-20 °C) overnight. Small water droplets appear, and the organic is removed to a new vial and stored overnight. Droplets did not form again. ^{1}H NMR (400 MHz, CDCl$_3$ and TMS) δ 7.22 (s, 1.00, 4.73%, CHBr$_2$NO$_2$), 5.72 (s, 36.32, 85.59%, CH$_2$BrNO$_2$) and 4.33 (s, 5.91, 9.32%, CH$_3$NO$_2$).

Table 9. Composition of Brominated Nitromethane by ^{1}H NMR

Substance	Proton Integration value (I.V.)	I.V. / total # of protons	% Compound[a]
CH$_3$NO$_2$	5.91	1.97	9.32
CH$_2$BrNO$_2$	36.3	18.2	85.6
CHBr$_2$NO$_2$	1.00	1.00	4.73

[a] 100% × (integration value ÷ total # of protons) ÷ (1.97 + 18.16 + 1.00)

Crude product in Chapter 2.9, 2-formylbenzoic acid reaction with

bromonitromethane to produce 7.5 Hz doublets attributed to

(R*, R*)-3-[bromo(nitro)methyl]-2-benzofuran-1(3H)-one (36):

2-Formylbenzoic acid (150 mg, 1 mmol) and sodium bicarbonate (86 mg, 1

mmol) were dissolved in water and EtOH (1 mL each) in a 25 mL RBF that was

placed on an ice-water bath. Methylamine (40% in water, 8 mg, 0.1 mmol) and

sodium carbonate (15 mg, 0.15 mmol) were added to the RBF and stirred

magnetically. Bromonitromethane (490 mg, < 3.5 mmol) was dissolved in EtOH

(5 mL) and added over 65 min to the stirred solution. The solution was faintly red

by complete addition and stirring was continued. After an additional 2.5 h, water

(15 mL) and 10% H_2SO_4 (3 mL) were added, and the acidic solution was stirred

overnight at rt. The faintly yellow precipitate was collected by filtration and dried;

mp (116–119 °C) and ^{1}H NMR (Major:Minor, i.e., **36**:BNLA product, ~ 6.6:1). ^{1}H

NMR (400 MHz, $CDCl_3$ and TMS) δ 7.99 (d, 1H, $J = 7.7$ Hz), 7.78 (m, 2H), 7.70

(m, 1H), 6.13 (d, 1H, $J = 7.5$Hz), 6.02 (d, 1H, $J = 7.5$Hz).

Minor product: δ 8.41 (d, 1H, $J = 7.9$ Hz), 7.92 (m, 2H), everything else was

overlapped by the major product, suspected **36**.

PTP assay with DIFMUP (for **24**, **29**, **33**, **35** and **37**):

Compounds were prepared as 5 mM DMSO stock solutions except for **29**, which

was prepared as a 2.5 mM solution after UV solubility results (see page 134).

They were diluted 2 µL into a total volume of 100 µL of appropriate buffer

(correspondence with Millipore, Ltd.) with 0.1 mM DTT at pH 7.2 containing

individual PTP enzymes (CD45, PTP1B, SHP1, SHP2 and TCPTP). The

fluorescence measurement obtained by hydrolysis of the substrate from wells with a compound were compared to control wells without the compound to which 2 µL of DMSO was added, to determine the activity of each enzyme. This assay was conducted by Millipore Corporation under their Enzyme Profiling Services, and the assay results were released on March 13, 2012 (QA Report: George, Charles; QC Report: Jackson, Wayne).

Assay, pNPP (**2–5**, **14**, **23**, **24**, **27**, **28** and **29**)

Original buffer stock solution:

1 mM EDTA, 0.5 mM 3,3-dimethylglutaric acid, 0.15 M NaCl, and 0.01% Triton X-100 was prepared at pH 7 for the stock buffer. The assay buffer contained 1–10 mM DTT added to the stock buffer. The pNPP substrate was prepared from pellets purchased from Sigma Aldrich and dissolved in the stock buffer. The final pNPP concentration in the enzyme assay was typically 10 mM.

PTPβ was purchased from U.S. Biological as the *E. coli* expressed catalytic domain (a.a. 1675–1996) that was 90% by SDS-PAGE with a specific activity of 40 U/µg. Manufacture's definition, "One unit will hydrolyze 1 nmole of pNPP per minute at pH 7.4 and 30 °C." It was supplied as 20 µg (800 units) in 25 mM Tris-HCl, pH 8.0, 75 mM NaCl, 0.05% Tween-20, 50% glycerol, 2 mM EDTA, 3 mM DTT and 10 mM glutathione. This was diluted with stock buffer to slightly more than twice the original volume and separated into nine aliquots. Eight of the aliquots, 4 µL, were estimated to contain 94 units each, and the last vial, ~ 2 µL, had 47 units. These aliquots were stored at -70 °C and diluted with additional stock buffer prior to use in assays.

PTP1B was purchased from U.S. Biological as the *E. coli* expressed catalytic domain (a.a. 1–321) that was 95% by SDS-PAGE with a specific acitivity of 6,000–12,000 units/mg. Manufacture's definition, "One unit will hydrolyze 1 nmole of pNPP per minute at pH 7.4, 37 °C using 10 mM substrate." It was supplied as 250 µg (1500–3000 units) in 25 mM Tris-HCl, pH 7.5, 2 mM β-mercaptoethanol, 1 mM EDTA, 1 mM DTT and 20% glycerol. Stock buffer was added to nearly double the volume, and eleven aliquots were made from this dilution. Ten aliquots had about 23 µg (138–376 units) and the final one had 18.5 µg (111–222 units). These aliquots were stored at -70 °C and diluted with additional buffer prior to use in assays.

Enzyme assays used stock buffer with added DTT (1–10 mM). The enzyme aliquots were diluted to 250 µL with the DTT buffer, and 5 µL of the enzyme in buffer was used per well (PTPβ ~ 1.88 units & PTP1B ~ 2.31 µg, 13–27 units). Potential inhibitors were dissolved in DMSO solutions to a final concentration of 40–73 mM. An inhibition assay was attempted by dilution of the DMSO stocks into assay buffer with enzymes for a few of the compounds, but not all appeared to remain soluble. The DMSO-stock of each compound was then diluted into stock buffer to achieve soluble concentrations of 0.12–1.06 mM. These solutions were stored in the dark at about 4 °C overnight and allowed to warm to room temperature without precipitate forming, before being used. These pre-diluted mixtures were used in the assays in varying amounts, usually between 10–20 µL, to obtain final assay concentrations between 50–120 µM.

The inhibition of the enzymes was monitored by addition of the compound solutions or stock solution (blank) to the enzyme. After incubation for 10–60 min, pNPP was added. After 1–3 min, 1 M NaOH (aq) was added to stop the reaction, and the absorbance at 405 nm was measured. Regardless of the compound used or its concentration, there was never a consistently measurable difference between the wells with compounds and the control.

UV experimental:

Solubility determination for **24**, **29**, **33**, **35** and **37** prior to submission for DIFMUP assay[107]

A 5 mM DMSO stock solution was made for each compound. The experiment was conducted in duplicate, with DMSO stock solutions diluted 2 µL of 5 mM of compound into 98 µL of phosphate-buffered saline (PBS), pH 7.4 (purchased from Sigma) to acquire 100 µM concentration of compound. Blank wells were included by dilution of 2 µL of DMSO into 98 µL of PBS. Absorbance readings were taken at 630 nm at room temperature initially and then at the planned DIFMUP-PTP assay temperature of 37 °C. The absorbance value for every compound except **29** was below or between the absorbance readings for the two blank wells when at room temperature. The absorbance value for every compound well was below the blank readings upon warming to 37 °C except for the wells with **29** in them. They still returned absorbance values up to five times greater than the blank readings. Reducing the concentration of **29** by half (by addition of 1 µL of 5 mM **29** and 1 µL of DMSO to 98 µL of PBS) and reacquisition of the absorbance resulted in values below the blank absorbance

values.

33, **35** and **37** were again made into 5 mM DMSO stock solutions. For PBS spectra, 2 µL of the DMSO stock was diluted to 100 µL in a Costar UV plate with PBS, pH 7. The spectra were acquired from 200–400 nm. Glass-distilled water, pH 7, was used for the water spectra, and they were collected at 100 µL volumes similar to PBS spectra. For the figure with spectra titled as having 50 µL of 2 M NaOH (aq) added (Figure 39), the final volume was 150 µL. Blank spectra were acquired with DMSO in place of the DMSO-inhibitor stock solution and addition of the same amount of 2 M NaOH (aq). Absorbance values of blank wells were subtracted from experimental wells, and molar absorptivity was determined as described below.

Molar absorptivity (ε, $M^{-1}cm^{-1}$) is calculated from the Beer's Law (eqn1).

1. $A = \varepsilon c \ell$

The absorbance (A) is found as optical density, and the concentration (c) is known from the inhibitor preparation. The path length (ℓ) was calculated from the dimensions of the wells of the plate as provided by Corning, the manufacturer of Costar plates.[108] Well dimensions of Costar UV plate are as follows:

Well depth = 10.67 mm; diameter (top; bottom) = 6.86 mm; 6.35 mm; Well Volume = 360 µL. Since the well diameter varies, the calculation is an approximation, but the volume is similar to a cylinder (eqn 2):

2.
$$V_{cylinder} = \frac{\pi h D^2}{4}$$

The beam passes through a length of solution equal to the height of the cylinder (eqn 3):

$$h = \frac{4V_{cylinder}}{\pi D^2}$$

3.

The diameter at the top of the solution depends on the final volume, and it must be between the maximum and minimum diameter. If V_F is the final volume of the solution, then D′ will be the new diameter at the top of the solution with that volume (eqn 4):

$$D' = \left(\frac{V_F}{360 \ \mu L}\right) \Delta D + D_{bottom}$$

4.

If the final volume in equation 4 is the same as the maximum well volume (360 µL), then D′ will be equal to D_{top} because $\Delta D + D_{bottom} = D_{top}$. Replacing D in equation 3 with D′ from equation 4 provides the height (h). Taking V_F as 100 µL, affords D′ as 6.492 mm and height as 3.02 mm (or 0.302 cm) as the path length traveled. This calculation was used to find ℓ in equation 1 that afforded values for molar absorptivity, ε. It should be noted that simpler calculations have been used to determine ℓ, in which the height is determined using equation 3 with the lower well diameter being used for D.[109]

Description of reactions with **35** found in Table 7.

For the reaction mixture with pyridine only:

Mercaptoethanesulfonate sodium salt, MESNA, and pyridine, which was

128

previously distilled from CaO and stored over 3 Å Molecular Sieves, were added

to a 5 mL conical vial and magnetically stirred in an ice-water bath. Solid was still

present after stirring for 30 min. After **35** was added to the vial, all solids

appeared to be more soluble with a distinct yellowing of the liquid. Within 10

min, the solution was orange. After warming to 16 °C over 2 h, the reaction

mixture was acidified with 1% aq H_2SO_4 and extracted with DCM. The organic

phase was washed with brine and dried with sodium sulfate before the solvent

was evaporated to yield a dark yellow solid. A ^1H NMR spectrum of the crude

material matched **31** with minor impurities.

For every other reaction in Table 7:

35 was added to PBS, followed by addition of the indicated thiol (for the two-

phase system, **35** was first dissolved in DCM, then PBS was added and MESNA,

previously dissolved in PBS, was added last). For aqueous-only reactions, **35** was

not entirely soluble. The reaction mixture was stirred for at least 24 h (24–32 h),

and the amount of precipitate noticeably increased over that time. The solid was

collected by vacuum filtration, and a ^1H NMR spectrum of the material was

collected.

5. FUTURE WORK

Protein tyrosine phosphatase assays would need to be continued for the

bromo nitro lactones **33**, **34**, **35** and **37**. The single concentration inhibitor assay

with DIFMUP supports PTPs as a potential target during cancer cell inhibition.

However, detailed inhibition kinetics for these inhibitors are still in their infancy.

There are a number of issues that would need to be addressed during these

investigations, though. The catalytic cysteine requires a reducing agent, usually in

the form of DTT, to generate the reactive thiolate. Oxidation of cysteine by

hydrogen peroxide *in vivo* is believed to be a control mechanism utilized by

cells.[109] Excess DTT is needed to reduce any sulfenic acid or intramolecular

disulfide bonds (Figure 48).
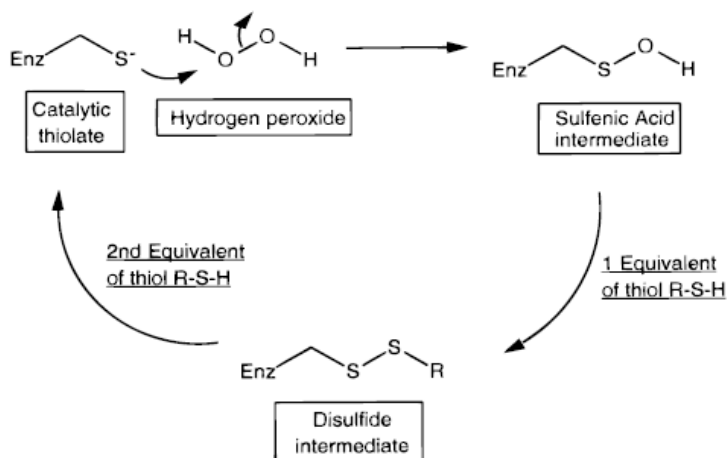
Figure 48. Cysteine-enzyme oxidation by hydrogen peroxide and reduction by
thiol (from Denu and Tanner[110]).

Excessive oxidation of the cysteine can lead to formation of a sulfonic acid, which

is not reduced by DTT back to the active thiolate (Figure 49). PTPs can protect

the cysteine thiol by forming an intramolecular sulfenamide with a nitrogen on the

backbone. However, this protective mechanism does not last in high peroxide

concentration (Figure 49).
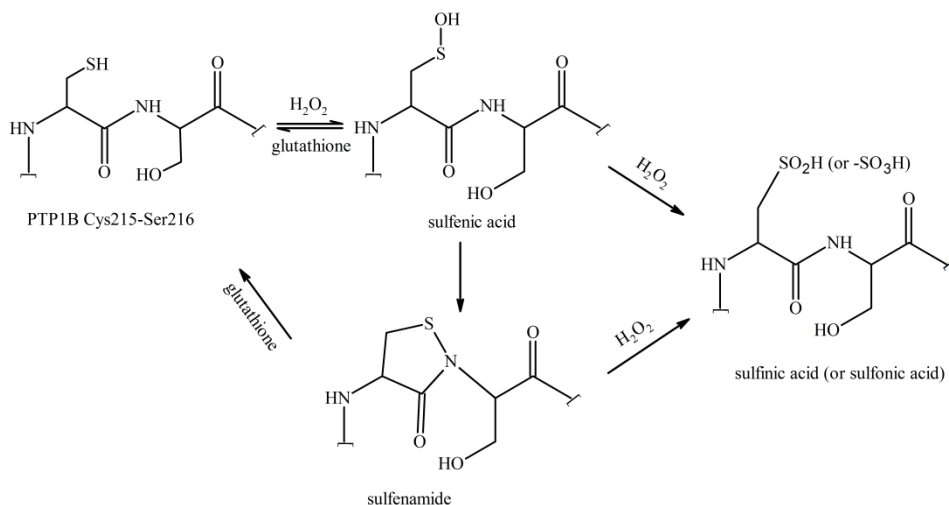
Figure 49. Cyclic sulfenamide formation upon cysteine oxidation; see
Blaskovich.[95]

Oxidation of the cysteine has led to incorrectly labeling compounds as

irreversible alkylating inhibitors when they were inhibiting by oxidization of the

cysteine. Unusual inhibition kinetics have been observed, and in some cases, the

only variation from one assay to another was the concentration of DTT

(Blaskovich;[95] specifically see reference 448 and 489 cited within). In general,

reactive oxygen species (ROS) are generated in the form of peroxides that oxidize

the cysteine to a sulfenic or a sulfonic acid. Furthermore, inhibitors that function

via oxidation of the cysteine will not selectively inhibit a single PTP but the entire

family will be targeted. False hits brought on by peroxide-induced oxidation can

be examined during the assay by including antioxidant enzymes like catalase or

superoxide.[111]

Inhibition kinetic studies would need to follow if the inhibitors are not acting as oxidizing agents. The rate of irreversible inhibition can be checked during enzyme assays.[112] Briefly, an aliquot of the pre-incubated enzyme-inhibitor is removed at various time points, and the enzyme activity is measured and compared to control, i.e. enzyme-only aliquot. Reversible inhibitors are more likely to disassociate from the enzyme when aliquots are taken, and enzyme activity would be expected to recover partially or completely.

Additional investigation by HSQC can be done as described in Chapter 1.4, regardless of the irreversible or reversible nature of inhibition. HSQC experiments done by Pei and colleagues[48, 50] were used to propose a slow-binding reversible inhibition profile for peptidyl nitrostyrenes. The inhibitors would need to be synthesized from ^{13}C enriched nitromethane, however.

There was some evidence to suggest **33** is able to form a bromo nitro lactone alkene (BNLA). A more basic solution possibly generated an analogue of phthalic acid. By extension, **34** can likely generate similar products. The BNLA analogue is believed to be the inhibitory compound for **33**, and not the phthalate analogue. Phthalic acids have been investigated previously for any toxic potential since phthalate esters are commonly used plasticizers. Phthalic acid is not toxic and readily excreted when given to mice.[113, 114] Therefore, it is not expected to be inhibiting cell growth or the PTPs. An enzyme assay using phthalic acid can be done at the same time as the bromo nitro lactones for additional confirmation, however.

132

6 CONCLUSION

The modification of the oxalylamino group that incorporated halogens was intended to irreversibly bind to the catalytic cysteine of PTPs. Some cinnamic acid analogues inhibited cancer-cell growth, but none of them were able to inhibit PTP1B or PTPβ in an assay with pNPP as substrate. The most effective cinnamic acid analogues at inhibiting cancer-cell growth, **24** and **29**, were also analyzed in an assay with PTP1B and four different PTPs using DIFMUP as a substrate (Table 6). Enzyme activity for PTP1B was unaffected at 100 μM (**23**) and 50 μM (**29**) concentration of inhibitor. The same result was obtained for three of the four other PTPs. Enzyme activity for SHP-2 was slightly reduced by these two compounds, however.

The replacement of carboxyl group on the propenoate substituent with a nitro group along with bromine substitution led to inhibition of cancer-cell growth and cancer cell death. Additionally, all the PTPs were found to be inhibited in the same DIFMUP assay that the cinnamic acid analogues were not active in. A bromo nitro alkene may be formed in buffer by these compounds (**33**, **34**, **35** and **37**). UV experiments with **33** indicate a possible bromo nitro lactone alkene forming in buffer, and it may be the compound responsible for inhibition. Confirmation of **35**'s ability to undergo lactone ring opening and form a bromonitrostyrene intermediate was not as convincing. The UV experiments indicated a slowly emerging peak around 340 nm after 19 h in PBS that may have been from the conjugated bromonitrostyrene. However, this intermediate could

not be confirmed, as only reduction from **35** to **31** seemed to be occurring with thiols.

Nitrostyrenes have been investigated for their ability to alkylate nucleophiles and inhibit cancer cell growth and protein tyrosine phosphatases. The brominated nitro lactone compounds will need to be studied further to identify their mode of inhibition and to determine if they can be modified to selectively target specific PTPs or other relevant targets.

REFERENCES

1. Howlader, N.; Noone, A. M.; Krapcho, M.; Neyman, N.; Aminou, R.; Waldron, W.; Altekruse, S. F.; Kosary, C. L.; Ruhl, J.; Tatalovich, Z.; Cho, H.; Mariotto, A.; Eisner, M. P.; Lewis, D. R.; Chen, H. S.; Feuer, E. J.; Cronin, K. A. (eds). *SEER Cancer Statistics Review*, 1975–2009 (Vintage 2009 Populations), National Cancer Institute. Bethesda, MD, http://seer.cancer.gov/csr/1975_2009_pops09/, based on November 2011 SEER data submission, posted to the SEER website, April 2012.

2. Croce, C. M. *N. Eng. J. Med.* **2008,** *358,* 502–511.

3. Goodman, L. S.; Wintrobe, M. X.; Dameshek, W.; Goodman, M. J.; Gilman, M. A.; McLennan, M. T. *J. Am. Med. Assoc.* **1946,** *132,* 126–132.

4. Bjorge, J. D.; Jakymiw, A.; Fujita, D. J. *Oncogene* **2009,** *19,* 5620–5635.

5. Stehelin, D.; Varmus, H. E.; Bishop, J. M.; Vogt, P. K. *Nature* **1976,** *260,* 170–173.

6. Martin, G. S. *Oncogene* **2004,** *23,* 7910–7917.

7. Madhusudan, S.; Ganesan, T. S. *Clinical Biochemistry* **2004,** *37,* 618–635.

8. Javier, R. T.; Butel, J. S. *Cancer Res.* **2008,** *68,* 7693–7706.

9. Bulaj, G.; Kortemme, T.; Goldenberg, D. P. *Biochemistry* **1998,** *37,* 8965–8972.

10. Tsou, H. R.; Overbeek-Klumpers, E. G.; Hallet, W. A.; Reich, M. F.; Floyd, M. B.; Johnson, B. D.; Michalak, R. S.; Nilakantan, R.; Discafani, C.; Golas, J.; Rabindran, S. K.; Shen, R.; Shi, X.; Wang, Y.-F.; Upeslacis, J.; Wissner, A. *J. Med. Chem.* **2005,** *48,* 1107–1131.

11. Tonks, N. A.; Diltz, C. D.; Fischer, E. H. *J. Biol. Chem.* **1988,** *263,* 6722–6730.

12. Eckhart, W.; Hutchinson, M. A.; Hunter, T. *Cell* **1979,** *18,* 925–933.

13. Elchebly, M.; Payette, P.; Michaliszyn, E.; Cromlish, W.; Collins, S.; Loy, A. L.; Normandin, D.; Cheng, A.; Himms-Hagen, J.; Chan, C.-C.; Ramachandran, C.; Gresser, M. J.; Tremblay, M. L.; Kennedy, B. P. *Science* **1999,** *283,* 1544–1548.

14. Alonso, A.; Sasin, J.; Bottini, N.; Friedberg, I.; Friedberg, I.; Osterman, A.; Godzik, A.; Hunter, T.; Dixon, J.; Mustelin, T. *Cell* **2004,** *117,* 699–711.

15. Julien, S. G.; Dubé, N.; Hardy, S.; Tremblay, M. L. *Nat. Rev. Cancer* **2011,** *11,* 35–49.

16. Tonks, N. K. *Nat. Rev. Cancer* **2006,** *7,* 833–846.

17. Neel, B. G.; Tonks, N. K. *Curr. Opin. Cell Bio.* **1997,** *9,* 193–204.

18. Dewang, P. M.; Hsu, N.-M.; Peng, S.-Z.; Li, W.-R. *Curr. Med. Chem.* **2005,** *12,* 1–22.

19. Andersen, J. N.; Jansen, P. G.; Echwald, S. M.; Mortensen, O. H.; Fukada, T.; Vecchio, R. D.; Tonks, N. K.; Møller, N. P. H. *FASEB J.* **2004,** *18,* 8–30.

20. Kristjánsdóttir, K.; Rudolph, J. *Chem. Biol.* **2004,** *11,* 1043–1051.

21. Viry, E.; Anwar, A.; Kirsch, G.; Jacob, C.; Diederich, M.; Bagrel, D. *Int. J. Oncology* **2001,** *38,* 1103–1111.

22. Wang, Z.; Kar, S.; Carr, B. I. *Anti-Cancer Agents Med. Chem.* **2008,** *8,* 863–871.

23. Li, J.; Yen, C.; Liaw, D.; Podsypanina, K.; Bose, S.; Wang, S. I.; Puc, J.; Miliaresis, C.; Rodgers, L.; McCombie, R.; Bigner, S. H.; Giovanella, B. C.; Ittmann, M.; Tycko, B.; Hibshoosh, H.; Wigler, M. H.; Parsons, R. *Science* **1997,** *275,* 1943–1946.

24. Futreal, P. A.; Coin, L.; Marshall, M.; Down, T.; Hubbard, T.; Wooster, R.; Rahman, N.; Stratton, M. R. *Nat. Rev. Cancer* **2004,** *4,* 177–183. Additional information, including updated status of oncogenes, can be found at http://www.sanger.ac.uk/research/projects/cancergenome/ and http://www.sanger.ac.uk/genetics/CGP/Census/.

25. Loh, M. L.; Vattikuti, S.; Schubbert, S.; Reynolds, M. G.; Carlson, E.; Lieuw, K. H.; Cheng, J. W.; Lee, M. C.; Stokoe, D.; Bonifas, J. M.; Curtiss, N. P.; Meshinchi, S.; Le Beau, M. M.; Emanuel, P. D.; Shannon, K. M. *Blood* **2004,** *103,* 2325–2331.

26. Tartaglia, M.; Gelb, B. D. *Eur. J. Medical Genetics* **2005,** *48,* 81–96.

27. Wishart, M. J.; Dixon, J. E. *Trends in Cell Biology* **2002,** *12,* 579–585.

28. Steck, P. A.; Pershouse, M. A.; Jasser, S. A.; Yung, W. K. A.; Lin, H.; Ligon, A. H.; Langford, L. A.; Baumgard, M. L.; Hattier, T.; Davis, T.; Frye, C.; Hu, R.; Swedlund, B.; Teng, D. H. F.; Tavtigian, S. V. *Nature Genetics* **1997,** *15,* 356–362.

29. Julien, S. G.; Dubé, N.; Read, M.; Penney, H.; Paquet, M.; Han, Y.; Kennedy, B. P.; Muller, W. J.; Tremblay, M. L. *Nature Genetics* **2007,** *39,* 338–346. Also see references 4–7 in this reference.

30. Hutchinson, J. N.; Muller, W. J. *Oncogene* **2000,** *19,* 6130–6137.

31. Wiener, J. R.; Hurteau, J. A.; Kerns, B.-J. M.; Whitaker, R. S.; Conaway, M. R.; Berchuck, A.; Bast, R.C. *Am. J. Obstet. Gynecol.* **1994,** *170,* 1177–1183.

32. Bentires-Alj, M.; Neel, B. G. *Cancer Res.* **2007,** *67,* 2420–2424.

33. Tonks, N. K.; Muthuswamy, S. K. *Cancer Cell* **2007,** *11,* 214–216.

34. Iversen, L. F.; Møller, K. B.; Pedersen, A. K.; Peters, G. H.; Petersen, A. S.; Sune, H. S.; Branner, S.; Mortensen, S. B.; Møller, N. P. H. *J. Biol. Chem.* **2002,** *277,* 19982–19990.

35. You-Ten, K. E.; Muise, E. S.; Itié, A.; Michaliszyn, E.; Wagner, J.; Jothy, S.; Lapp, W. S.; Tremblay, M. L. *J. Exp. Med.* **1997,** *186,* 683–693.

36. Dubé, N.; Tremblay, M. L. *Biochim. Biophys. Acta Proteins Proteomics* **2005,** *1754,* 108–117. Also see references 34, 35, 39 and 40 in this reference.

37. Ibarra-Sanchez, M. J.; Tremblay, M. L. *Oncogene* **2001,** *20,* 4728–4739.

38. Gibrat, J. F.; Madej, T.; Bryant, S. H. *Curr. Opin. Struct. Biol.* **1996,** *6,* 377–385. http://www.ncbi.nlm.nih.gov/Structure/VAST/vast.shtml.

39. Wang, Y.; Greer, L. Y.; Chappey, C.; Kands, J. A.; Bryant, S. H. *Trends Biochem. Sci.* **2000,** *25,* 300–302. http://structure.ncbi.nlm.nih.gov/CN3D/cn3d.shtml

40. Burke, T. R.; Kole, H. K.; Roller, P. P. *Biochem. Biophys. Res. Commun.* **1994,** *204,* 129–134.

41. Burke, T. R.; Ye, B.; Yan, X.; Wang, S.; Jia, Z.; Chen, L.; Zhang, Z.-Y.; Barfod, D. *Biochemistry* **1996,** *35,* 15989–15996.

42. Andersen, H. S.; Iversen, L. F.; Jeppesen, C. B.; Branner, S.; Norris, K.; Rasmussen, H. B.; Møller, K. B.; Møller, N. P. H. *J. Biol. Chem.* **2000,** *275,* 7101–7108.

43. Jia, Z. C.; Barford, D.; Flint, A. J.; Tonks, N. K. *Science* **1995,** *268,* 1754–1758.

44. Peters, G. H.; Branner, S.; Møller, K. B.; Andersen, J. N.; Møller, N. P. H. *Biochimie* **2003,** *85,* 527–534.

45. Settleman, J.; Kurie, J. M. *Cancer Cell* **2007,** *12,* 6–8.

46. Esterbauer, H.; Ertl, A.; Scholz, N. *Tetrahedron* **1976,** *32,* 285–289.

47. Seiner, D. R.; LaButti, J. N.; Gates, K. S. *Chem. Res. Toxicol.* **2007,** *20,* 1315–1320.

48. Fu, H.; Park, J.; Pei, D. *Biochemistry* **2002,** *41,* 10700–10709.

49. Moran, E. J.; Sarshar, S.; Cargill, J. F.; Shahbaz, M. M.; Lio, A.; Mjalli, A. M. M.; Armstrong, R. W. *J. Am. Chem. Soc.* **1995,** *117,* 10787–10788.

50. Park, J.; Pei, D. *Biochemistry* **2004,** *43,* 15014–15021.

51. Doré, J. C.; Viel, C. *Farmaco. [Sci.]* **1975,** *30,* 81–109.

52. Nicolletti, A.; White, K. S. Protein Tyrosine Phosphatase Modulators. WO 2008/061308 A1, May 29, 2008; *Scifinder Scholar.* 2008:639170 (accessed Sep 27, 2012).

53. Chatterji, T.; Kizil, M.; Keerthi, K.; Chowdhury, G.; Pospísil, T.; Gates, K. S.; *J. Am. Chem. Soc.* **2003,** *125,* 4996–4997.

54. Fekry, M. I.; Price, N. E.; Zang, H.; Huang, C.; Harmata, M.; Brown, P.; Daniels, J. S.; Gates, K. S. *Chem. Res. Toxicol.* **2011,** *24,* 217–228.

55. Barhate, N. B.; Gajare, A. S.; Wakharkar, R. D.; Bedekar, A. V. *Tetrahedron* **1999,** *55,* 11127–11142.

56. Herlihy, K. P. *Aust. J. Chem.* **1983,** *36,* 203–209.

57. Marko, I. E.; Richardson, P. R.; Bailey, M.; Maguire, A. R.; Coughlan, N. *Tetrahedron Lett.* **1997,** *38,* 2339–2342.

58. De Luca, L.; Giacomelli, G.; Masala, S.; Porcheddu, A. *J. Org. Chem.* **2003,** *68,* 4999–5001.

59. Elvidge, J. A.; Jones, D. E. H. *J. Chem. Soc., C* **1971,** 2424–2427.

60. Riordan, J. F.; Vallee, B. L. *Meth. Enzymol.* **1972,** *25,* 451–456.

61. Fadgen, C. J.; Groy, T. L.; Rose, S. D. *Acta Crystallogr., Sect. E: Struct. Rep. Online* **2010,** *E66*, o376.

62. Kraszkiewicz, L.; Sosnowski, M.; and Skulski, L. *Tetrahedron* **2004,** *60,* 9113–9119.

63. Breau, L.; Kayser, M. M.; *Can. J. Chem.* **1989,** *67,* 569–573.

64. Chopard, P. A.; Hudson, R. F.; Searle, R. J. G. *Tetrahedron Lett.* **1965,** *6,* 2357–2360.

65. Zhu, J.; Kayser, M. M.; *Synth. Commun.* **1994,** *24,* 1179–1186.

66. Baer, H. H.; Kienzle, F.; *Can. J. Chem.* **1964,** *43,* 190–196.

67. Whelton, B. D.; Huitric, A. C. *J. Org. Chem.* **1970,** *35,* 3143–3144.

68. Hashimoto, T.; Nagase, S. *J. Pharm. Soc. Jpn.* **1960,** *80,* 1637–1638.

69. Wheeler, D. D.; Young, D. C.; Erley, D. S.; *J. Org. Chem.* **1957,** *22,* 547–556.

70. Ukhin, L. Y.; Suponitsky, K. Y.; Belousova, L. V.; Orlova, Z. I. *Russ. Chem. Bull.* (International) **2009,** *58,* 2478–2487.

71. Erickson, A. S.; Kornblum, N. *J. Org. Chem.* **1977,** *42,* 3764–3765.

72. Slagh, H. R. Production of Monobromonitromethane. U.S. Patent 2632776, Mar. 24, 1953; *Scifinder Scholar.* 1954:7354 (accessed Oct 16, 2012).

73. Gleason, J. G.; Harpp, D. N. *Tetrahedron Lett.* **1970,** *39,* 3431–3434.

74. Djerassi, C.; Scholz, C. R. *Experientia* **1947,** *3,* 107.

75. Djerassi, C.; Scholz, C. R. *J. Am. Chem. Soc.* **1948,** *70,* 417–418.

76. McKenna, C. E.; Khawli, L. A. *J. Org. Chem.* **1986,** *51,* 5467–5471.

77. Luk'yanov, O. A.; Ternikova, T. V.; Shlykova, N. I.; Salamonov, Y. B. *Russ. Chem. Bull.* (International) **2009,** *58,* 2063–2069.

78. McCoy, W. F.; Thornburgh, S. A New Industrial Antimicrobial: Uses for 2-(2-bromo-2-nitroethenyl)-furan and a New Process of Forming 2-(2-bromo-2-nitroethenyl)-furan. WO 8911793, Dec. 14, 1989; *Scifinder Scholar.* 1990:402007 (accessed Oct 16, 2012).

79. Alexander, R. G.; Buckle, D. R.; Tedder, J. M. *J. Chem. Soc., Perkin Trans. 1* **1977,** 1191–1193.

80. Knepper, K.; Ziegert, R. E.; Bräse, S. *Tetrahedron* **2004,** *60,* 8591–8603.

81. Rubinstein, L. V.; Shoemaker, R. H.; Paull, K. D.; Simon, R. M.; Tosini, S.; Skehan, P.; Scudiero, D. A.; Monks, A.; Boyd, M. R. *J. Natl. Cancer Inst.* **1990,** *82,* 1113–1118.

82. Skehan, P.; Storeng, R.; Scudiero, D.; Monks, A.; McMahon, J.; Cistica, D.; Warren, J. T.; Bokesch, H.; Kenney, S.; Boyd, M. R. *J. Natl. Cancer Inst.* **1990,** *82,* 1107–1112.

83. NCI website for inhibitor concentration determination; http://dtp.nci.nih.gov/branches/btb/ivclsp.html.

84. Bowers, G. N.; McComb, R. B.; Christensen, R. G.; Schaffer, R. *Clin. Chem.* **1980,** *26,* 724–729.

85. Montalibet, J.; Skorey, K. I.; Kennedy, B. P. *Methods* **2005,** *35,* 2–8.

86. Mikalsen, S.-O.; Kaalhus, O. *J. Biol. Chem.* **1998,** *273,* 10036–10045.

87. Zhou, A.; Pittman, C. U.; *Tetrahedron Lett.* **2004,** *45,* 8899–8903.

88. Abraham, R. J.; Parry, K.; Thomas, W. A.; *J. Chem. Soc. B* **1971,** 446–453.

89. *TOPSPIN,* version 2.1, Bruker Biospin: 2008. http://www.bruker-biospin.com/.

90. Adam, W.; Hadjiarapoglou, L.; Wang, X.; *Tetrahedron Lett.* **1989,** *30,* 6497–6500.

91. Murray, R. W.; Singh, M. *Organic Syntheses, Coll. Vol.* **1998,** *8,* 288.

92. Kraft, G. A.; Katzenellenbogen, J. A. *J. Am. Chem. Soc.* **1981,** *103,* 5459–5466.

93. Doré, J. C.; Montagnier, L.; Viel, C. *Chim. Ther.* **1971,** *6,* 167–185.

94. Welte, S.; Baringhaus, K. H.; Schmider, W.; Müller, G.; Petry, S.; Tennagels, N. *Anal. Biochem.* **2005,** *338,* 32–38.

95. Blaskovich, M. A. T. *Curr. Med. Chem.* **2009,** *16,* 2095–2176.

96. Baranski, A.; Cholewka, E. *Chem. Papers* **1991,** *45,* 449–455.

97. Watarai, S.; Yamamura, K.; Kinugasa, T. *Bull. Chem. Soc. Jpn.* **1967,** *40,* 1448–1452.

98. Berestovitskaya, V. M.; Bel'skii, V. K.; Macmillan, G. H.; Makarenko, S. V.; Trukhin, E. V. *Russ. J. Gen. Chem.* **1999,** *69,* 803–808.

99. Shchukina, L. *Zh. Obshch. Khim.* **1965,** *31,* 3041–3045.

100. *Spectral Database for Organic Compounds (SDBS)*; carbon NMR; SDBS No.: 6270; RN 3674-33-7; http://riodb01.ibase.aist.go.jp/sdbs/cgi-bin/cre_index.cgi (accessed October 26, 2012).

101. Shemyakin, M. M.; Shigorin, D. N.; Shchukina, L. A.; Semkin, E. P. *Russ. Chem. Bull.* **1959,** *8,* 664–668.

102. Metro, S. J.; Taurins, A. *Can. J. Chem.* **1952,** *30,* 466–470.

103. Bellucci, G.; Berti, G.; Bianchini, R.; Orsini, L. *Tetrahedron Lett.* **1982,** *23,* 3635–3638.

104. Gottlieb, H. E.; Kotlyar, V.; Nudelman, A. *J. Org. Chem.* **1997,** *62,* 7512–7515.

105. Pettit, G. R.; Tan, R.; Bao, G. H.; Melody, N.; Doubek, D. L.; Gao, S.; Chapuis, J.-C.; Williams, L. *J. Nat. Prod.* **2012,** *75,* 771–773. Also see reference 12 within this reference.

106. Kalemkerian, G. P.; Ou, X.; Adil, M. R.; Rosati, R.; Khoulani, M. M.; Madan, S. K.; Pettit, G. R. *Cancer Chemother. Pharmacol.* **1999,** *43,* 507–515.

107. Lipinski, C. A.; Lombardo, F.; Dominy, B. W.; Feeney, P. J. *Adv. Drug Delivery Rev.* **1997,** *23*, 3–25.

108. Corning Life Sciences Microplate Dimensions for Corning 96 Well Microplates. http://catalog2.corning.com/Lifesciences/media/pdf/MD_Microplate_Dimension_Sheets_96_Well.pdf (February 2012). Costar UV Cat. # 3635.

109. Greiner Bio-one Application Note. http://www.greinerbioone.com/en/germany/files/1143349/UV-Spectroscopy.pdf (December 2012).

110. Denu, J. M.; Tanner, K. G. *Biochemistry* **1998,** *37*, 5633–5642.

111. Doroshow, J. H. *Proc. Natl. Acad. Sci. USA* **1986,** *83,* 4514–4518.

112. Kitz, R.; Wilson, I. B. *J. Biol. Chem.* **1962,** *237,* 3245–3249.

113. Lim, D. S.; Shin, B. S.; Yoo, S. D.; Kim, H. S.; Kwack, S. J.; Ahn, M. Y.; Lee, B. Y. *J. Toxicol. Environ. Health, Part A* **2007,** *70,* 1344–1349.

114. Lee, K. H.; Lee, B. M. *J. Toxicol. Environ. Health, Part A* **2007,** *70,* 1329–1335.